Wnt secretion is regulated by the Claudin-like Protein, HIC-1 through its interaction with Neurabin/NAB-1

A thesis

Submitted for the degree of

Doctor of Philosophy

By

Vina Tikiyani

Department of Biological Sciences

Indian Institute of Science Education and Research (IISER)

Mohali-140306

INDIAN INSTITUTE OF SCIENCE EDUCATION AND RESEARCH MOHALI
Sector 81, SAS Nagar, Mohali,
PO Manuali, Punjab, 140306, India

DECLARATION

The work presented in this thesis entitled "Wnt secretion is regulated by a Claudin-like protein, HIC-1 through its interaction with Neurabin/NAB-1'' has been carried out by me under the supervision of Dr. Kavita Babu at the Department of Biological Sciences, Indian Institute of Science Education and Research (IISER) Mohali.

This work has not been submitted in part or full for a degree, a diploma, or a fellowship to any other university or institute. Whenever contributions of others are involved, every effort is made to indicate this clearly, with due acknowledgment of collaborative research and discussions. This thesis is a bonafide record of original work done by me and all sources listed within have been detailed in the bibliography.

(Vina Tikiyani)

Date:

Place:

In my capacity as supervisor of the candidate's doctoral thesis work, I certify that above statements by the candidate are true to the best of my knowledge.

(Dr. Kavita Babu)

Department of Biological Sciences
Indian Institute of Science Education and Research Mohali

Table of contents

List of Figures

Number ***Page***

List of Tables

Number ***Page***

Acknowledgment

Looking back at the journey of my PhD, I have been blessed with many people who have helped me directly or indirectly in this endeavour. I would like to acknowledge everyone who helped and supported me during the entire process. First and foremost, I owe my greatest debt and heartfelt gratitude to my PhD supervisor Dr. Kavita Babu, who has been the soul behind every effort that I have put forth in this thesis. Words may fall short when I try to describe her greatness as my PhD supervisor and as a human being. Before PhD, I worked as a Project JRF with her for 18 months. I will always remain indebted to her for accepting me in her lab as a JRF and a PhD and providing me her esteemed guidance and support at every moment. From the day I joined her lab, she showed immense confidence in me. She used to get excited seeing my results and progress which was the key for my perseverance towards my goals. She always made me positive whenever I was at my low. I have learned so much from her not only professionally but also personally. Her promptness to work, time management and organizational skills are incomparable. She taught me every basic thing starting from performing experiments to think scientifically. It was under her tutelage that I developed an understanding of the subject and the research curriculum. In spite of my shortcomings, she always continued her support and guidance to me. I admire and respect her for

her loving and caring nature, valuable feedbacks and the amount of freedom she renders to each of her students. She has always been a great mentor and her exceptional dedication, guidance and enthusiasm has helped me to expand my knowledge and horizon throughout the journey of my thesis work. Thank you very much Kavita for everything!

I express my immense gratitude to my doctoral committee members, Dr. Samarjit Bhattacharyya, Dr. Mahak Sharma, and Dr. Rajesh Ramachandran for their critical comments and timely review of the progress of my work. Their constant motivation and valuable discussions have always improved the quality of my work. Thank you!

I would like to thank Prof. N. Sathymurthy, former Director, IISER Mohali, and Prof. Debi P. Sarkar, current Director, IISER Mohali for giving me the opportunity to work at this premier institute and avail the excellent infrastructure to carry out my research work.

I would like to thank all DBS faculty members for their suggestions and help during the entire period. My heartfelt gratitude goes to Dr. Shravan Kumar Mishra for his continuous help in my research project. The story of HIC-1 and NAB-1 would not have been completed without the experiments he suggested. Special thanks to Prof. Anand Bachhawat, Prof. Purnananda Guptasarma, Dr. Sudip Mandal, Dr. Lolitika Mandal, Dr. Kaushik, Dr. Arunika, and Dr. Rachna Chaba for their constant motivation and help whenever I needed them.

I am extremely grateful to have incredible lab members. Their active interest in my work, useful suggestions and constructive criticism improved the quality of my work. Special thanks to our two postdocs Dr.

Pratima Sharma Pandey and Dr. Yogesh Dahiya, the two strong pillars of the Babu lab. They not only taught me the basics of the research but were always there for me whenever I needed them. I am grateful to have wonderful seniors; Shruti Thapliyal, Pallavi Sharma, and Ashwani Bhardwaj for their constant help and support. I really admire Shruti for her hardwork and passion for science. Pallavi and I together started the Claudin project, many thanks to her for teaching me the basics during my initial days in the lab. Thanks to Ashwani for making lab a joyful environment to work. I am extremely grateful to have Nagesh and Anuradha around me as lab mates. Being the junior most graduate in the lab and apart from her own work, Anuradha is managing the ordering responsibilities incredibly well. Hats-off to her! Many thanks to Ankit Negi for his help in the lab and all the present and past students of BS-MS I have worked with (Diwakar, Nandini Tripathi, Nandini Natrajan, Dipannita).

I am thankful to my batch-mates Sonal, Alok, Namrata, Deepinder, Richa and Aparajita for their help, specially to Namrata and Deepinder who have helped me in performing few experiments in their labs.

I consider myself extremely lucky to be a part of the IISER Mohali community. I am indebted to them for making it a home away from home. I have been surrounded by wonderful colleagues and friends such as Saurabh Pandey, Ravinder Gulia, Saikat Ghosh, Rohan Sharma, Prabhat Mahato, Prince Tiwari, Nidhi Kundu, Prachi Ojha, Mekhla Rudra, Manisha, Poonam Thakran, Nisha Arora, Surabhi, Harleen

Kaur, Simran Kaur, and Muskan for their constant help and cheerful moments. Thank you and love you all!

Words are never enough to describe the gratitude one feels towards their family. As always, I fell short of words to describe what I feel for my Mom. She has been my strongest support system. All of my achievements in life till date have been and will always be because of the constant love, prayers, support, encouragement and sacrifices my Mom has made for me. Her immense unwavering faith in me and my abilities, greater than my own has always driven me to aspire for the pinnacle of success and this thesis is dedicated to her. Thank you very much to my family Mom, Nilu, Saurabh, Mummiji, Papaji, Monu, Didi, Jijju, Ansh and Abhi for always being there for me.

I owe my deepest gratitude to my husband Saurabh Pandey for his constant support and understanding of my goals and aspirations. Many experiments in the thesis work have been carried out after hour long discussions with him. His suggestions and criticism have always improved my work. I am thankful to him for teaching me imaging and data quantitation skills. His valuable suggestions have improved my presentation skills a lot. His unconditional love, support, care and encouragement have always been my biggest strength.

Thank you very much for being with me!

Thank you, All!

Funding agencies

Vina Tikiyani thanks the Council of Scientific and Industrial Research (CSIR) for a graduate fellowship. This work was supported by the Wellcome Trust/DBT India Alliance Fellowship [Grant number IA/I/12/1/500516] awarded to Kavita Babu. This work was also partially supported by grant [BT/05/IYBA/2011] to Kavita Babu.

List of Publications

1.**Tikiyani V.,** Li L., Sharma P., Hu Z., and Babu K. Wnt secretion is regulated by a Claudin, HIC-1, through its interaction with Neurabin/NAB-1. *Cell Reports* **2018** Nov 13; 25, 1856-1871.

2. Sharma P*., Li L*., Liu H., **Tikiyani V.,** Hu Z©., and Babu K©.(2018); The Claudin-like protein, HPO-30, is required to maintain LAChRs at the *C. elegans* neuromuscular junction. *The Journal of Neuroscience* **2018** Aug 08; 38(32): 7072-87

*= equal contribution, ©= co-corresponding authors

Glossary

Weights and measures

%	Percent
°C	Degree centigrade
bp, kb	Base pair, kilobase
rpm	Revolutions per minute
RT	Room temperature
sec, min, h	Second, minute, hour
µg, mg, g	Microgram, Milligram, Gram
µl, ml, L	Microliter, Milliliter, Liter,
µM, mM, M,	Micromolar, Millimolar, Molar
mV,V	Millivolt,Volt

Symbols

α	Alpha
β	Beta
γ	Gamma
Δ	Delta

Techniques

BiFC	Bimolecular Fluorescence Complementation assay
PCR	Polymerase Chain Reaction
FRAP	Fluorescence Recovery after Photobleaching
RNAi	RNA Interference

qPCR	Quantitative PCR
Chemicals	
Amp	Ampicillin
DMSO	Dimethyl Sulphoxide
dNTPs	2'-deoxyadenosine 5'-triphosphate
DTT	Dithiothreitol
EDTA	Ethylenediamine-tetra-acetic acid
BDM	2, 3-butanedione monoxamine
Miscellaneous	
aa	Amino acids
Ach	Acetylcholine
BLAST	Basic Local Alignment Search Tool
Ca2+	Calcium ion
CAM	Cell Adhesion Molecule
CGC	*C. elegans* Genetics Center
CIP	Calf Intestinal Phosphatase
C-terminal	Carboxy- terminal
DNA	Deoxyribonucleic acid
DNC	Dorsal Nerve Cord
EPSC	Excitatory Postsynaptic Current
FP	Forward primer
GABA	Gamma-aminobutyric acid
GFP	Green Fluorescent Protein
GPCR	G-protein-coupled receptor
IPSC	Inhibitory Postsynaptic Current

LB	Luria Bertani
NGM	Nematode Growth Medium
NMJ	Neuro-Muscular Junction
N-terminal	Amino- terminal
ORF	Open Reading Frame
RNA	Ribonucleic acid
ROI	Region of interest
RP	Reverse primer
SEM	Standard error mean
SNB	Synaptobrevin
SV	Synaptic Vesicle
VNC	Ventral Nerve Cord
WT	Wild-type
YFP	Yellow Fluorescent Protein

Synopsis

Introduction:

To maintain proper communication between pre- and postsynaptic sites, neurons are equipped with accessory molecules such as cell adhesion molecules (CAMs). Apart from the basal neurotransmission machinery, these CAMs help maintain stringent control of synaptic transmission (reviewed in (Cox, 2004; Togashi et al., 2009; Yamagata et al., 2003a) and (Charles et al., 2000; Pollerberg et al., 2013)) . Claudins are a family of CAMs that have not been studied for their function at the synapse. The Claudin super-family consists of four transmembrane domain proteins, which are important functional and structural components of tight junctions. They maintain paracellular permeability and barrier functions across epithelial and endothelial cells (Van Itallie and Anderson, 2006). Recent reports indicate their functional roles in the brain and in brain disorders (Devaux et al., 2010; Jia et al., 2014; Stork et al., 2008). However, how they function in the brain and at the synapses is poorly understood. A previous RNAi based screen that was performed using the acetylcholine esterase inhibitor, aldicarb, to identify various CAM at the *C.elegans* Neuromuscular Junctions (NMJs), pulled out multiple claudins as possible regulators of NMJ function (Babu et al., 2011a) and Babu K. and Kaplan J.M.; unpublished data)). The aldicarb drug inhibits the activity of acetylcholine esterase, which in turn leads to increased acetylcholine at the synaptic cleft and ultimate paralysis of the worms. The paralysis pattern of mutants is observed with respect to wild type worms. Mutations that cause increased synaptic transmission often results in aldicarb hypersensitivity

while the mutants with decreased synaptic transmission have been seen with aldicarb resistance (Mahoney et al., 2006b; Sieburth et al., 2005a).

Since multiple Claudins came out as positive in the screen described above, we were interested in further understanding how these Claudins function at the NMJ. To this end we screened through all the available mutants for Claudin-like molecules in *C.elegans* in the aldicarb assay. In the screen, we found one Claudin homolog; T28B4.4/HIC-1 which showed hypersensitivity to aldicarb. We found that the HIC-1 hypersensitivity phenotype was rescued by expressing HIC-1 specifically in the cholinergic neurons. This allowed us to hypothesize that this particular Claudin homolog could be functioning in the cholinergic neurons of *C.elegans*. We were then interested in elucidating the synaptic functions of HIC-1. In order to address the role of HIC-1 at the synapse, we framed the following objectives:

1) Understanding the role of HIC-1 at the *C.elegans* NMJ.

2) Delineating the molecular pathway through which HIC-1 functions at the NMJ.

3) Identifying possible interacting partner/s for HIC-1 at the NMJ.

Results:

1. HIC-1, a novel Claudin like molecule is expressed in cholinergic motor neurons

The *hic-1* mutant worms showed increased paralysis or a hypersensitivity phenotype on aldicarb. This hypersensitivity of HIC-1 was rescued to wild-type (WT) levels when HIC-1 gene was expressed in the cholinergic neurons. Expression pattern studies of HIC-1 also revealed that HIC-1 is expressed at the cholinergic synapses. In a series of experiments to decipher how HIC-1 could be functioning at the cholinergic neuromuscular synapse, we found that HIC-1 is required to maintain

normal levels of postsynaptic acetylcholine receptor (AChR/ACR-16) through its function in cholinergic neurons.

2. HIC-1 regulates postsynaptic Acetylcholine receptor (AChR/ACR-16) levels by controlling Wnt secretion from the cholinergic neurons

After establishing that HIC-1 is affecting AChR/ACR-16 receptors levels, we went on to investigate the mechanism by which HIC-1 could be regulating AChR/ACR-16 receptors levels.

A class of secretory proteins, Wnts, are key players in various aspects of brain development (Inestrosa and Arenas, 2010; Inestrosa and Varela-Nallar, 2014; Oliva et al., 2013). They have been shown to be required in aspects of neurogenesis (Hawkins et al., 2005; Valvezan and Klein, 2012), axon guidance, development of neuronal polarity (Chien et al., 2015; Hilliard and Bargmann, 2006; Pan et al., 2006), neural circuit development (Fradkin, 2005), neuromuscular junction development (Barik et al., 2014a; Henriquez et al., 2008b; Klassen and Shen, 2007a; Koles and Budnik, 2012b) and synaptic plasticity (Babu et al., 2011a; Dickins and Salinas, 2013; Jensen et al., 2012b). Through genetic studies, we have discovered that HIC-1 is a component of the Wnt signalling pathway which is known to regulate AChR/ACR-16 receptor translocation at the postsynaptic body-wall muscle membrane (Jensen et al., 2012b). We show here that HIC-1 functions upstream of the Wnt pathway molecules *mig-14/Wntless* and *lin-17/Frizzeled*. We demonstrate using coelomocyte uptake assays that *hic-1* mutants show increased Wnt secretion from the cholinergic neurons.

Claudins are known to interact with the actin cytoskeleton via PDZ domain scaffold proteins such as ZO-1/2/3 (Van Itallie et al., 2017). To test if HIC-1, being a Claudin

homolog could also interact with actin, we visualized actin binding protein gelsolin and stable F- actin in *hic-1* mutants. Both gelsolin and F-actin levels were found to be reduced in the absence of *hic-1*, indicating that HIC-1 could alter a normal actin cytoskeleton. Disruption of the actin cytoskeleton in *hic-1* mutants led us to hypothesize that the actin cytoskeleton could have a role in the secretion of Wnts, since Wnt release is enhanced in the *hic-1* worms. We disrupted actin cytoskeleton pharmacologically in the wild type worms and checked Wnt secretion. We were surprised to see that disrupting actin indeed phenocopied *hic-1* and we found increased Wnt secretion in these animals.

3. HIC-1 interacts with NAB-1 to maintain normal Wnt release at the *C. elegans* NMJ

The structural analysis of HIC-1 showed that HIC-1 also contained a putative PDZ binding motif at its C-terminus which is required for bonafide Claudins to interact and participate in intracellular signalling. Deleting last four amino acids, the putative PDZ binding motif, from HIC-1, resulted in non-functioning of HIC-1 at the synapses while the localization of the protein was not affected. These data suggested that HIC-1 could be interacting with other molecules via its PDZ binding motif. This prompted us to look for possible actin binding molecules through which HIC-1 could interact with the actin cytoskeleton. We searched through known proteins in literature and Wormbase using the following criteria: 1) that molecule should be present at the synapses 2) it should have a PDZ motif and 3) it should also have an actin binding motif. While searching through the literature, we came across one molecule that fit the above three criteria, NAB-1/Neurabin. NAB-1 showed genetic and physical interaction with HIC-1 and was also involved in the same signalling

pathway to regulate Wnt secretion together with HIC-1. Furthermore, we also found that actin binding domain of NAB-1 anchored onto HIC-1 lacking the last four amino acids was sufficient enough to partially rescue NAB-1 and HIC-1 functions in the *nab-1; hic-1* double mutants, suggesting that NAB-1 could be acting as an adaptor molecule to link HIC-1 to actin cytoskeleton.

Conclusions:

We have characterized the synaptic functions of HIC-1, a novel Claudin-like molecule in *C.elegans*. We show that HIC-1 and the *C. elegans* Neurabin, NAB-1 function together to regulate the actin cytoskeleton and Wnt secretion. To our knowledge, these data potentially indicate the first characterization of a loss of function mutants that causes an increase in Wnt sectretion. More comprehensive studies on how Wnt secretion is deregulated could be helpful in treating illnesses where blocking Wnt secretion or designing therapeutic targets against Wnt signaling have been proven to be helpful (reviewed in (Inestrosa and Varela-Nallar, 2014)).

References:

Wnt signaling regulates experience dependent synaptic plasticity in the adult nervous system.

Babu, K., Hu, Z., Chien, S.-C., Garriga, G., and Kaplan, Joshua M. (2011). The Immunoglobulin Super Family Protein RIG-3 Prevents Synaptic Potentiation and Regulates Wnt Signaling. Neuron *71*, 103-116.

Barik, A., Zhang, B., Sohal, G.S., Xiong, W.-C., and Mei, L. (2014). Crosstalk between Agrin and Wnt signaling pathways in development of vertebrate neuromuscular junction. Developmental Neurobiology *74*, 828-838.

Charles, P., Hernandez, M.P., Stankoff, B., Aigrot, M.S., Colin, C., Rougon, G., Zalc, B., and Lubetzki, C. (2000). Negative regulation of central nervous system myelination by polysialylated-neural cell adhesion molecule. Proceedings of the National Academy of Sciences *97*, 7585.
Chien, S.C., Gurling, M., Kim, C., Craft, T., Forrester, W., and Garriga, G. (2015). Autonomous and nonautonomous regulation of Wnt-mediated neuronal polarity by the C. elegans Ror kinase CAM-1. Developmental biology *404*, 55-65.
Cox, E.A. (2004). Sticky worms: adhesion complexes in C. elegans. Journal of Cell Science *117*, 1885-1897.
Devaux, J., Fykkolodziej, B., and Gow, A. (2010). Claudin Proteins And Neuronal Function. Current topics in membranes *65*, 229-253.
Dickins, E.M., and Salinas, P.C. (2013). Wnts in action: from synapse formation to synaptic maintenance. Frontiers in Cellular Neuroscience *7*.
Fradkin, L.G. (2005). Wnt Signaling in Neural Circuit Development. Journal of Neuroscience *25*, 10376-10378.
Hawkins, N.C., Ellis, G.C., Bowerman, B., and Garriga, G. (2005). MOM-5 frizzled regulates the distribution of DSH-2 to control C. elegans asymmetric neuroblast divisions. Developmental biology *284*, 246-259.
Henriquez, J.P., Webb, A., Bence, M., Bildsoe, H., Sahores, M., Hughes, S.M., and Salinas, P.C. (2008). Wnt signaling promotes AChR aggregation at the neuromuscular synapse in collaboration with agrin. Proceedings of the National Academy of Sciences *105*, 18812-18817.
Hilliard, M.A., and Bargmann, C.I. (2006). Wnt signals and frizzled activity orient anterior-posterior axon outgrowth in C. elegans. Developmental Cell *10*, 379-390.
Inestrosa, N.C., and Arenas, E. (2010). Emerging roles of Wnts in the adult nervous system. Nat Rev Neurosci *11*, 77-86.
Inestrosa, N.C., and Varela-Nallar, L. (2014). Wnt signaling in the nervous system and in Alzheimer's disease. Journal of Molecular Cell Biology *6*, 64-74.
Jensen, M., Hoerndli, Frédéric J., Brockie, Penelope J., Wang, R., Johnson, E., Maxfield, D., Francis, Michael M., Madsen, David M., and Maricq, Andres V. (2012). Wnt Signaling Regulates Acetylcholine Receptor Translocation and Synaptic Plasticity in the Adult Nervous System. Cell *149*, 173-187.
Jia, W., Lu, R., Martin, T.A., and Jiang, W.G. (2014). The role of claudin-5 in blood-brain barrier (BBB) and brain metastases (Review). Molecular Medicine Reports *9*, 779-785.
Klassen, M.P., and Shen, K. (2007). Wnt Signaling Positions Neuromuscular Connectivity by Inhibiting Synapse Formation in C. elegans. Cell *130*, 704-716.

Koles, K., and Budnik, V. (2012). Wnt Signaling in Neuromuscular Junction Development. Cold Spring Harbor Perspectives in Biology *4*, a008045-a008045.
Mahoney, T.R., Luo, S., and Nonet, M.L. (2006). Analysis of synaptic transmission in Caenorhabditis elegans using an aldicarb-sensitivity assay. Nature Protocols *1*, 1772-1777.
Oliva, C.A., Vargas, J.Y., and Inestrosa, N.C. (2013). Wnts in adult brain: from synaptic plasticity to cognitive deficiencies. Frontiers in Cellular Neuroscience *7*, 224.
Pan, C.L., Howell, J.E., Clark, S.G., Hilliard, M., Cordes, S., Bargmann, C.I., and Garriga, G. (2006). Multiple Wnts and frizzled receptors regulate anteriorly directed cell and growth cone migrations in Caenorhabditis elegans. Developmental Cell *10*, 367-377.
Pollerberg, G.E., Thelen, K., Theiss, M.O., and Hochlehnert, B.C. (2013). The role of cell adhesion molecules for navigating axons: density matters. Mech Dev *130*, 359-372.
Sieburth, D., Ch'ng, Q., Dybbs, M., Tavazoie, M., Kennedy, S., Wang, D., Dupuy, D., Rual, J.-F., Hill, D.E., Vidal, M.*, et al.* (2005). Systematic analysis of genes required for synapse structure and function. Nature *436*, 510-517.
Stork, T., Engelen, D., Krudewig, A., Silies, M., Bainton, R.J., and Klämbt, C. (2008). Organization and Function of the Blood–Brain Barrier in Drosophila. The Journal of Neuroscience *28*, 587-597.
Togashi, H., Sakisaka, T., and Takai, Y. (2009). Cell adhesion molecules in the central nervous system. Cell Adhesion & Migration *3*, 29-35.
Valvezan, A., and Klein, P. (2012). GSK-3 and Wnt Signaling in Neurogenesis and Bipolar Disorder. Frontiers in Molecular Neuroscience *5*.
Van Itallie, C.M., and Anderson, J.M. (2006). CLAUDINS AND EPITHELIAL PARACELLULAR TRANSPORT. Annual Review of Physiology *68*, 403-429.
Van Itallie, C.M., Tietgens, A.J., Anderson, J.M., and Nusrat, A. (2017). Visualizing the dynamic coupling of claudin strands to the actin cytoskeleton through ZO-1. Molecular Biology of the Cell *28*, 524-534.
Yamagata, M., Sanes, J.R., and Weiner, J.A. (2003). Synaptic adhesion molecules. Current Opinion in Cell Biology *15*, 621-632.

Prelude to the present study

The brain is one of the most complex organs of the human body. Neurons or nerve cells are the building blocks of this amazing structure; they perform all the communication and processing functions within the brain. The neurons "talk" to each other at very specialized structural points called synapses. These synapses consist of two components; the presynapse and the postsynapse (Frotscher et al., 2014).The neuronal signal travels down in the form of an action potential generated in the presynaptic neuron and is received by the postsynaptic neuron (in case of neuron-neuron junctions) or the muscle (in case of neuromuscular junctions). To maintain proper communication at the synapse (between pre- and postsynaptic sites), the brain has evolved accessory molecules such as secretory proteins and cell adhesion molecules in addition to the basal synaptic transmission machinery.

Wnt proteins are a class of secretory molecules that are also known to enable synaptic communication through their function in both pre- and postsynaptic compartments (Oliva et al., 2013). At the presynapse, they regulate active zone formation and recycling of synaptic vesicles, and at the postsynaptic site, they maintain dendritic spine morphogenesis and postsynaptic receptors (reviewed in (Inestrosa and Varela-Nallar, 2014)) . At the *C. elegans* NMJ, the Wnt signaling pathway modulates postsynaptic acetylcholine receptor levels allowing activity-dependent synaptic plasticity (Babu et al., 2011b; Jensen et al., 2012a; Pandey et al., 2017) . Here the Wnt signaling pathway involves presynaptic Wnt/CWN-2 and it's postsynaptic receptor Frizzled/LIN-17 in the translocation of AChR/ACR-16 receptors at the *C.elegans* NMJ (Jensen et al., 2012b). Although the components of the Wnt signaling pathways and their mechanism of action have been studied in

great detail, how Wnt secretion itself is mediated by the Wnt-producing cells, is poorly understood to date. Consistent with the previous findings, we demonstrate in the current thesis work that a claudin-like molecule in *C.elegans*, HIC-1, regulates postsynaptic AChR/ACR-16 receptors by controlling Wnt secretion from the cholinergic motor neurons.

Chapter 1:
General Introduction

1.1 *C.elegans* as a model system

Caenorhabditis elegans is a free-living soil nematode. In 1965, Sydney Brenner first established *C.elegans* as a model system to study animal development and neurobiology (Brenner, 1974a). Over the years, this system has contributed immensely in the understanding of the various biological problems, which has led to remarkable discoveries such as apoptotic pathway genes (Ellis and Horvitz, 1986), RNA interference (RNAi) (Tabara et al., 1998), Ras and Notch signaling pathway genes (Fitzgerald et al., 2000), synaptic functional genes, axon pathfinding (Culotti, 1994), longevity (Lin et al., 1997), developmental timing (Liu and Thomas, 1994), nicotine dependence (Shimohama et al., 1998), animal sleep or lethargus (Cassada and Russell, 1975). Also, it was the first invertebrate used in spaceflight research (Adenle et al., 2009). Ever since its discovery as a model system, three noble prizes have been awarded for research on *C.elegans*:

(1) In 2002, Sydney Brenner, H. Robert Horvitz and John Sulston for their work on the genetics of organ development and programmed cell death,

(2) In 2006, Andrew Fire and Craig C. Mello for their discovery of RNA interference (Fire et al., 1998),

(3) In 2008, Martin Chalfie for his work on green fluorescent protein using *C.elegans* (Chalfie et al., 1994).

Some of the notable features that make *C.elegans* an attractive model system to study biological functions are:

1. Small size (1mm long) and rapid life-cycle (3 days) makes it easy for laboratory cultivation.

2. Genetically tractable (*C.elegans* was the first model system with completely sequenced genome), consists of only 100 million bases (humans: 3 billion bases), with 20000 genes (humans: 30000) and about 6000 *C.elegans* genes have human homologs (Hillier et al., 2005).

3. Anatomically simple (<1000 cells) and a well defined neural circuitry with only 302 neurons in the hermaphrodite.

4. The transparent body makes it amenable to tag endogenous proteins with fluorescent marker proteins.

5. Strains can be frozen at -80^{0}C and in liquid nitrogen. They can be recovered after a period of more than 25 years later similar to cell lines.

1.2 *C.elegans* Neuromuscular Junctions (NMJs) to study synaptic function

The NMJs use different neurotransmitters in different species like at the vertebrate NMJs, acetylcholine is the major excitatory neurotransmitter while in case of *C.elegans*, there are two kinds of NMJs; one is excitatory, uses acetylcholine and causes muscles to contract, another is inhibitory and uses GABA to relax the muscles (Wu et al., 2010). The *C.elegans* neuromuscular junction shares many characteristics with the mammalian synapses (Francis et al., 2005a), mainly one GABA and two acetylcholine receptors are functional at the NMJs (Richmond and Jorgensen, 1999a), **Figure 1.1)**). To study genes that are involved in the function of worm NMJs, a drug based behavioral assay, aldicarb assay, has been used widely (Mahoney et al., 2006b).

Aldicarb (2-methyl-2[methylthio]proprionaldehyde O-[methylcarbamoyl]-oxime) is a nematicide, which is a competitive inhibitor of acetylcholinesterase.

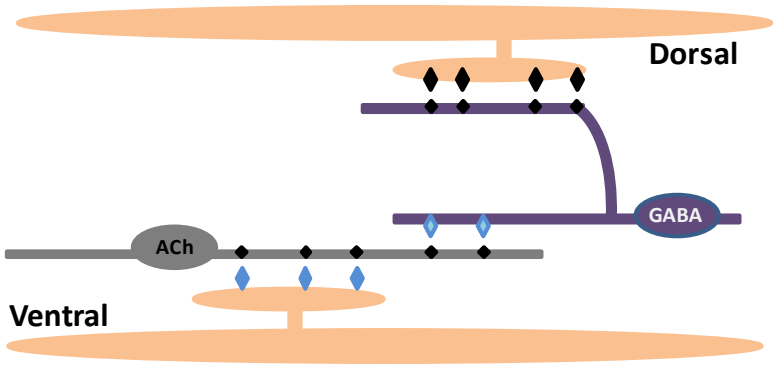

Figure 1.1 Schematic of *C.elegans* Neuromuscular junction: Acetylcholine (ACh) motor neurons present at the dorsal side of the worm make synapses with ventral muscles and with GABA motor neurons. GABA MNs present at the ventral side make synapses with dorsal muscle (image modified from (Philbrook et al., 2013)).

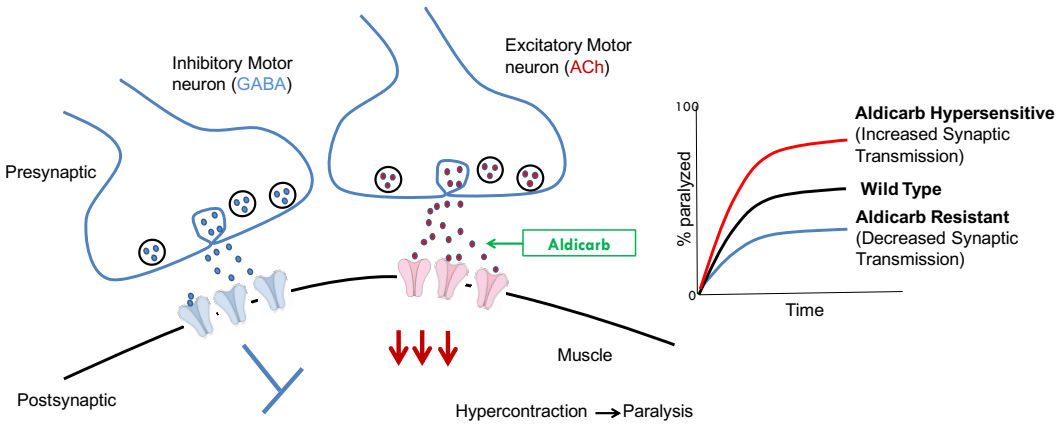

Figure 1.2 Aldicarb Assay: (A) a cartoon illustrates *C.elegans* neuromuscular junction comprises motor neurons (acetylcholine and GABA) and body-wall muscles and the activity of aldicarb drug. Aldicarb inactivates acetylcholinesterase enzyme which leads to an increased build-up acetylcholine neurotransmitter at the NMJs. (B) Possible aldicarb outcomes compared to WT (image modified from Kowalski lab research page, Butler University).

Acetylcholinesterase is responsible for the disintegration of acetylcholine; it breaks acetylcholine into acetate and choline at the synaptic cleft (**Figure 1.2A**). Aldicarb blocks the normal activity of acetylcholinesterase and hence the levels of the acetylcholine neurotransmitter build-up at the synaptic cleft, which leads to the increased activation of the postsynaptic receptors and a consequent hypercontraction of the muscles that in turn causes paralysis of the *C. elegans*. This paralysis follows a well-defined time-course in the WT worms.

Mutants that have a functional role at the *C.elegans* NMJ can be identified by their differences in paralysis pattern relative to WT animals. Mutants that disrupt the normal paralysis to aldicarb are classified as RIC (Resistant to Inhibitors of Cholinesterase) or HIC (Hypersensitive to Inhibitors of Cholinesterase) Mutants (**Figure1.2B**). The worm body–wall muscles receive excitatory signals from cholinergic motor neurons, which leads to contraction of the muscles, and inhibitory signals from GABA motor neurons that leads to relaxation of the muscles. This coordinated action of contraction and relaxation of the muscles results in the sinusoidal wave movements of the worms (Jorgensen and Nonet, 1995).

Resistance to aldicarb could be due to:

(1) Lower amounts of acetylcholine neurotransmitter release (Nonet et al., 1993) or decreased numbers of cholinergic receptors activated (Philbrook et al., 2013) .

(2) More GABA release or more GABA receptors activated (Vashlishan et al., 2008).

Whereas, hypersensitivity to aldicarb could be caused by:

(1) More acetylcholine release (Lackner et al., 1999) or more activated acetylcholine receptors at the NMJ (Babu et al., 2011b).

(2) Lower amounts of GABA release or decrease in activated GABA receptor levels (Vashlishan et al., 2008) .

1.3 Acetylcholine receptors

Acetylcholine receptors are responsible for various brain activities both in vertebrates and invertebrates. As the name suggests, all acetylcholine receptors respond to the neurotransmitter acetylcholine, but they respond to different pharmacological agents as well, depending on their subunit compositions (Jospin et al., 2009). There are two main classes of acetylcholine receptors in vertebrates:

1.3.1 Nicotinic acetylcholine receptors(*nAChRs*) –

The nAChRs are ligand-gated ion channels and are made up of five protein subunits (two α, and one each of β, δ, and ε subunits) (Albuquerque et al., 2009). They are arranged symmetrically in a barrel or cylindrical shape to make a pore lining to allow for passage of cations. The composition of the subunits varies in different tissues and organisms. They were characterized for their activation by nicotine; an active compound in tobacco. *nAChRs* are involved in wide variety of physiological processes. They are present both at the muscles and on the neurons. In the CNS, they are involved in cognition, learning and memory, arousal, reward, motor control and analgesia ((Gotti and Clementi, 2004; Jensen et al., 2005) and reviewed in (Hogg et al., 2003)). At the neuromuscular junction, binding of acetylcholine to the acetylcholine receptor causes a rapid change in the permeability of the muscle membrane towards Na^{2+} or Ca^{2+} ions which leads to depolarization and subsequent contraction of the muscle. nAChRs are responsible for fast synaptic actions (Alkondon et al., 1998). In humans, they are divided into

six subcategories based on their subunit composition and localization (Lukas et al., 1999):

- Muscle nicotinic AChRs- present at the adult neuromuscular junction and made up of α1-ε-α1-β1-δ (Mishina et al., 1986; Witzemann et al., 1987).
- Muscle nicotinic AChRs- present at the fetal extrajunctional site of NMJ and consists of α1-γ-α1-β1-δ (Raftery et al., 1980).
- Neuronal nicotinic AChRs-present in the CNS, PNS and developing muscle, made up of homopentameric subunits of α7 (Schoepfer et al., 1990).
- Neuronal and autonomic nicotinic AChRs- localized at the ganglion and consists of α3-β4-α3-β4-β4 and α3-β2- α3-β4-α5 (reviewed in (McGehee and Role, 1995)).
- Neuronal and autonomic nicotinic AChRs- expressed in the brain, consists of α4-β2-α4-β2-β2 (reviewed in(McGehee and Role, 1995)).
- Epithelial and neuronal nicotinic AChRs- expressed in the cochlear hair cells, made up of five subunits of α9 (Zuo et al., 1999).

Each subunit contains four transmembrane regions (TM1-TM4). TM2 forms the pore lining (reviewed in(Albuquerque et al., 2009)). Acetylcholine neurotransmitter binds to the N termini of two α subunits which leads to conformational changes in the all TM2 regions and hence the opening of the ion pores. The acetylcholine receptors allow Na^{+2}, K^{+2}, and Ca^{+2} ions inside the cells (reviewed in(Albuquerque et al., 2009)).

1.3.1.1 Postsynaptic Acetylcholine receptors in *C.elegans*

The *C.elegans* genome encodes a plethora of acetylcholine receptors which differ in their subunit composition and pharmacology. The genome encodes for at least 27 subunits (Jones and Sattelle, 2004). Two kinds of acetylcholine receptors are well studied at the *C.elegans* neuromuscular junctions based on electrophysiology and reconstitution studies in the heterologous systems (Richmond and Jorgensen, 1999a):

1.3.1.1.1 levamisole-sensitive acetylcholine receptor (*L-AChRs*)-

The L-AChRs are the most extensively studied subtype of acetylcholine receptors in *C.elegans.* They respond to the anthelmintic drug, levamisole. They are worm-specific and consist of five different subunits; UNC-38, UNC-29, UNC-63, LEV-8, and LEV-1 (**Figure 1.3**). Each subunit is approximately 500 amino acid long and has four domains (M1, M2, M3, and M4). Similar to other acetylcholine receptors, here too the M2 region forms the lining of the pore (Martin et al., 2012).

1.3.1.1.2 nicotine-sensitive acetylcholine receptors (*nAChRs*)-

These receptors are thought to respond to nicotine and not to levamisole, they are responsible for more than 90% of the currents mediated by acetylcholine (Touroutine et al., 2005). They are made up of homomeric ACR-16 subunits. The ACR-16 receptors are homologs of vertebrate α7 acetylcholine receptors (Touroutine, 2009) (**Figure 1.4**).

1.3.2 Muscarinic acetylcholine receptors (*mAChRs*)-

These receptors are also known as metabotropic or G-protein coupled acetylcholine receptors activated by the drug muscarine. They mainly play modulatory acetylcholine functions in the CNS and are involved in cognition, memory and

motor control (Chan et al., 2013). GAR-3 is an example of a Muscarinic acetylcholine receptor present on the extrasynaptic site in *C.elegans* neurons which allows for cholinergic signaling during acetylcholine spillover from a distant source or neuron (Chan et al., 2013).

2. Cell adhesion molecules in the nervous system

A number of studies in the last decade have identified the role of Cell adhesion molecules (CAMs) in the functioning of synapses (reviewed in (Abbas, 2003; Tallafuss et al., 2010; Wu et al., 2010; Yamagata et al., 2003b)). Apart from reports on the function of CAMs in maintaining cell-cell and cell-extracellular matrix contacts (reviewed in (Albelda, 1991)), there are various modes by which CAMs could function at the synapse; they could function in target recognition such as SYG-1 and sidekicks among other molecules (Shen and Bargmann, 2003; Yamagata et al., 2002), formation and alignment of synaptic specializations such as SynCAMs, neurexins and neuroligins (Biederer et al., 2002; Hu et al., 2012), regulation of synaptic structure and function such as Cadherins and Syndecan (reviewed in (Couchman, 2003)) as well as the regulation of activity dependent synaptic plasticity such as *rig-3* which prevents synaptic potentiation by regulating Wnt signaling (Babu et al., 2011b; Pandey, 2017). Claudins are a subset of CAMs whose function at the synapse remains largely unknown.

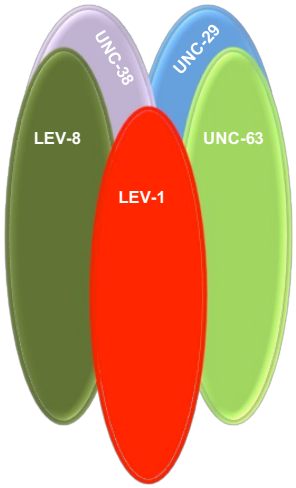

Figure 1.3 Levamisole-sensitive acetylcholine receptor: Consists of heteromeric subunits UNC-29, UNC-63, UNC-38, LEV-1, and LEV-8.

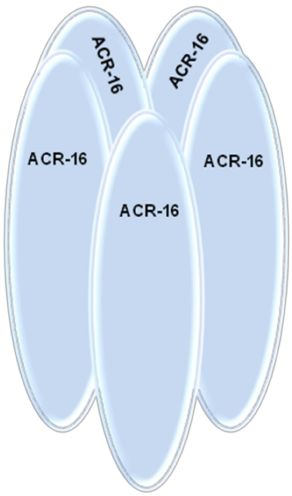

Figure 1.4 Nicotine-sensitive acetylcholine receptor: Consists of homomeric subunits of ACR-16.

3. Claudins

3.1 Claudin Superfamily of proteins

Claudins are four transmembrane domain proteins and are important structural and functional components of tight junctions (**Figure 1.5**). They are known to maintain epithelial and endothelial tissue integrity and barrier functions (reviewed in (Tsukita and Furuse, 2000). The tetraspan superfamily of claudins belongs to PMP22/EMP/MP20/claudin class (PFAM family 00822) (Van Itallie and Anderson, 2006). Claudins are conserved structurally but are highly divergent at the sequence level (reviewed in (Krause et al., 2008b)). There are 24 gene families of claudins in mammals, which exhibit a complex tissue-specific pattern of expression and function. Differential expression and function of the claudins in mammals has been reported in many tissues including intestine, kidney, gall bladder, inner ear, retina, prostate glands, brain, etc. (reviewed in (Krause et al., 2008a)). Apart from canonical roles of claudins in maintaining barrier functions, they also play diverse noncanonical functions in cell signaling. They regulate cell proliferation, differentiation and gene expression in different cell types such as differentiation of bone cells osteoclasts and osteoblasts (reviewed in (Alshbool and Mohan, 2014)). Although, there are no typical tight junction structures reported in invertebrates, the components required for making TJs such as claudin proteins are expressed widely in invertebrates as well. A claudin-like molecule called sinuous in *drosophila* is required to maintain septate junctions. The septate junctions are considered to be equivalent to the vertebrate tight junctions in terms of maintaining barrier and paracellular permeability functions in the epithelium (Wu et al., 2004). In *C. elegans*, 18 claudin and claudin-like molecules are thought to be present, including

CLC-1, CLC-2, CLC-3 and CLC-4 that show structural similarity to vertebrate claudins. (Reviewed in (Cox and Hardin, 2004; Cox et al., 2004) and wormbase). These claudins function to regulate channel activity, intercellular signaling, and cell morphology. CLC-1 is expressed in the epithelial cell junctions in the pharynx and regulates barrier function while CLC-2 is expressed in the seam cells of the hypodermis where it maintains hypodermis barrier functions (Asano et al., 2003a). The functions of the remaining CLC proteins are as yet unknown. VAB-9, a divergent claudin-like protein most similar to vertebrate BCMP1 (brain cell membrane protein 1) localizes to epithelial cell contacts and interacts with the cadherin-catenin complex during epidermal morphogenesis (Simske et al., 2003). Together, the diversified expression and the function of the claudin superfamily of proteins suggests that their involvement in maintaining homeostasis in different tissues is far beyond than being just tight junction protein at the epithelium.

3.2 Role of claudins in the nervous system

A growing body of evidence suggests functional roles for claudins in the brain. These proteins have been shown to be essentials component of the blood-brain - barrier. The deregulation of claudins is associated with various brain disorders such as Alzheimer's disease, multiple sclerosis, diabetic retinopathy and retinopathy of prematurity (reviewed in (Goncalves et al., 2013)). The Blood-Brain Barrier (BBB) helps protect a delicate, intricate network of neurons from noxious blood-borne or surrounding stimuli. Claudins-1,3,5,11,12,19, occludin, Zona occludens-1(ZO-1), and tricellulin have been identified as key proteins in making neural barriers (Reinhold and Rittner, 2016). Claudin-5 positive leukocytes have been detected in

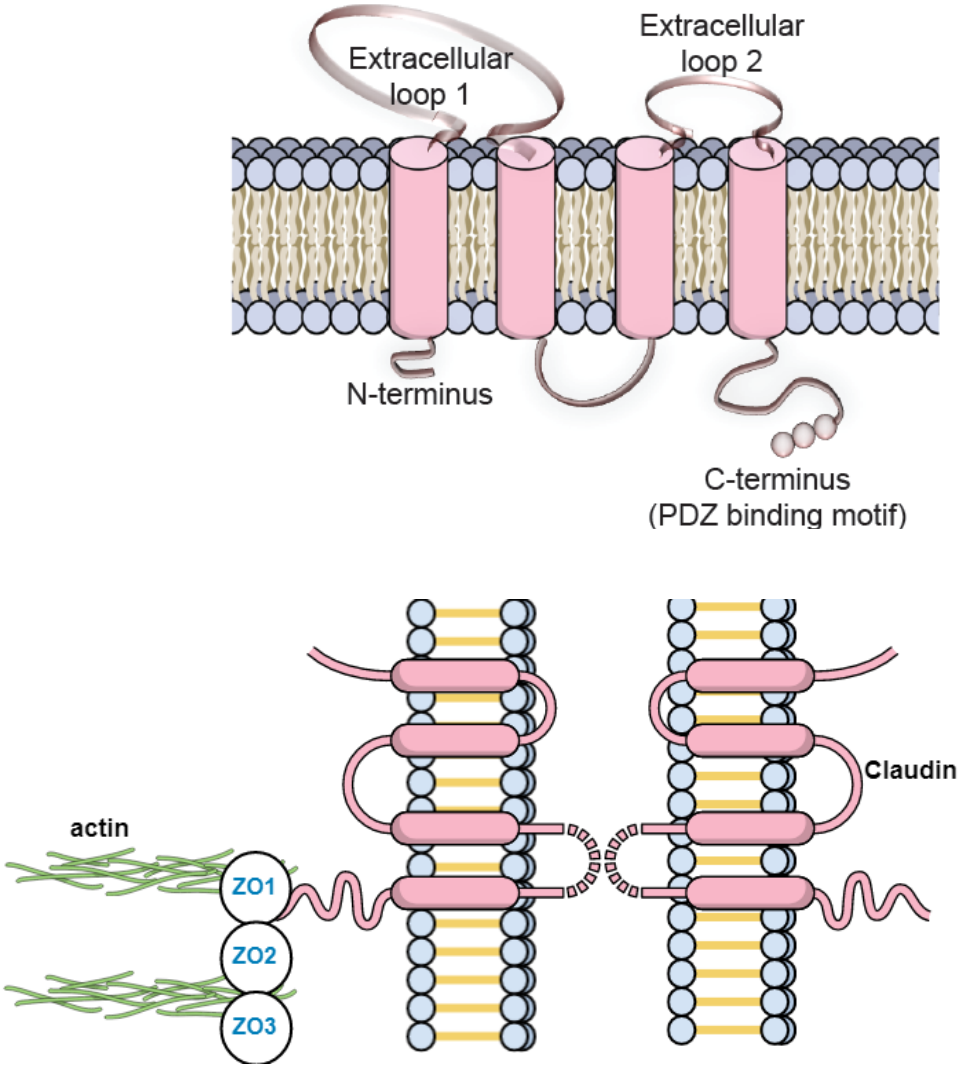

Figure 1.5 Structure of Claudins: The cartoon in the upper panel shows the different domains of Claudins; Claudins are four transmembrane domain-containing proteins with both their N and C terminus present inside the cell, they possess two highly conserved extracellular loops. The lower panel depicts intracellular interactions of Claudins with the actin cytoskeleton via scaffold proteins ZO-1, ZO-2, and ZO-3(image modified from (Aktories and Barbieri, 2005)).

the brain during neuroinflammation (Paul et al., 2016). Furthermore, it has been shown that claudin-5 in the central nervous system regulates both paracellular ionic selectivity and tumor cell motility across the BBB. Hence, mutants in claudin-5 are involved in the brain tumor metastasis (Jia et al., 2014). Moreover, activation of matrix metalloproteinases (MMPs) regulates the BBB by degrading the tight junction proteins claudins-5 and occludin (Yang and Rosenberg, 2011).

Claudin-11 is thought to regulate magnesium ion permeability across the myelin sheath membrane, which is crucial for maintaining brain homeostasis.

More recently researchers have started to investigate the function of claudin proteins in the nervous system of invertebrate organisms. Out of six claudin-like molecules found in the *drosophila*, two have been reported to be essential to make septate junctions to allow for maintaining blood-brain barrier integrity in the fly brain. (Stork et al., 2008). Claudin-5a in *zebrafish* is required for the brain ventricle morphogenesis where it establishes neuroepithelial-ventricular barriers which maintain the hydrostatic pressure within the ventricular cavity (Zhang et al., 2012) and reviewed in (Abdelilah-Seyfried, 2010)). NSY-4, a claudin-like protein in *C.elegans* is required for the stochastic activation of AWC ($^{on/off}$) asymmetric olfactory neurons. In each worm, one AWC neuron is activated or ON at any given time, while the other remains inactivated or OFF. NSY-4 coordinates lateral signaling between the AWC neurons which allows them to be either ON or OFF (Hsieh et al., 2014). Another claudin superfamily member, STG-1 in *C.elegans* acts as an obligate auxiliary subunit or TARPs (transmembrane AMPA receptor regulatory proteins) for AMPA receptors and is required for glutamate-mediated currents. Further, the STG-1 function as a TARP protein for AMPA receptor has

been shown to be conserved across species (Walker et al., 2006; Wang et al., 2008b). A claudin-like molecule HPO-30 in *C.elegans* is required for maintaining dendrite morphology (Smith et al., 2013) and for the stability or trafficking of a subtype-specific levamisole-sensitive acetylcholine receptor at the NMJ (Sharma et al., 2018). The above examples bring home the point that claudins play essential roles in the nervous system. However, how they might be performing their function in the brain or at the synapse and their mechanism of action remains largely unexplored. The current thesis work shows that HIC-1, a claudin-like molecule in *C.elegans*, is functioning at the synapses through its interaction with an actin-binding protein, Neurabin which it directly interacts with via its PDZ binding motif.

3.3 PDZ binding motif of claudins

Based on sequence similarity, claudin superfamily proteins have been divided into two groups in humans: classical (1-10,14,15,17,19) and nonclassical claudins (11-13,16,18,20-24). The tetraspan claudin proteins have two extracellular loops. The first large extracellular loop is required for specific ion permeability and for making a paracellular barrier and the second shorter extracellular loop is thought to be involved in the holding function between the apposing cell membranes and making homo/heterophilic interactions. Further, most claudins possess a PDZ binding motif at their C-terminus tail by which they interact to PDZ domain-containing scaffolding proteins such as ZOs, PATJ, and MUPP1, which in turn act as an adaptor that links claudins to the actin cytoskeleton in epithelial cells (reviewed in(Gunzel and Yu, 2013). The PDZ-binding motif, for example -K/R/H-X-Y-V is present mostly at -3,-2,-1, 0 positions at the C-terminal tail of the claudins. The –Y-V motif at the C-

terminal positions -1 and 0 shows high conservation in the classic claudins in comparison to the large variations in the non-classic claudins (H/S/Y/D/E/R-V/L). It is thought that because of conserved –Y-V motif in the classic claudins, they bind to the PDZ1 domain of ZO-1 in the epithelium (reviewed in(Krause et al., 2008a)).

4. Neurabin, an actin-binding protein

Neurabin (neural tissue-specific F-actin binding protein) was purified from rat brain and was shown to be expressed specifically in neural tissues (Nakanishi et al., 1997b). The localization and function of neurabin appear to be conserved across the species (Oliver et al., 2002). Neurabin localizes at synapses, specifically at the periactive zone (adjacent to active zone) of synapses (Sieburth et al., 2005a) and at the growth cone in developing neurons (Nakanishi et al., 1997b). Neurabin is a multidomain protein with an F-actin-binding domain at the N-terminus, a PSD-95 domain, a DlgA domain, a ZO-1 like domain present in the middle of the protein (for interact with transmembrane proteins), and a domain predicted to form coiled-coil structures at the C-terminus (Nakanishi et al., 1997b). Neurabin binds to F-actin at the synapse and shows cross-linking activity. Cyclin-dependent kinase (CDK)-5 is a key regulator of neuronal actin remodeling and is involved in different processes mediated by rapid turnover of the actin cytoskeleton (Shah and Rossie, 2017). Neurabin has been found to be one of the substrates for the cdk5 kinase and hence is a key player in pathways associated with actin remodelings such as axon pathfinding, LTP, LTD, etc. (Shah and Rossie, 2017). Due to its multidomain structure, neurabin could interact with many different synaptic proteins strongly or transiently; Neurabin interacts with Rho-specific GEFs through its coiled-coil

domain to regulate dendritic spine morphology (Ryan et al., 2005), and through its PDZ domain, it interacts with a mitogen-activated protein kinase p70 S6($p70S^{6k}$) which plays a central role in mRNA translation (Burnett et al., 1998), and a SAD-1 kinase to maintain neuronal polarity in *C.elegans* (Hung et al., 2007). Neurabin acts as an adaptor or scaffolding protein for cell adhesion molecules and helps connect them to the actin cytoskeleton (Chia et al., 2013). Previous studies on the *C.elegans* HSN neurons have shown that the specificity determining cell adhesion molecules, SYG-1 and SYG-2 (Shen and Bargmann, 2003), locally assemble F-actin in HSN neurons and NAB-1/Neurabin then binds to F-actin and goes on to recruit the active zone proteins SYD-1 and SYD-2 (Chia et al., 2012a). Neurabin has been studied in diverse neuronal insults including in anxiety-like behavior (Kim et al., 2011), as an anti-seizure molecule (Chen et al., 2012), as a neuroprotective molecule (Cattabeni, 2012), and in glioblastoma (Cheerathodi et al., 2016).

The findings from the current thesis work have revealed that HIC-1 directly interacts with Neurabin via its PDZ binding motif, i.e. Neurabin acts as an adaptor protein to link HIC-1 to the actin cytoskeleton.

5. Wnt signaling and secretion

The Wingless- type (Wnt) family of secretory proteins are highly conserved across the metazoans. The First Wnt mutant with glazed eyes were discovered in *Drosophila* in 1936 by Thomas Hunt Morgan (Morgan, 1936). After this a lot of work has been done in understanding the function of Wnts by developmental biologists who have studied the role of Wnt in embryogenesis, cell fate determination and cell proliferation (reviewed in (Cadigan and Nusse, 1997)). More

recent studies have brought to light the function of Wnts in the brain, where they are involved in various aspects of development (Inestrosa and Arenas, 2010; Inestrosa and Varela-Nallar, 2014; Oliva et al., 2013). Wnts have been implicated in regulating neurogenesis (Hawkins et al., 2005; Valvezan and Klein, 2012), axon guidance or polarity (Chien et al., 2015; Hilliard and Bargmann, 2006; Pan et al., 2006), neural circuit development (Fradkin, 2005), neuromuscular junction development (Barik et al., 2014a; Henriquez et al., 2008b; Klassen and Shen, 2007a; Koles and Budnik, 2012b) and plasticity (Babu et al., 2011a; Dickins and Salinas, 2013; Jensen et al., 2012b) among other functions in the nervous system.

Although a lot of work has been done to delineate various Wnts and their molecular pathways, only a few studies have looked at Wnt ligand secretion from the Wnt producing cells (Inestrosa et al., 2007; Koles and Budnik, 2012a; Langton et al., 2016; Pan et al., 2008; Yang et al., 2008). Since deregulated Wnt secretion is implicated in various forms of cancers (reviewed in (Zhan et al., 2017) and (Wang et al., 2016a)) and inflammatory disorders (Inestrosa and Varela-Nallar, 2014), more studies are needed to fully understand how Wnt secretion is regulated at every step for developing better therapeutic interventions to circumvent these illnesses.

This thesis delineates a signaling pathway at the *C.elegans* NMJ, where a presynaptic claudin-like protein, HIC-1 is involved in regulating Wnt secretion through it's role in maintaining the actin cytoskeleton in motor neurons.

Chapter 2:

Materials and Methods

2.1 Genetic Work

2.1.1 Mutant Strains:

All strains were maintained on Nematode Growth Medium (NGM) plates seeded with OP50 *Escherichia coli* at 20°C under standard conditions (Brenner, 1974b). The *C. elegans* Bristol strain N2 was used as the WT control. Mutant strains used were: *hic-1* (*ok3475*), *mig-14* (*ga62), lin-17* (*e1456*), *acr-16* (*ok789*), and *nab-1(ok943);* all of which are available from CGC. A brief description of all the mutants used in the study is listed here.

Table1. Description of mutant strains used in the study:

Genotype	Strain name and allele description	Source
hic-1(ok3475) X	RB2512 *ok3457* is a deletion allele; the deletion is 381 bp of the *hic-1* gene that is 656 base pairs long.	CGC
nab-1(ok943) I	RB1017 WT PCR product of neurabin gene is 3254 base pair long. Deletion allele *ok943* deletes 1032 base pairs of the gene.	CGC
acr-16(ok789) V	RB918 WT PCR Product is 3196 bp. Estimated deletion size 1100 bp.	CGC

mig-14(mu71) II	CF367 A small protrusion can be seen near the vulva in the mutants. The animals make extra turns. Mild Egl.	CGC
lin-17(n671) I	MT1306 Slightly unc. Long irregularly shaped tail. Many hermaphrodites (50%) have a small protrusion posterior to the vulva, some gonadal abnormality, and sterility.	CGC

2.1.2 Genetic crosses:

C.elegans genome consists of six chromosomes (Brenner, 1974b); four autosomes, and two sex chromosomes ((Hermaphrodite (XX) and male (XO)). Since the frequency of males present in the growth plates are so rare (~0.002 percent of the total population), the males are produced/maintained either by mating with hermaphrodites or by simulating a nondisjunction event by giving heat shock at 30^0C for 60 mins (reviewed in (Anderson et al., 2010)).

The mating is set on a plate with minimal OP50 seeding (~ 10µl) just in the middle of the NGM plate to increase the chances of the mating process. Around 8-10 males and 2-3 hermaphrodites are picked for a cross. All the mutant strains were outcrossed with WT worms at least 4X times to get rid of any background mutation before beginning any experiment.

2.1.3 Single worm PCR and genotyping:

To know the genetic background of a worm, PCR based genotyping is performed after worm lysis (Zwaal et al., 1993).

The lysis buffer is made from 100µl of 1X Phusion buffer by adding 2.5µl of proteinaseK. The single adult worm is picked and placed in a PCR tube containing lysis buffer. The worm lysis is performed at 60^0 C for 60 mins followed by 15mins incubation at 95^0C to inactivate the proteinaseK activity in a thermal cycler.

After worm lysis, the lysate is subjected to PCR reaction.

2.2 Generation of transgenics

2.2.1 *C. elegans* genomic DNA isolation:

Worms were grown on OP50 plates until the food was depleted. Worms were washed from the plates using M9 buffer and transferred to 1ml Eppendorf tubes. Worms were successively (3-4 times) washed using an M9 buffer by gently pelleting them at low spin, throwing the supernatant and resuspending the worm pellet in the fresh M9 buffer. Washing with M9 buffer facilitated complete removal of bacteria.

The worm pellet was finally suspended in 500 µl of worm Lysis solution (100mM Tris pH 8.5, 100mM NaCl, 50mM EDTA, 1% SDS, and proteinase K 100µg/ml). Worms suspended in lysis solution were incubated at 60^0C for 90 minutes. RNaseA (20µg/ml) was then added and the tube was incubated at 37^0C for 30 minutes. The tube was spun in a microfuge and the supernatant transferred to new tube and an equal volume of Phenol: Chloroform was added. It was gently mixed which was followed by centrifugation at 13000 rpm for 3 minutes. The aqueous phase obtained was extracted. To this extract 2.5 volumes of absolute ethanol was added. Whole mixture was spun at 13000 rpm for 15 minutes. The pellet was

washed with 70% ethanol to remove salt. The pellet was then re-suspended in 100µl TE buffer and was stored at -20^{0}C.

2.2.2 *C. elegans* RNA isolation:

Worms were grown on OP50 plates for a mixed-stage population. Worms were washed from the plates using M9 buffer in an RNase-free Eppendorf tube and were pelleted by spinning briefly at 14,000 rpm. Supernatant was removed leaving 100µl of solution on top of the sample. In the hood, 400 µL of Trizol reagent was added followed by vortexing for about 2 minutes. Samples were freeze-thawed thrice in liquid nitrogen. Again, 200 µL of Trizol reagent was added and samples were allowed to sit at room temperature for 5 minutes. To this 140µl of chloroform was added followed by vigorous shaking for 15 seconds. Samples were incubated at room temperature for 2 minutes. Further, samples were centrifuged at 12,000xG for 15 minutes in the cold room (4°C). The aqueous phase was transferred to a new 1.5 ml tube and slowly an equal volume of 70% EtOH was added. The mixture was taken in a Qiagen RNeasy spin column. Samples were spun at maximum speed for 15 seconds. This was followed by washing with 700µl of buffer RW1 and 500µl of buffer RPE (twice). Every time centrifugation was done at maximum speed for 15 seconds. After the final wash, columns were transferred to a new 1.5 ml tube, and RNA was eluted in 50µl of RNase-free water.

2.2.3 Molecular Cloning:

Standard restriction digestion or PCR based cloning was performed for all the experiments in this study (Russell, 2001). cDNA or genomic DNA were amplified using either Phusion enzyme (NEB)or PCR master mix from Takara.

The vectors used in this study are pPD49.26, pPD95.25 and PCFJ910, all obtained from addgene. A detailed description of all the constructs generated for the study and their respective oligos are mentioned here:

2.2.3.1 Primers and constructs:

1. pBAB# 0101: P*hic-1*::mCherry

VT156 (*PstI*) AAAACTGCAGcctgcggagatatggagtctcaaagacaagg

VT86 (*BamHI*) CGCGGATCCcatggtttggtggagtttgg

2.4 Kb upstream of the *hic-1* gene was amplified and cloned into pPD49.26 vector containing mCherry.

2. pBAB# 0102: P*hic-1*::HIC-1::mCherry

VT111 (*PstI*) AACTGCAGggcgttttaggctttcagaa

VT112 (*BamHI*) CGCGGATCCcattgcaggtatgacaagaagac

A 3.1kb of the whole genomic region of *hic-1* (Promoter and gene) were amplified and cloned upstream to mcherry in the pPD49.26 vector.

3. pBAB# 0103: P*rab-3*::HIC-1

VT48 (*XhoI*) CCGCTCGAGcggatgcatcatcatcaccatcacgcacc

VT49 *(BglII*) GAAGATCTTCttatcggtattccgagtatgctccatatccagtt

VT149 (*AgeI)* CTCTCTACCGGTcttcagatgggagcagtggac

VT150 (*SbfI)* CTCTCTCCTGCAGGgcctgctttttgtacaaacttgtcatct

The genomic region of *hic-1* was cloned in the pCFJ910 vector under *XhoI* and *BglII* sites. The promoter of *rab-3* was cloned upstream to HIC-1 using *AgeI* and S*bfI* sites.

4. pBAB# 0104: P*let-413*::HIC-1

VT119 (*AflII*) AGACTTAAGccttggtagcagcacagcag

VT120 (*XhoI*) CCGCTCGAGcggccatcttctgcttcttcttctcc

The promoter of *let-413* was amplified from *C. elegans* genomic DNA and cloned into the PCFJ910 vector using *AflII* and *XhoI* restriction sites to drive the expression of HIC-1 in the epithelial tissue.

5. pBAB# 0105: P*myo-3*::HIC-1

DM11 (*BamHI*) CGCGGATCCatgcatcatcatcaccatcacgc

DM12 *(NheI*) CTAGCTAGCgacgaattcaactgagcttgtacaattgtc

DM13 (*XbaI*) CTAGTCTAGAggctgcaacaaagatcagg

DM14 (*BamHI*) CGCGGATCCggagaacaatggtaaagcgtgg

The cDNA and the 3'UTR of HIC-1 was cloned in pPD49.26 vector in *BamHI* and *NheI* restriction sites. The *myo-3* promoter was amplified from the PCF104 vector and cloned upstream to HIC-1.

6. pBAB# 0106: P*unc-17*::HIC-1

DM09 (*SbfI*) CTCTCTCCTGCAGGgtcgaccatgacaaagtggtgacac

DM10 (*BamHI*) CGCGGATCCgactccaccgagttaccttaaaaaattgc

The *unc-17* promoter was cloned upstream to HIC-1 in pPD49.26 vector using *SbfI* and *BamHI* restriction sites to drive expression in the cholinergic neurons.

7. pBAB# 0107: P*unc-25*::HIC-1

VT245 (*SbfI*) CCTGCAGGccgacttaagggtcaaaagccg

VT246 (*BamHI*) CGCGGATCCagcaactacacaactgagccacc

P*unc-17* was replaced with the *unc-25* promoter in pBAB#106 plasmid by using the same restriction sites.

8. pBAB# 0108: P*unc-17*::HIC-1ΔC(4aa)

DM11 (*BamHI*) CGCGGATCCatgcatcatcatcaccatcacgc

VT182 (*NheI*) CTAGCTAGCttagtatgctccatatccagttgcacttcc

The cDNA of HIC-1 was amplified without the last 12 nucleotide bases encoding four amino acids (Putative PDZ binding motif) and cloned into pBAB# 0106 by replacing the full-length HIC-1 gene.

9. pBAB# 0109: P*unc-17*::CWN-2::mCherry

VT 239 (*SphI*) CATGCATGCgtcgaccatgacaaagtggtgacac

VT 240 (*AvrII*) CTCTCTCCTAGGgactccaccgagttaccttaaaaaattgc

VT 241(*AvrII)* CTCTCTCCTAGGatgattccacggagaagttgttggc

VT242(*BamHI*) CGCGGATCCtttacaaatatccacttgtgtcacattattgcaagtttgacataccac

The cDNA of the CWN-2 gene was cloned under *AvrII* and *BamHI* sites in the pPD49.26 vector containing mCherry. The *unc-17* promoter was cloned upstream to it using *SphI* and *AvrII* sites to drive the expression of CWN-2 in cholinergic motor neurons.

<u>Sequences and constructs for the BiFC experiments:</u>

10.pBAB# 0110: P*unc-17*::NAB-1::Linker::VN173

ATGACAACGGCTTCCGAGCTGCTGTCAGACGACGCAAGAGCTCGATTCTCACATAC
AAAGGCTCTTTTTGAGCAGCTTGAGAGACAGCAAGACGTTCCATCATTCTACTCTCC
ACGTCTTCAACGTCAACCACCACCTCCATTACCCCCAAAACCTCCATCTCAATGTCC
GCCGAGTCCGATGTCACAGGTCGAACGAAATTTCTCTGATTTGGCCGCGGATCTCGA
TCGGATCCAATCATCGCCGGCAACGTCTAGGTTTATACAAAATAAATCATCAACTCT
TCCGTCATCATATTCCGATTCCACACAGCAGTATTCGTTCGAAAATACGGTTGCCAC
GTCGCAATATGGAGGACTTCAAACCAACAACAATAATAATAATATTAATATGAATT
CATTTGAACCCTATTGGAGAAATGGATCAATATATCGGAGGCAATTCGAAGGAAAT

GGCAAACCTTTTGGCGAGGAAAACGATGGAATCTCACCAACGACGAATGGAGTGAA
GCACACGACATACGCCGTCGTCAAAACACCAAAGGAAACAGAACTTGAAACAACAT
CAGAAAACAGAGGACTCATGGAAACACGGAGGGGTCTGAGTCCAGAGAGGCCTGA
CGTGGATTTAACGAATCGAAAGGTCTCGTTCAGCACTGCACCTATTCCGGTCTTCTC
GGCGTTTTCCGTTGAAGACTACGATCGCAAGAATGAAGACATTGATCCGGTGGCAA
GTTGTGCTGAATATGAATTGGAGAGACGACTTGAAAGAATGGATTTGTTTGAAGTTG
ATTTGGAAAAGGGTGCCGAGGGACTTGGAGTCTCTATTATTGGTATGGGTGTTGGTG
CAGACTCGGGTCTTGAAAAGCTGGGAATCTTTGTAAAGAGCATCACACCTGGCGGA
GCTGTTCATCGAGATGGACGAATTCGTGTCTGCGATCAAATTGTTTCAGTCGATGGA
AAGAGTTTGGTCGGTGTCTCACAGTTGTATGCTGCAAACACGTTGAGATCCACCAGC
AATCGAGTCACTTTCACAATTGGTCGCGAACAAAACCTTGAAGAATCCGAAGTTGCT
CAGCTAATTCAACAAAGTCTTGAACACGACAGAATGAGAATGATGGGAGACGAGGA
AGACGATATCGAAGAGCCGCCACCACCACCATCTCAAATGCCACAGCTACCAATTG
AACAGGATCGTCCGACAACTTCAATGATCACAAAAGAAGAAATTGAGATTCGTTCG
AAGATTGCTGCTCTTGAACTGGAACTTGATGTTACTCATAAGAAAGCAGAGCAATAT
CATGAAGTGTTGAGCTCAACGAAATCACATTGTGATCAACTGGAAAAGCAGAATGA
GCAGGCAAATTATATGATTAAAAACTATCAGGAAAGAGAAAAAGAGTTGTTGAATC
GAGAAGAGAATCATGTGGAACAATTGAGAGATAAGGATGTACATTATGCATCATTA
GTTCGTCAATTGAAAGAACGAATTGATGAGTTGGAATCGAAATTGGAAGAAGCTGA
AGAGAGAAGGCATTCTATTCAGAATCTTGAGCTTATCGAGTTGAGAGAGAAGTTAA
AGGAGAAAGTTGAGAAGAGGAATGAAGGAATGGCGTATAGACCAGGTGGAGAGCT
TCCTCACGAGGATAAGGCTGTTATGGTTAATTTGGAGACTATTACTCCATCAACCAA
AAAAGATGCGGAAGTATCAGTTGGAAGTAGTTGGACAGAAGAGTACTCATCACCAT
GCGAGTCGCCAGTCCCTCGTATCTCCGAGCCAGCATCTCCGGCTCTTCCACATAAAT
TGACGCATCGCAAACTTCTGTTCCCACTCCGAAAGAAGTACGCCGAAAACGAGTTCT
GGCGTGCCACGTGTCAACCAGTTGGTCTTCAAGCTCTTCATTGGACGGTGGACGATG
TTTGTCAGTTGCTCGTTTCAATGGGCTTGGACAAATATGTGCCAGAGTTCACCATTA
ATAAGATCGATGGAGCCAAGTTCCTCGAGCTCGACGGAAATAAACTGAAGGCAATG

GGAATTCAAAATCACTCGGATCGTTCTCTAATTAAAAAGAAAGTAAAAGGAATGAA
GAATAAAATTGAAAGAGAACGAAAACAGTTGGAACGAGAAAGCCGTACCCGAGTC
ATTGCACACACAATTCCCATGcgcccggcgtgcaaaattccgaacgatctgaaacagaaagtgatgaaccatGTGA
GCAAGGGCGAGGAGCTGTTCACCGGGGTGGTGCCCATCCTGGTCGAGCTGGACGGC
GACGTAAACGGCCACAAGTTCAGCGTGTCCGGCGAGGGCGAGGGCGATGCCACCTA
CGGCAAGCTGACCCTGAAGCTGATCTGCACCACCGGCAAGCTGCCCGTGCCCTGGC
CCACCCTCGTGACCACCCTGGGCTACGGCCTGCAGTGCTTCGCCCGCTACCCCGACC
ACATGAAGCAGCACGACTTCTTCAAGTCCGCCATGCCCGAAGGCTACGTCCAGGAG
CGCACCATCTTCTTCAAGGACGACGGCAACTACAAGACCCGCGCCGAGGTGAAGTT
CGAGGGCGACACCCTGGTGAACCGCATCGAGCTGAAGGGCATCGACTTCAAGGAGG
ACGGCAACATCCTGGGGCACAGCTGGAGTACAACTACAACAGCCACAACGTCTATA
TCACCGCCGACAAGCAGAAGAACGGCATCAAGGCCAACTTCAAGATCCGCCACAAC
ATCGAGTGA

The sequence shown above is for a construct where the Neurabin gene (black) and VN173 fragment of YFP gene (green) are separated by a linker sequence (red). The linker sequence was incorporated using the primers VT188 and VT189.

VT199 (*SbfI*) NAB-1 Forward

CCTGCAGGatgacaacggcttccgagctgc

VT188Linker-NAB-1Reverse

ATGGTTCATCACTTTCTGTTTCAGATCGTTCGGAATTTTGCACGCCGGG
CGCATGGGAATTGTGTGTGCAATGACTCGGG

VT189LinkerForwardVN173

CGCCCGGCGTGCAAAATTCCGAACGATCTGAAACAGAAAGTGATGAAC
CATGTGAGCAAGGGCGAGGAGC

VT190(*KpnI*)VN173Reverse

GGGGTACCTCACTCGATGTTGTGGCGGATCTTGAAGTTGGC

11. pBAB# 0111: P*unc-17*::HIC-1::Linker::VC155

ATGCATCATCATCACCATCACGCACCATTCGCCATTGCTGGCCTTCTGATTATTGTT
ACAATACTAACCGGAGTGGGAACTTTTACAAATTATTGGGGTGTTTCTGGAAACTT
GCACATGGGAATTTATCAATGGGGACAGGCAGGCGCGAACAGAAGTTTCCAAAGA
AGTGCGGGGTGGCTGCAATGTGTCGTGGTTTGTCAATTAATGGCATTCTCATTTGAG
CTCTTGTTTTGTCTTCTTGTCATACCTGCAATAGTTTTCCGAAGAATGATGCCGGTTC
ATGCAGCGTGTACTCTTCTCTCCTTGATCATATTCATTTTACTTCTTATTTCCATCAT
TGTATTCGCGGCAAATATTGGAAGCTTCTATTACAACGCATTGATTTCGTTAAAGCT
CGGATGGTCATGGGGAATCACTTTGGCTGCTACAATTCTTTCATTTCTTTTACTACT
AGTATCTGGAAGTGCAACTGGATATGGAGCATACTCGGAATACCGAcgcccggcgtgcaaa
attccgaacgatctgaaacagaaagtgatgaaccatCAGAAGAACGGCATCAAGGCCAACTTCAAGATC
CGCCACAACATCGAGGACGGCGGCGTGCAGCTCGCCGACCACTACCAGCAGAACA
CCCCCATCGGCGACGGCCCCGTGCTGCTGCCCGACAACCACTACCTGAGCTACCAG
TCCAAACTGAGCAAAGACCCAACGAGAAGCGCGATCACATGGTCCTGCTGGAGTT
CGTGACCGCCGCCGGGATCACTCTCGGCATGGACGAG CTGTACAAGTAA

The sequences shown above is for a construct where the HIC-1 gene (black) and VC155 fragment of YFP gene (green) is separated by a linker sequence (red). The linker sequence was added in the primers VT184 and VT185 as highlighted below.

VT183 *(BamHI*) HIC-1 Forward

CGCGGATCCATGCATCATCATCACCATCACGCACC

VT184HIC-1LinkerReverse

ATGGTTCATCACTTTCTGTTTCAGATCGTTCGGAATTTTGCACGCCGGG
CGTCGGTATTCCGAGTATGCTCCATATCC

VT185LinkerVC155Forward

CGCCCGGCGTGCAAAATTCCGAACGATCTGAAACAGAAAGTGATGAAC
CATCAGAAGAACGGCATCAAGGCC

VT186 (*NheI*) VC155 Reverse

CTAGCTAGCTTACTTGTACAGCTCGTCCATGCCG

12. pBAB# 0112: *Punc-17*:: HIC-1ΔC(4aa)::Linker::VC155

VT183(*BamHI)*HIC-1Forward

CGCGGATCCATGCATCATCATCACCATCACGCACC

VT200LinkerHIC-1ΔC(4aa)Reverse

ATGGTTCATCACTTTCTGTTTCAGATCGTTCGGAATTTTGCACGCCGGG

CG GTATGCTCCATATCCAGTTGC

The cDNA of HIC-1 was replaced with HIC-1ΔC (4aa) using the same enzymatic sites used for cloning HIC-1 in pBAB# 0111.

13. pBAB# 0113: P*unc-17*:: GFP-UtrCH

VT233 (*BamHI*) CGCGGATCCATGGTGAGCAAGGGCGAGGAG

VT234 (*NheI*) CTAGCTAGCTTAGTCTATGGTGACTTGCTGAGG

The GFP-UtrCH sequence was amplified from plasmid #26740 (addgene) and cloned into pBAB# 0105 by replacing HIC-1 using *BamHI* and *NheI* sites.

14. pBAB# 0114: P*unc-25*:: GFP-UtrCH

VT245 (*SbfI*) CCTGCAGGCCGACTTAAGGGTCAAAAGCCG

VT246 (*BamHI*) CGCGGATCCAGCAACTACACAACTGAGCCACC

Promoter of *unc-25* was replaced with *unc-17* promoter in pBAB# 0113 using *SbfI* and *BamHI* sites.

15. pBAB# 0115: P*hic-1*::HIC-1ΔC(4aa)::mCherry

VT255 (*PstI*) AAAACTGCAGcctgcggagatatggagtctcaaagacaagg

VT256 (*BamHI*) CGCGGATCCttagtatgctccatatccagttgcacttcc

The HIC-1 gene was replaced with HIC-1ΔC (4aa) in pBAB# 0102 using *PstI* and *BamHI* sites.

16. pBAB# 0116: *Punc-17*:: HIC-1(ΔC(4aa)+NAB-1(ABD))

The HIC-1 gene was replaced with HIC-1(ΔC(4aa)+NAB-1(ABD)) in pBAB# 0105 using BamHI and NheI sites.

2.2.3.2 Preparation of chemical competent cells:

A single DH5β bacterial colony from a culture plate was taken and incubated in 10 ml LB broth for overnight at 37°C. From this primary culture, 100 µl of culture was taken and incubated in 100 ml LB media till the optical density of the culture reached to 0.4 - 0.6. Subsequently, the culture was centrifuged at 6000 rpm at 4°C for 15 min. Afterward, the supernatant was decanted, and the pellet was resuspended in 10 ml of 0.1 M ice-cold CaCl2 solution and incubated on ice for 15 min. After that, the solution was centrifuged at 6000 rpm at 4°C for 15 min. The supernatant was discarded, and then the pellet was resuspended in 5 ml of 0.05 M CaCl2 solution and kept in ice for 45 min. Subsequently, recovery of the cells was made by centrifugation at 2000 rpm at 4°C for 5 min. Finally, the pellet was resuspended in 85% 0.1 M CaCl2 solution and 15% glycerol and aliquoted into 1.5 ml microcentrifuge tubes and stored at -80°C.

2.2.3.3 Transformation:

The competent cells were kept on ice for 10 min for thawing. Afterward, 100-200 ng of DNA was added and incubated on ice for 30 min. Subsequently, heat shock was given for 60 sec at 42°C and after that cells were kept on ice for 5 min. On

completion of the incubation time, 1 ml LB media was added and the culture was placed on a water bath for one hr at 37°C. Cells were then centrifuged at 5000 rpm for 5 min. Around 800ul of LB media is discarded, leaving behind minimal volume containing the pellet. Subsequently, the pellet was resuspended in LB media and was plated on antibiotic containing LB agar plates.

2.2.4 Microinjections:

C.elegans transformants were obtained as described previously (Mello and Fire, 1995). Briefly; 100 ng/ul concentration injection mix was prepared with 10-50 ng of transgene DNA, 5-15 ng/ul of co-injection marker (P*myo-2*::mCherry)/(P*myo-3*::mCherry/P*ttx*::GFP or P*unc-122*::GFP) and rest of the concentration was made-up by using pBluescript (PBS) plasmid. The injection mix is prepared in elution buffer and all the plasmid DNAs are also eluted in elution buffer supplied in the plasmid isolation Kit (Quigen or genei). An additional cleaning step is used to get higher transmission rate of the transgene, we have seen that a protocol suggested by morris maduro in 'the worm breeder's Gazette' uses ethanol precipitation after plasmid purification is quite helpful. Briefly, the original plasmid preparation was adjusted to 200µl by adding ddH_2O, followed by addition of 20µl of 3M sodium acetate (pH4.8) and 550µl of 95% ethanol and placing it at -20^{0}C for 15mins. After this, the preparation was spun at 13,000 rpm for 10 mins; the pellet was rinsed in 80% ethanol and suspended in the elution buffer.

The injection mix was spun at 13,000 rpm for 10 mins, and the supernatant was carefully taken and filled in the injection needle to avoid any debris which can clog the needle during injections.

2.2.5 Integration of Arrays:

The extrachromosomal arrays with high-frequency transmission rate were integrated as described previously (Mariol et al., 2013).

Briefly, higher transmission rate (>80%) containing arrays/lines were selected for integration. Around 300 young *C.elegans,* adults from the line were picked and placed on five separate NGM plates without OP50. A UV crosslinker was used for giving UV treatment to the worms. 30 Joules for 60 seconds dose of UV radiation has been proven successful for integration in our case. After UV treatment, the worms were left at 20^0C overnight to recover, next day they were placed on NGM plates with OP50 to grow. After 10-15 days, the plates were chunked, and around 100 L1-L2 worms were singled out. They were observed after two days for integration events such as high transmission rates (preferably 100%) and any abnormalities such egg-laying defective or slow movement. Around four worms from each selected plates were further singled out to confirm the integration.

The list of integrated lines generated in the current study and others with their sources used for this work is listed in table2, the list of arrays used in this study is listed in table3. The list of all the strains used in this work is listed in table4.

Table 2. List of Integrated Lines:

S. no.	Plasmid	Integrated Line no.	Source and reference
1	P*unc-17*::RFP	*nuIs321*	Josh Kaplan Lab (Babu et al., 2011b)
2	P*unc-25*::GFP	*juIs76*	CGC strain number CZ1200 (Ackley et al., 2005)
3	P*unc-129*::GFP::SNB-1	*nuIs152*	Josh Kaplan Lab (Sieburth et al., 2005b
4	P*unc-25::SNB-1::GFP*	*nuIs376*	Josh Kaplan Lab (Hao et al., 2012)
5	P*acr-2*::mCherry::RAB-3(pPRB47)	*uIfs63*	Mike Francis Lab (Petrash et al., 2013)
6	P*unc-129*::SYD-2::YFP	*nuIs159*	Josh Kaplan Lab (Sieburth et al., 2005b)
7	P*unc-25*::SYD-2::GFP	*hpIs3*	CGC strain number ZM54 (Yeh et al., 2005)
8	P*myo-3*::UNC-29::GFP	*akIs38*	Villu Maricq lab (Francis et al., 2005b)
9	P*myo-3*::ACR-16::GFP	*nuIs299*	Josh Kaplan Lab (Babu et al., 2011b)
10	P*myo-3*::UNC-49::GFP	*nuIs283*	Josh Kaplan Lab (Babu et al., 2011b)
11	P*myo-3*::GCaMP3.35	*goels3*	CGC strain number HBR4 (Schwarz et al., 2011)
12	P*nab-1*::NAB-1::GFP	*hpIs66*	Mei Zhen Lab (Hung et al., 2007)
13	P*unc-17*:: GFP-UtrCH	*indIs001*	This study
14	P*unc-129*::LIN-44::mCherry	*indIs002*	This study, array number *IndEx32* from (Pandey et al., 2017)

15	P*unc-17*::CWN-2::mCherry	*indIs003*	This study
16	P*unc-17*::NLP-21::YFP (pDS269)	*vjIs30*	Derek Sieburth Lab (Staab et al., 2013)
17	P*unc-129*::GSLN-1::YFP	*nuIs169*	Josh Kaplan Lab (Sieburth et al., 2005b)

Table 3. List of Transgenes and Arrays:

S. no.	Plasmid	Plasmid number	Array number/ Line number
1	P*hic-1*::mCherry *(injected into WT)*	BAB#0101	*IndEx001*/BAB347
2	P*hic-1*::HIC-1::mCherry *(injected into WT)*	BAB#0102	*IndEx002*/BAB348
3	P*rab-3*::HIC-1 *(injected into hic-1)*	BAB#0103	*IndEx003*/BAB349
4	P*let-413*::HIC-1 *(injected into hic-1)*	BAB#0104	*IndEx004*/BAB350
5	P*myo-3*::HIC-1 *(injected into hic-1)*	BAB#0105	*IndEx005*/BAB351
6	P*unc-17*::HIC-1 *(injected into hic-1)*	BAB#0106	*IndEx006*/BAB352
7	P*unc-25*::HIC-1 *(injected into hic-1)*	BAB#0107	*IndEx007*/BAB353
8	P*unc-17*::HIC-1ΔC(4aa) *(injected into hic-1)*	BAB#0108	*IndEx008*/BAB354
9	P*unc-17*::NAB-1::VN173 *(injected into uIfs63)*	BAB#0110	*IndEx009*/BAB355
10	P*unc-17*::HIC-1::VC155 *(injected*	BAB#0111	*IndEx010*/BAB356

	into uIfs63)		
11	P*unc-17*::HIC-1ΔC(4aa)::VC155 *(injected into uIfs63)*	BAB#0112	*IndEx011*/BAB357
12	P*hic-1*::HIC-1ΔC(4aa)::mCherry*(injected into nuIs152))*	BAB#0115	*IndEx012*/BAB358
13	P*unc-25*:: GFP-UtrCH *(injected into WT)*	BAB#0114	*IndEx013*/BAB359
14	P*unc-17*::NAB-1::VN173 *(injected into nab-1)*	BAB#0110	*IndEx014*/BAB360
15	P*unc-17*::CWN-2::mCherry *(injected into WT)*	BAB#0109	*IndEx015/BAB361*
16	P*unc-17*::HIC-1::VC155;P*unc17*::NAB-1::VN173 *(injected into uIfs63)*	BAB#0110, BAB#0111	*IndEx016*/BAB362
17	P*unc-17*::HIC-1ΔC(4aa)::VC155; P*unc17*::NAB-1 ::VN173 *(injected into uIfs63)*	BAB#0110, BAB#0112	*IndEx017*/BAB363
18	*Punc-17*:: HIC-1(ΔC(4aa)+NAB-1(ABD)) *(injected into BAB323)*	BAB#0116	*IndEx018*/BAB364
19	*Punc-17*:: HIC-1(ΔC(4aa)+NAB-1(ABD))	BAB#0116	*IndEx019*/BAB365

	(injected into BAB330)		
20	*Punc-17*:: HIC-1(ΔC(4aa)+NAB-1(ABD)) *(injected into BAB333)*	BAB#0116	*IndEx020*/BAB366
21	P*unc-17*::HIC-1ΔC(4aa) *(injected into BAB323)*	BAB#0108	*IndEx021*/BAB367
22	P*unc-17*::HIC-1ΔC(4aa) *(injected into BAB330)*	BAB#0108	*IndEx022*/BAB368
23	P*unc-17*::HIC-1ΔC(4aa) *(injected into BAB333)*	BAB#0108	*IndEx023*/BAB369

Table 4. List of strains

S. no.	Genotype	Strain number	Source and reference
1	*hic-1(ok3475)*	RB2512	CGC
2	*nab-1(ok943)*	RB1017	CGC
3	*mig-14(mu71)*	CF367	CGC
4	*lin-17(sy277)*	PS1403	CGC
5	*acr-16(ok789)*	RB918	CGC
6	*hic-1(ok3475); nuIs321*	BAB302	This study
7	*hic-1(ok3475); juIs73*	BAB303	This study
8	*hic-1(ok3475); nuIs152*	BAB304	This study
9	*hic-1(ok3475); juIs76*	BAB305	This study
10	*hic-1(ok3475); uIfs63*	BAB306	This study
11	*hic-1(ok3475); nuIs159*	BAB307	This study

12	*hic-1(ok3475); hpIs3*	BAB308	This study
13	*hic-1(ok3475); nuIs169*	BAB309	This study
14	*hic-1(ok3475); nuIs169; IndEx006*	BAB310	This study
15	*hic-(ok3475); akIs38*	BAB311	This study
16	*hic-1(ok3475); nuIs299*	BAB312	This study
17	*hic-1(ok3475); nuIs299; IndEx006*	BAB313	This study
18	*hic-1(ok3475); nuIs283*	BAB314	This study
19	*hic-1(ok3475); goels3*	BAB315	This study
20	*hic-1(ok3475); goels3; IndEx006*	BAB316	This study
21	*hic-1(ok3475); indIs001*	BAB317	This study
22	*hic-1(ok3475); indIs001; IndEx006*	BAB318	This study
23	*hic-1(ok3475); indIs002*	BAB319	This study
24	*hic-1(ok3475); indIs002; IndEx006*	BAB320	This study
25	*hic-1(ok3475); IndIs003*	BAB321	This study
26	*hic-1(ok3475); IndIs003; IndEx006*	BAB322	This study
27	*nab-1(ok943);hic-1(ok3475)*	BAB323	This study
28	*mig-14(mu71);hic-1(ok3475)*	BAB324	This study
29	*lin-17(sy277); hic-1(ok3475)*	BAB325	This study
30	*nab-1(ok943); IndEx014*	BAB326	This study
31	*nab-1(ok943); hpIs66*	BAB327	This study
32	*nab-1(ok943); IndIs001*	BAB328	This study
33	*nab-1(ok943); IndEx014; IndIs001*	BAB329	This study
34	*nab-1(ok943); hic-1(ok3475);*	BAB330	This study

	IndIs001		
35	*nab-1(ok943); IndIs003*	BAB331	This study
36	*nab-1(ok943); IndEx014; IndIs003*	BAB332	This study
37	*nab-1(ok943); hic-1(ok3475);IndIs003*	BAB333	This study
38	*mig-14(mu71);IndIs003*	BAB334	This study
39	*mig-14(mu71); hic-1(ok3475); IndIs003*	BAB335	This study
40	*hic-1(ok3475); hpIs66*	BAB336	This study
41	*hpIs66; IndEx002*	BAB337	This study
42	*hic-1(ok3475); vjIs30*	BAB348	This study
43	*nab-1(ok943); nuIs299*	BAB349	This study
44	*nab-1(ok943);nuIs299; IndEx014*	BAB350	This study
45	*nab-1(ok943); hic-1(ok3475); nuIs299*	BAB351	This study
46	*hic-1(ok3475); acr-16(ok789)*	BAB352	This study
47	*hic-1(ok3475);hpIs66; IndEx006*	BAB355	This study

2.3 Behavioral assays

2.3.1 Aldicarb assay:

This assay was performed as previously described (Mahoney et al., 2006b). Briefly, the aldicarb plates were prepared one day before the experiment, 100 mM stock of aldicarb (Sigma-Aldrich, St. Louis, MO) was prepared in ethanol and incorporated in the NGM to make the final concentration of 1mM. At least 20 animals per genotype were picked at the late L4 stage for the assay. The number of paralyzed animals was counted at 10m intervals up to 120m. The assay was performed in triplicates with the experimenter being blind to the genotype of the *C. elegans*. Aldicarb assays were performed using multiple batched of aldicarb; this gave rise to small discrepancies in the rate of paralysis of WT animals. However, all the graphs were done with appropriate controls, with the experimenter being blind to the genotype of the animals, and showed a similar trend across the multiple batches of aldicarb. The worms which paralyze faster than the WT type are called 'hypersensitive' and the ones which paralyze slower than the WT are called as 'resistant' to the aldicarb assay.

2.3.2 Sytox green uptake assay:

To check epithelial membrane integrity, Sytox green assay was performed. Briefly, *C. elegans* were allowed to uptake sytox green dye at 22^{o} C or 37^{o}C for 1 hour (h). Images of the intestine of the *C. elegans* were captured using the 488nm filter and DIC after the sytox green treatment.

2.3.3 Coelomocyte uptake assay:

The secretion of Wnt ligands from the cholinergic neurons was monitored using a technique similar to that used previously for Neuropeptide uptake assays (Sieburth et al., 2006) and as has been previously published for Wnt (Jensen et al., 2012b). The fluorescence intensity of Wnts tagged with

mCherry was measured in the endocytic compartment of coelomocytes posterior to the vulva of the WT and mutant *C. elegans*. Laterally oriented young adults were imaged where the coelomocyte was not obscured by any other tissues. A maximum intensity projection was taken from image stacks of the coelomocyte; the fluorescence intensity was calculated from 3-4 vesicles in each coelomocyte, averaged and then averaged for all the coelomocytes for each genotype. The mean fluorescence intensity of coelomocytes from individual genotypes was divided by the wild type mean fluorescence intensity to normalize.

2.4 Microscopy and image analysis

2.4.1 Neuronal and synaptic markers:

Imaging of neuronal and synaptic markers was done by immobilizing *C. elegans* with 30mg/ml 2, 3-butanedione monoxamine (BDM) from Sigma on 2% agarose pads. A Zeiss AxioImager microscope with a 63x 1.4 NA Plan APOCHROMAT objective equipped with a Zeiss AxioCam MRm CCD camera controlled by Axiovision software (Zeiss Microimaging) was used for taking Z-stacks of the *C.elegans*. Maximum intensity projections of the line-scans were taken for Quantitation. Images were then quantitated using ImageJ software. The Prism 7 software was used for the statistical analyses of the data.

The Colocalization studies and the GFP-UtrCH imaging experiments were performed on the Leica SP8 confocal microscope using Argon laser at multiple

gains ranging from 10% to 15%. All the parameters were kept constant for any one set of imaging experiments plotted in the same graph.

2.4.2 Fluorescent recovery after photobleaching (FRAP) Experiment:

FRAP experiment was performed as mentioned before (Kourtis and Tavernarakis, 2008) on late L4 stage *C. elegans* that were immobilized on to 10% agarose pads. 0.2µl of 0.1 µm polystyrene beads (Polysciences) were added to the slides to further restrict the movement of the *C. elegans*. The SP8 confocal microscope (Leica Microsystem) with 23% bleaching power of 488 nm Argon laser was used to bleach the ACR-16::GFP puncta. The images were captured before and after photobleaching for up to 30m. The fluorescent intensities of neighboring puncta were also calculated and taken as a control to monitor the focal drift during the live imaging of the animals.

2.4.3 Latrunculin A (LAT-A) injections:

The Lat-A injections for actin depolymerization were performed as described previously (Chia et al., 2012a). L4 staged animals were immobilized by putting them on 2% agarose pads and adding halocarbon oil (Sigma), after immobilization, the *C. elegans* were injected with either 1mM of LAT-A (Sigma) in 25% vol/vol DMSO (Sigma) or 25% DMSO alone. The injections were done into the pseudocoelom of the *C. elegans* at a site slightly posterior to the vulva. The injected animals were then kept at 20^{o}C for 3h to recover. After recovery, the animals were imaged as has been described above in coelomocyte uptake assay.

2.4.4 Calcium imaging:

Calcium imaging in the *C.elegans* muscles was performed as described previously (Gong et al., 2016). For calcium imaging, animals were immobilized on 2%

agarose pads prepared in M9 buffer and 0.2µl of polystyrene beads were added to the slide. After immobilizing the *C. elegans*, time-lapse movies were taken for the muscles on the Zeiss fluorescence microscope at 1 frame/seconds speed for up to 40 seconds. From the movies, images were taken for different time points for all the genotypes, fluorescent intensities of calcium transients within a selected region of interest were calculated and subtracted from background to get rid of basal calcium signals. Data analysis was performed in the prism 7 software and images were quantitated using ImageJ software.

2.4.5 BiFC Assay:

To perform BiFC experiments, VN173 Fragment (N-terminus) of split YFP (Kerppola, 2013) was cloned downstream to Neurabin cDNA, and VC155 Fragment (C-terminus) of split YFP (Kerppola, 2013) was tagged to the C-terminus of HIC-1 cDNA. For the control experiment, HIC-1ΔC(4aa)::VC155 was generated. All the constructs for BiFC experiments were cloned under the *unc-17* promoter to drive the expression in the cholinergic neurons. Dorsal and ventral nerve cord of the worms was imaged under the confocal microscope. A summary of the sequences and the primers used for generating BiFC constructs are mentioned in the primers and constructs section.

2.5 Quantitative PCR experiment

For real-time PCR based gene expression analysis, Fresh RNA was isolated from a mixed staged population of *C. elegans* by first treating the freeze-thawed *C. elegans* pellets to Trizol and then purifying the lysate with an RNeasy Mini

Kit (Qiagen). cDNA was synthesized from the isolated RNA with random hexamers using the Transcriptor High Fidelity cDNA Synthesis Kit (Roche) according to manufacturer's protocols. The contamination of DNA in qPCR reaction was eliminated using DNAse treatment given in the kit. SYBR *Premix Ex Taq* II master mix (Clontech) was used to set up the real-time PCR reaction in triplicates. The normalized expression of genes in different mutants relative to WT controls was calculated using the $2^{-\Delta\Delta Ct}$ method (Livak and Schmittgen, 2001).

2.6 Electrophysiology Experiments

C.elegans dissection, Neuromuscular junctions exposure and Whole-cell voltage-clamp recordings were performed on body-wall muscles as previously described (Hu et al., 2012; Richmond and Jorgensen, 1999a). We recorded miniature excitatory postsynaptic currents by superfusing worms in an extracellular recording solution made up of 127mM NaCl, 5mM KCl, 26mM $NAHCO_3$,1.25mM NAH_2PO_4,20mM glucose,1mM $CaCl_2$, and 4mM $MgCl_2$ bubbled with 5% CO_2,95%O_2 at 20^0C. Endogenous EPSCs were recorded at -60Mv which is the reversal potential for the GABAA receptors. In this way, only mEPSCs were recorded (Hu et al., 2013). The intracellular recording solution is made up of 105mM $CsCH_3SO_3$,10mM CsCl,15mM CsF, 4mM $MgCl_2$,5mM EGTA,0.25mM $CaCl_2$, 10mM HEPES, and 4mM Na_2ATP at pH7.2 adjusted by adding CsOH. The stimulus-evoked EPSCs were performed by giving a gentle mechanical stimulus by placing a borosilicate pipette (5mm in open size) near the ventral nerve cord (one muscle distance from the recording pipette) and applying a 0.4 ms, 85μA square pulse using a stimulus current generator (WPI). The frequency was calculated by

counting the number of events in a given time frame while the mean amplitude represents the average value of all the peaks in a given time frame.

2.7 Quantification and Statistical Analysis

All statistical analysis was performed using GraphPad Prism V7. Experimental data are shown as Mean±SEM. Statistical comparisons were done using the Student's *t*-test, one-way ANOVA with Bonferroni's multiple comparison post-test or Kolmogorow–Smirnow-test (KS-test). A level of $p<0.05$ was considered significant. Multiple sequence Alignment amongst claudin homologs was analyzed using the Clustal Omega program (Sievers et al., 2011).

Chapter 3:
HIC-1, a novel Claudin like molecule is expressed in cholinergic motor neurons

Vina Tikiyani performed all the experiments except the electrophysiological recordings. Lei Li at Queensland Brain Institute performed the electrophysiological recordings. Pallavi Sharma and Vina Tikiyani did the initial aldicarb screen with the claudin mutants.

Introduction

Cell adhesion molecules play diverse roles at the synapses (Abbas, 2003; Benson et al., 2000; Togashi et al., 2009) and illustrated in **Figure 3.1**)). To study the role of cell adhesion molecules (CAMs) at the *C.elegans* Neuromuscular junction (NMJ) an aldicarb screen was performed by Dr. Kavita Babu during her postdoctoral fellowship in Professor Josh Kaplan's lab. An RNAi screen against CAMs followed by aldicarb assays was performed on the *C. elegans* that showed knock-down in CAM expression (Babu et al., 2011b). The screen revealed that tight junctional proteins, claudins may be functional at the *C.elegans* NMJ. Although, the function of claudins in the epithelium is very well studied, how they function in the neurons and at synapses are largely unknown. There are 18 known claudin-like molecules annotated in wormbase, out of which mutants were available for 11 claudin-like molecules from The *Caenorhabditis* genetics center (CGC). The claudin mutants were assayed using the aldicarb assay to analyze their function at the NMJ. We found that of the 11 mutant strains *clc-1,clc-2,clc-3,clc-4,nsy-4,hpo-30,f53.b3.5,f10a3.1,t28b4.4,stg-1,* and *f59c6.11* analyzed, 4 mutants *clc-3,clc-4,nsy-4,and t28b4.4* were hypersensitive to aldicarb, *3 mutants clc-2,hpo-30, and stg-1* were resistant to aldicarb and rest 4 mutants behaved like WT animals in the aldicarb assay (data not shown). Mutants in a claudin homolog, *t28b4.4* showed hypersensitivity to aldicarb. This prompted us to name the gene HIC-1 (Hypersensitive to Inhibitor of Cholinesterase). Since the *hic-1* mutant phenotype was robust, we decided to characterize this mutant. HIC-1 encodes a claudin

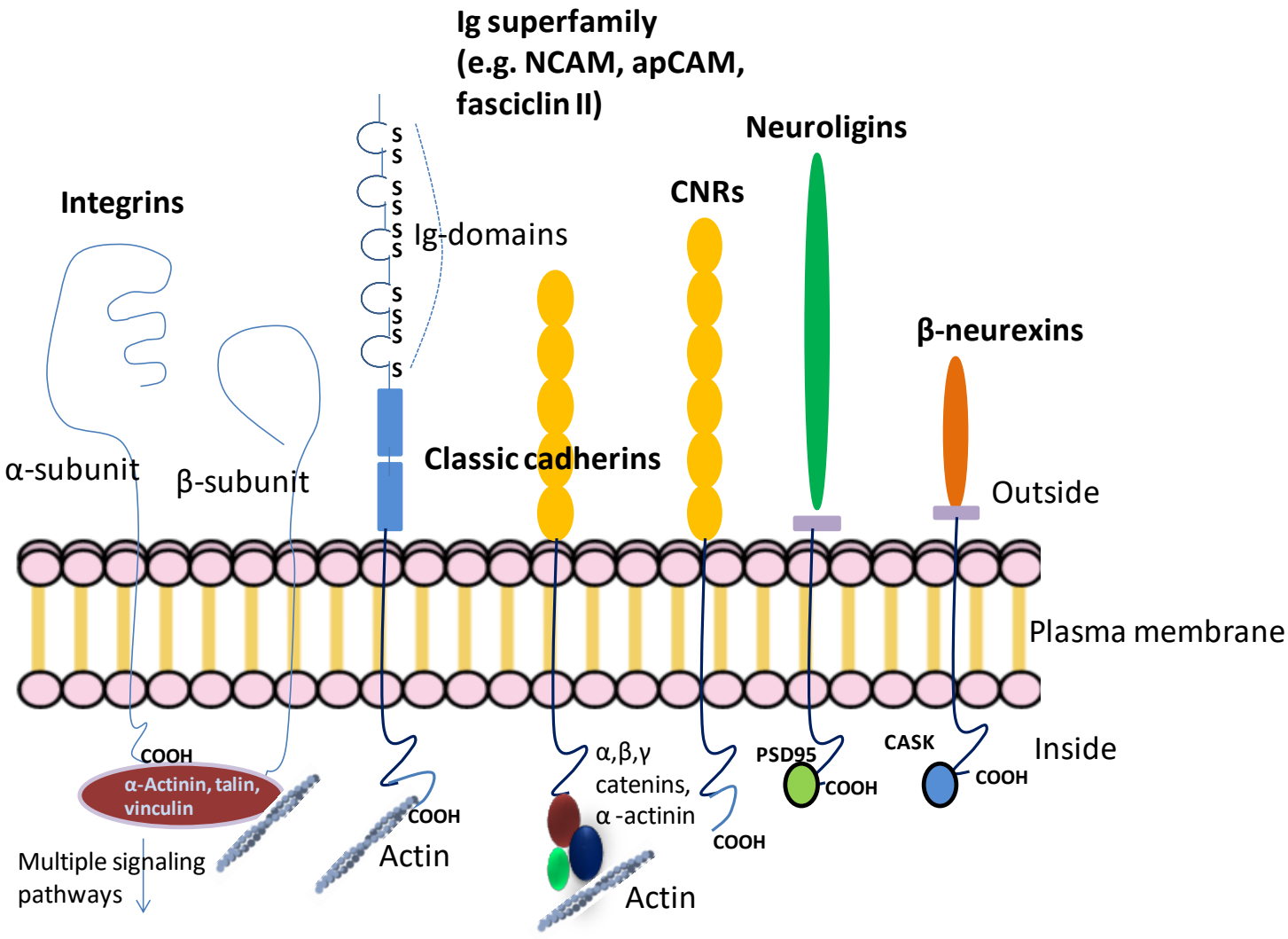

Figure 3.1 Illustration of cell adhesion molecules at the synapse (image adapted from (Benson et al., 2000)).Various Cell Adhesion Molecules (CAMs) that are present at the CNS postsynaptic terminus are indicated in the diagram. They are categorized mainly in four groups: classic cadherins, Immunoglobulin (Ig) superfamily, Integrins, and Neurexins and Neuroligins. They either make contacts with actin cytoskeleton directly or via adaptor proteins (α-Actinin, talin, vinculin) or to scaffold proteins such as PSD95 or CASK intracellularly.

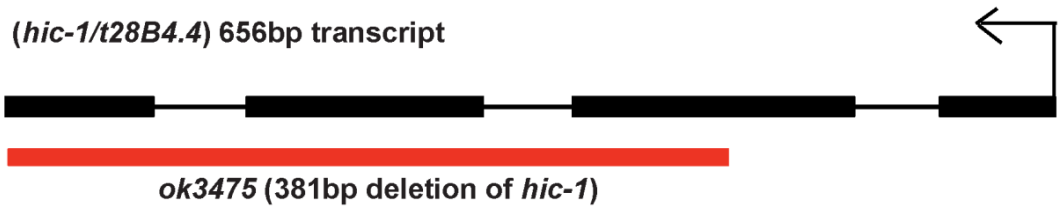

Figure 3.2 illustration of genomic region of T28B4.4/HIC-1 showing exonic and intronic regions. HIC-1 locus encodes for 656 base pair long transcript with four exons (black solid rectangles) and four introns (in between lines). Black arrow indicates the start of the transcription. The deletion allele *ok3475* was used in this study which makes a deletion from the second exon to the rest of the gene.

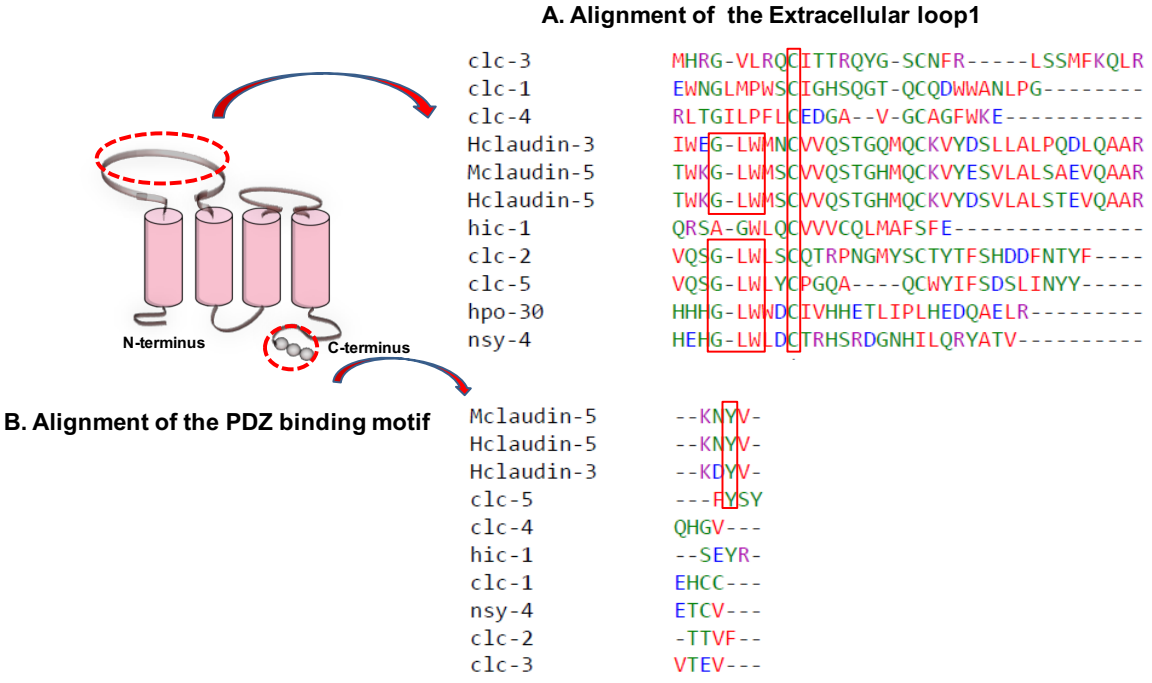

Figure 3.3 Claudin multialignment A. Multialignment of the extracellular loop 1 of different claudins shows the absence of the critical "GLW" residues in HIC-1. B. Multialignment of the C-terminus PDZ binding motif (bm) of different claudins indicating the conservation of the critical Tyrosine residue in HIC-1.

homolog (**Figure 1.1**) and shows weak sequence similarity to CLC (Claudin- Like in Caenorhabditis) -1 proteins (Asano et al., 2003b; Kamath et al., 2003). HIC-1 locus encompasses 504 base pair long coding region with four exons and four introns (wormbase). The mutant allele of *hic-1*(*ok3475)* which we used in this study is a deletion from the middle of the second exon to the end of the gene, making it a likely null allele (**Figure 3.2**).

The genomic region of tetraspan protein HIC-1 shares similarity with other claudins at its PDZ binding motif (C-terminus) but is poorly aligned with other claudins at the first extracellular loop (**Figure 3.3**), suggesting that HIC-1 might have functional roles similar to other claudins intracellularly.

Results

3.1 HIC- 1 functions in the nervous system:

WT worms usually take 120 minutes (m) to completely paralyze after aldicarb exposure (Mahoney et al., 2006b). However, 100% of the *hic-1* mutant worms were paralyzed at the 80m time-point (**Figure 3.4)**. HIC-1 cDNA was cloned under a pan-neuronal promoter (P*rab-3*,(Mahoney et al., 2006a; Nonet et al., 1997; Saheki and Bargmann, 2009)); the construct made was then injected into the *hic-1* worms. The neuronal rescue arrays showed a paralysis pattern similar to WT worms (**Figure 3.4 and 3.5**), i.e. HIC-1 function is restored in the nervous system, suggesting that this particular claudin homolog has a separate function to play in the nervous system apart from what is routinely assigned to its counterparts in the epithelium. For simplicity, we have just shown the percentage of paralysis at the 80m time- point in all future aldicarb experiments. Since aldicarb phenotypes are

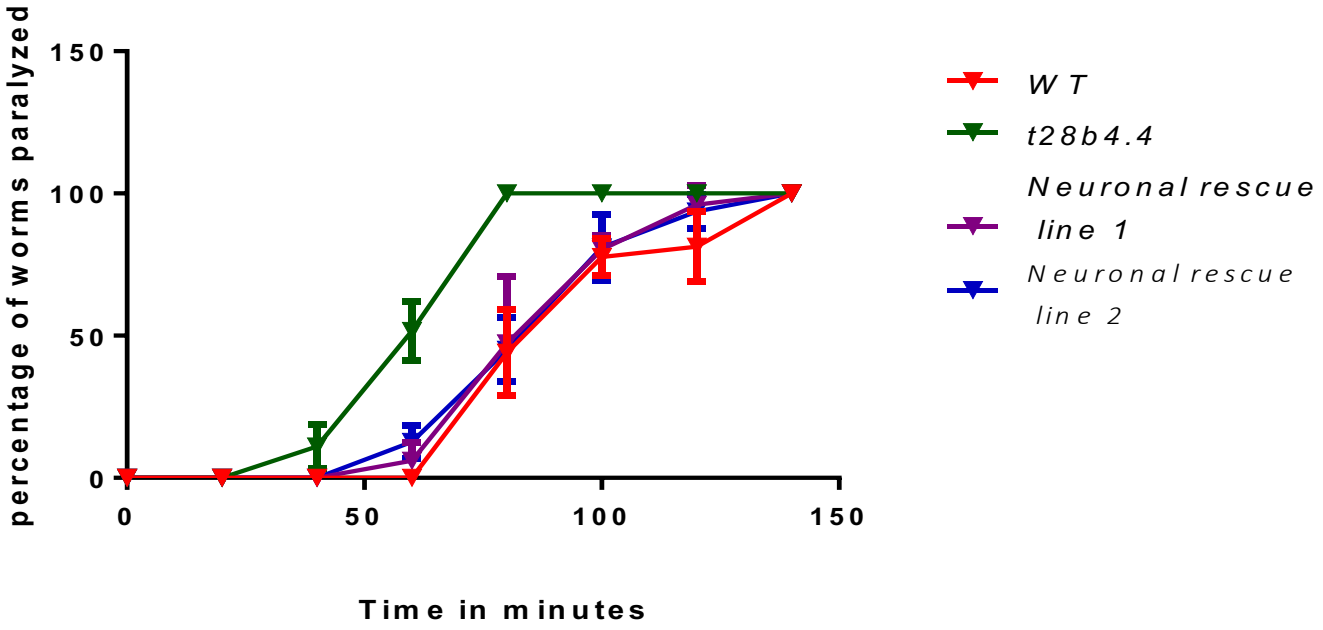

Figure 3.4 T28B4.4/HIC-1 functions in the neurons. Time-course paralysis shows *hic-1* worms (green line) are hypersensitive in the aldicarb assay compared to WT worms (orange line). Pan-neuronal rescue arrays (blue and purple lines) were able to rescue the hypersensitivity defects of HIC-1.

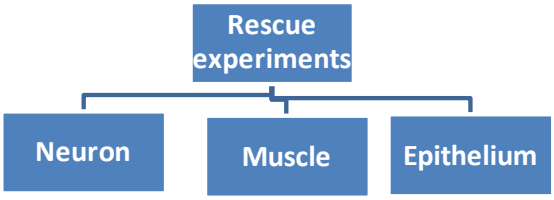

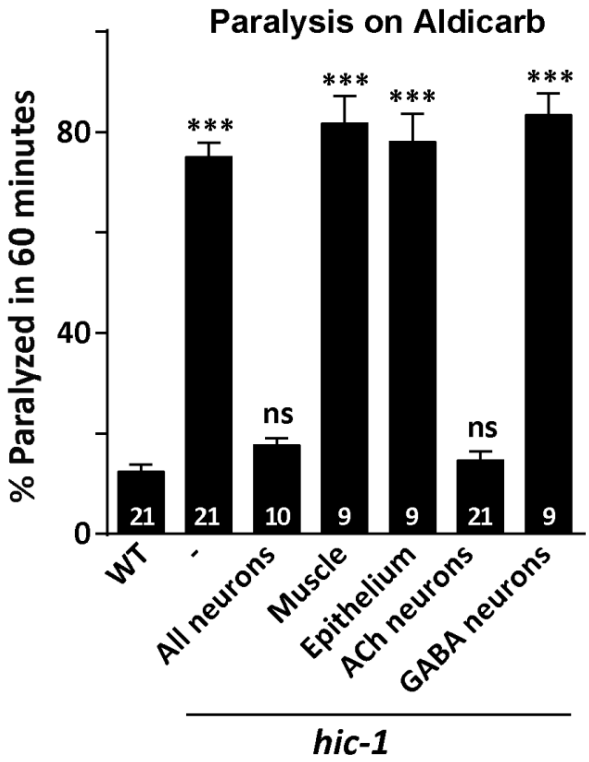

Figure 3.5 Percentage paralysis of *C. elegans* on 1mM aldicarb, plotted at the 60 minutes (m) time point. The graph indicates rescue of the aldicarb phenotype using the following promoters; P*rab-3* (pan-neuronal), P*myo-3* (body-wall muscles), P*let-413* (epithelium cells), P*unc-17* (Cholinergic neurons) and P*unc-25* (GABAergic neurons). The numbers at the base of the bar graphs represent the number of trials (20-25 animals per trial) for each genotype for all aldicarb graphs. Statistics for all aldicarb graphs is based on two-tailed unpaired student's t-test where "***" indicates $p<0.001$, "**" indicates $p<0.01$, "*" indicates $p<0.05$ and "ns" indicates not significant. The data are shown as mean ± SEM in all graphs unless otherwise stated.

largely due to defects in NMJ function (Mahoney et al., 2006b; Sieburth et al., 2005b), after rescuing HIC-1 function in the neurons, we next wanted to see if we could rescue the function of HIC-1 in body-wall muscles. When HIC-1 was expressed exclusively in the body-wall muscles using a body-wall muscle specific promoter (P*myo-3*,(Miller et al., 1986; Tabara et al., 1999)), it failed to rescue the hypersensitivity defects seen in *hic-1* mutants (**Figure 3.5**), indicating that HIC-1 is not required in the muscles. Since HIC-1 is a claudin homolog and claudins are known to be required to maintain epithelial membrane integrity (Gunzel and Yu, 2013), we wanted to check if the epithelial membrane in *hic-1* is affected.

Two experiments were done to understand the possible role of HIC-1 in epithelial integrity. First, we rescued HIC-1 in the epithelium using an epithelium-specific promoter (P*let-413*, (Firestein and Rongo, 2001; Legouis et al., 2000)). Arrays expressing HIC-1 in epithelial cells were not able to rescue the hypersensitive phenotype seen in the *hic-1* mutants. Next, we tested if the epithelial membrane integrity was compromised in *hic-1* mutants by measuring the uptake of the dye, sytox green in WT and mutant animals (Gill et al., 2003). The *hic-1* mutants behaved similarly to WT worms both at the 22^0C and at the 37^0C (**Figure 3.6**). Together, these data indicated that the aldicarb phenotype of HIC-1 is likely caused due to its function in the nervous system and not in the epithelium. Since both cholinergic and GABAergic neurons synapse onto the body-wall muscle, we wanted to see whether HIC-1 functions in both or one set of motor neurons. We observed that the HIC-1 expression in the cholinergic neurons (under P*unc-17*, (Alfonso et al., 1993; Liewald et al., 2008; Liu et al., 2009)) was sufficient to rescue the aldicarb

defect of *hic-1,* but HIC-1 expression in GABA neurons could not rescue this defect (under P*unc-25* promoter, (Hallam et al., 2000; Mclntire et al., 1993), **Figure 3.5)**).

3.2 HIC-1 expression pattern:

After establishing that HIC-1 could function in the nervous system, we went on to see its expression in the worm. First, we made a transcriptional fusion construct pBAB101 where we cloned the promoter region of the HIC-1 gene (approx 2100bp upstream of the start codon) to the mCherry sequence. The transcriptional array line showed that HIC-1 is expressed in head neurons, the tail neurons and the ventral nerve cord neurons (**Figure 3.7)**. Next, we went on to test if HIC-1 is expressed in cholinergic or GABAergic motor neurons. To address this, we crossed the transcriptional reporter line P*hic-1*::mCherry with marker lines where cholinergic neurons were specifically labeled with GFP (Babu et al., 2011b) and performed co-localization experiments. We found that P*hic-1*::mCherry co-localized with cholinergic neurons (**Figure 3.8**). The dorsal nerve cord in *C.elegans* represents NMJs whereas the ventral nerve cord largely consists of neuronal cell bodies (reviewed in (Debell, 1965)). To investigate the subcellular localization of HIC-1, we made a translational reporter line where we cloned entire genomic region of HIC-1 (promoter and gene) tagged to the mCherry sequence in the pBAB102 construct. The translational reporter line was then crossed with a presynaptic terminal marker protein Synaptobrevin (SNB-1) (Nonet, 1999) expressed under either cholinergic or GABAergic promoters (Babu et al., 2011b; Hao et al., 2012; Sieburth et al., 2005a).

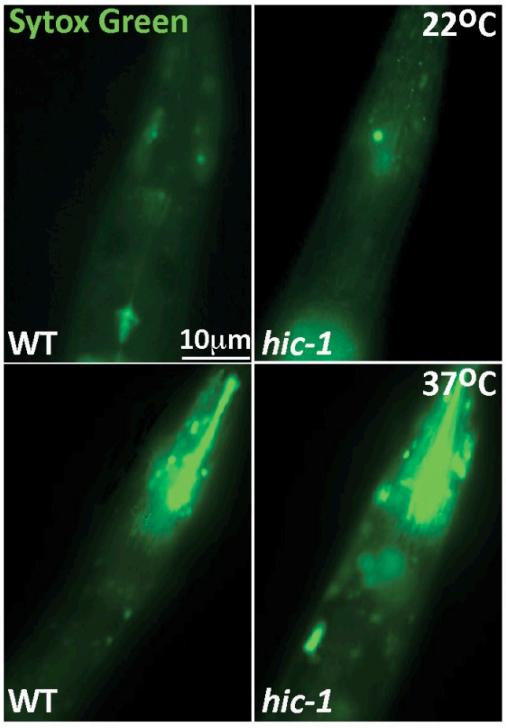

Figure 3.6 Sytox green uptake assay. Representative fluorescent images of the intestine after sytox green dye uptake at 22°C and 37°C in WT and *hic-1* mutant animals. Five animals were tested for each genotype and temperature.

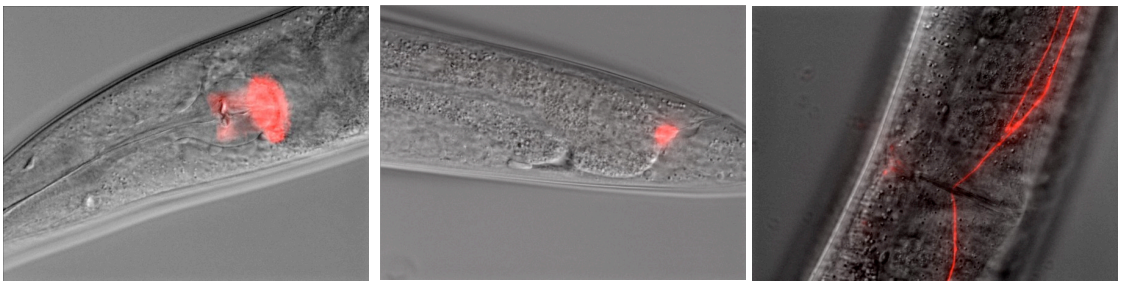

Figure 3.7 P*hic-1*::mCherry expression pattern. Representative DIC images of the head, tail, and the ventral cord of the animal showing expression of the P*hic-1*::mCherry transcriptional reporter line.

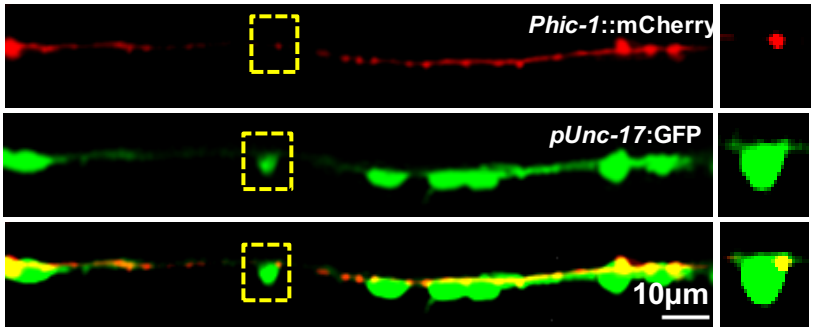

Figure 3.8 Representative ventral nerve cord confocal images of worms expressing P*hic-1*::mCherry (transcriptional reporter) and P*unc-17*::GFP (cholinergic neurons). P*hic-1*::mCherry (red) co-localizes with cholinergic neuronal cell bodies (green).

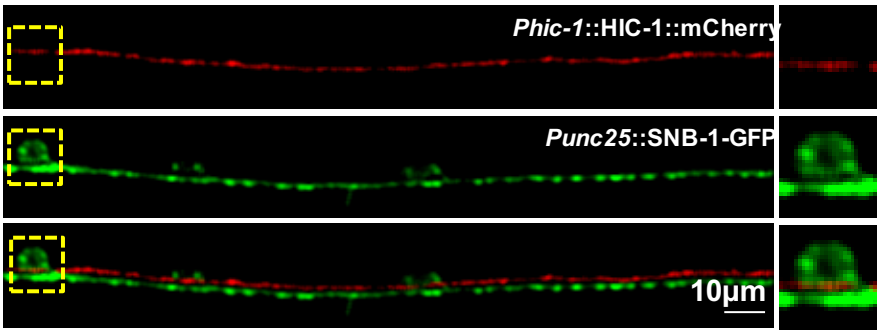

Figure 3.9 Representative ventral nerve cords of the worms expressing P*hic-1*::HIC-1::mCherry and P*unc-25*::SNB-1::GFP (GABA neurons). The expression of translation fusion array P*hic-1*::HIC-1::mCherry does not appear to be in GABA neurons.

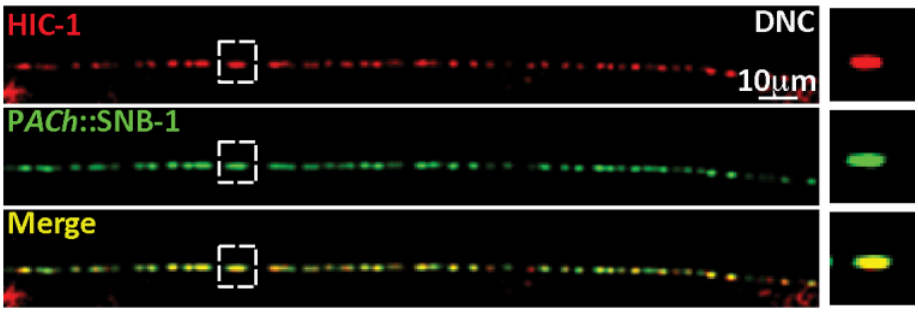

Figure 3.10 HIC-1 is co-localized with SNB-1 at the cholinergic synapse. Representative confocal image of the dorsal nerve cord (DNC) of the worm, expressing HIC-1 translational fusion reporter array and synaptobrevin (SNB-1)::GFP expressed as an integrated transgene under cholinergic promoter (P*ACh/Punc-17*). Percentage co-localization of HIC-1 was calculated using the formula: (number of HIC-1 puncta co-localized with SNB-1/total number of HIC-1 puncta)x100 in 100 µm.

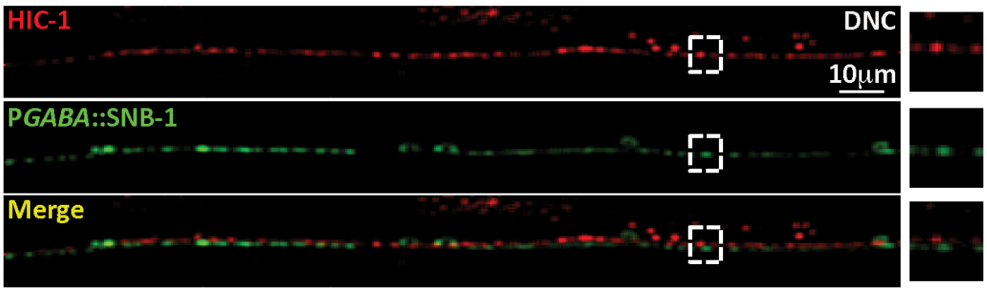

Figure 3.11 HIC-1 does not co-localize with SNB-1 at the GABA synapse. Representative confocal images of the dorsal nerve cord (DNC) of the worm, expressing the HIC-1 translational fusion reporter array and SNB-1::GFP which is expressed as an integrated transgene under the GABA promoter (P*unc-25*).

The co-localization experiments indicated that HIC-1 is significantly co-localized with SNB-1 in the cholinergic synapses (**Figure 3.10**) but not in the GABA neurons (**Figure 3.9**) or the synapses (**Figure 3.11**). To test if the mCherry tag is affecting the function of the HIC-1 protein, we crossed *hic-1* with the HIC-1 translational fusion reporter line and performed an aldicarb assay. The translational fusion reporter was able to rescue the aldicarb defects seen in the *hic-1* mutants, suggesting that the mCherry tag is not hampering the localization or the function of the HIC-1 protein (**Figure 3.12**).

3.3 HIC-1 regulates postsynaptic AChR/ACR-16 levels at the NMJ:

After establishing that HIC-1 is functional in the cholinergic neurons, we next went on to explore what it does in these neurons. To see if HIC-1 is required for the development of neurons or synapses, we first crossed the *hic-1* mutant animals into marker lines that showed expression in cholinergic or GABAergic neurons (Babu et al., 2011b). We found that the *hic-1* mutants did not show defects in the development of cholinergic or GABAergic neurons (**Figure 3.13**). Next, we went on to analyze the synaptic vesicle proteins SNB-1 and RAB-3 (Nonet et al., 1997; Petrash et al., 2013; Sieburth et al., 2005b) and again found no defects in presynaptic SNB-1 and RAB-3 fluorescence in *hic-1* mutants (**Figure 3.14 and Figure 3.15**). Further, on crossing the *hic-1* mutants with the active zone marker, α-Liprin/SYD-2 (Zhen and Jin, 1999) expressed specifically in cholinergic and GABAergic synapses (Hao et al., 2012; Sieburth et al., 2005b)

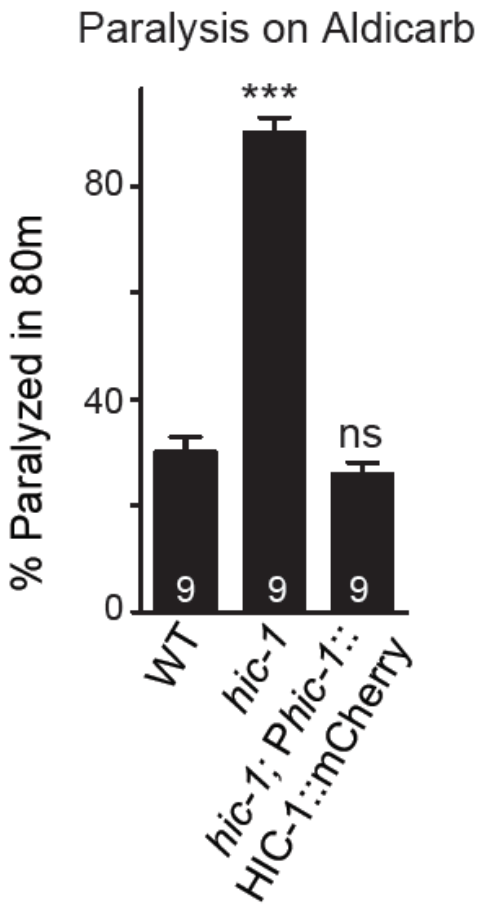

Figure 3.12 The translational fusion reporter of HIC-1 rescues the hypersensitivity to aldicarb seen in *hic-1* mutants. Percentage paralysis of different genotypes (WT, *hic-1, hic-1* P*hic-1*::HIC-1::mCherry) after 80 mins of aldicarb exposure.

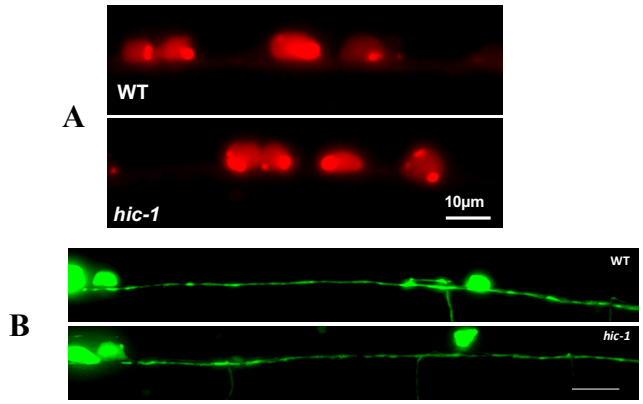

Figure 3.13 Neuronal development is normal in *hic-1* worms. (A) Representative ventral nerve cords showing cell bodies and neuronal projections of cholinergic neurons of WT and *hic-1* worms. Scale bar 10um. (B) Representative ventral nerve cords showing cell bodies and neuronal projections of GABA neurons of WT and *hic-1* worms.

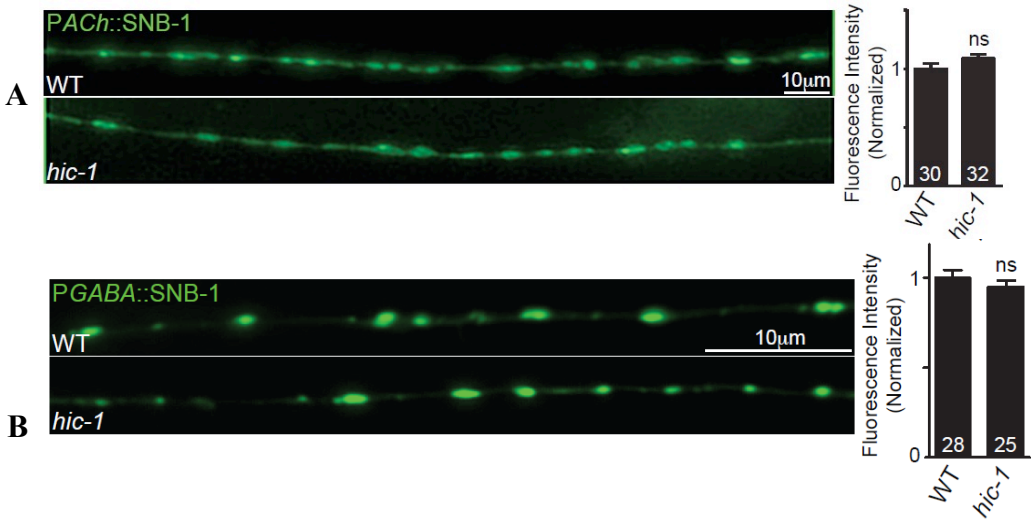

Figure 3.14 Synaptic vesicle numbers are not altered in *hic-1* worms. Representative images of dorsal nerve cords of WT and *hic-1* worms expressing synaptobrevin (SNB-1) in (A) cholinergic neurons (P*ACh*::SNB-1::*mCherry)* and in (B) GABA neurons (P*GABA*::SNB-1::GFP).The SNB-1::GFP fluorescence intensity has been normalized with respect to WT. Total number (N) of worms imaged for each genotype is indicated at the bottom in the bar graph. ns= non-significant compared to WT.

, we found no defects in neuromuscular synapse development (**Figure 3.16**). These data indicated that *hic-1* mutants do not appear to have any obvious presynaptic developmental defects. We next decided to analyze postsynaptic receptor levels at the NMJ in these mutants.

As mentioned earlier, The *C.elegans* body-wall muscle expresses one GABA and two types of Acetylcholine receptors (AChRs); one that is a nicotinic acetylcholine receptor (nAChR) and made up of homomeric subunits of AChR/ACR-16 and the other that is sensitive to the levamisole drug (LAChR) and is made up of heteropentameric αβ subunits (Richmond and Jorgensen, 1999b). We first went on to test the two AChRs (Babu et al., 2011b; Francis et al., 2005b) and found a significant increase in AChR/ACR-16 levels at the NMJ in *hic-1* mutants. This increase was completely rescued by expressing HIC-1 in cholinergic neurons (**Figure 3.17**). Testing a subunit of the LAChR/UNC-29 showed no obvious changes in LAChR/UNC-29 levels at the NMJ (**Figure 3.17**). Similarly, there were no significant defects in GABAR/UNC-49 levels in *hic-1* mutants (Babu et al., 2011b), **Figure 3.18**)). Further, to test if the increase in AChR/ACR-16 levels was due to increased expression of AChR/ACR-16, we performed quantitative PCR experiments to quantify the levels of *AChR/acr-16* RNA in WT and *hic-1* mutants, and found no differences in the RNA levels of AChR/ACR-16 in *hic-1* mutants (**Figure 3.19**). These data indicate that HIC-1 could be affecting AChR/ACR-16 levels specifically at the synapse. To further probe into whether *hic-1* affects AChR/ACR-16, we made double mutants of *hic-1* and *AChR/acr-16*. We found that the double mutants showed a paralysis response to aldicarb that was resistant in nature similar to the phenotype seen with the *AChR/acr-16* single mutants, i.e.

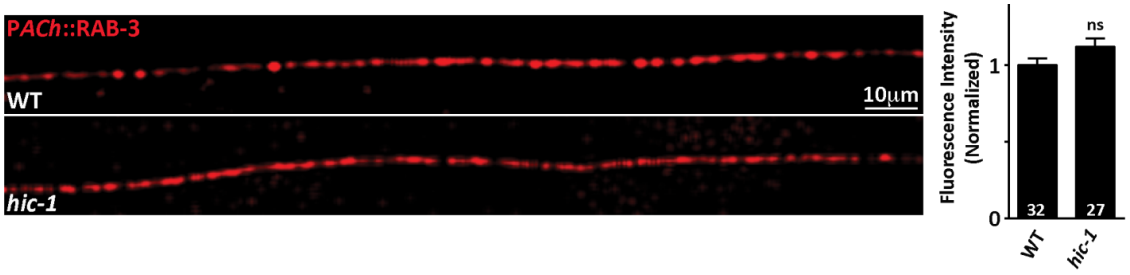

Figure 3.15 Cholinergic synaptic morphology is intact in *hic-1* mutants. Representative images of dorsal nerve cords of WT and *hic-1* worms expressing P*acr-2*::RAB-3::mCherry as a transgene. The summary data shows fluorescence intensity of RAB-3::mCherry.

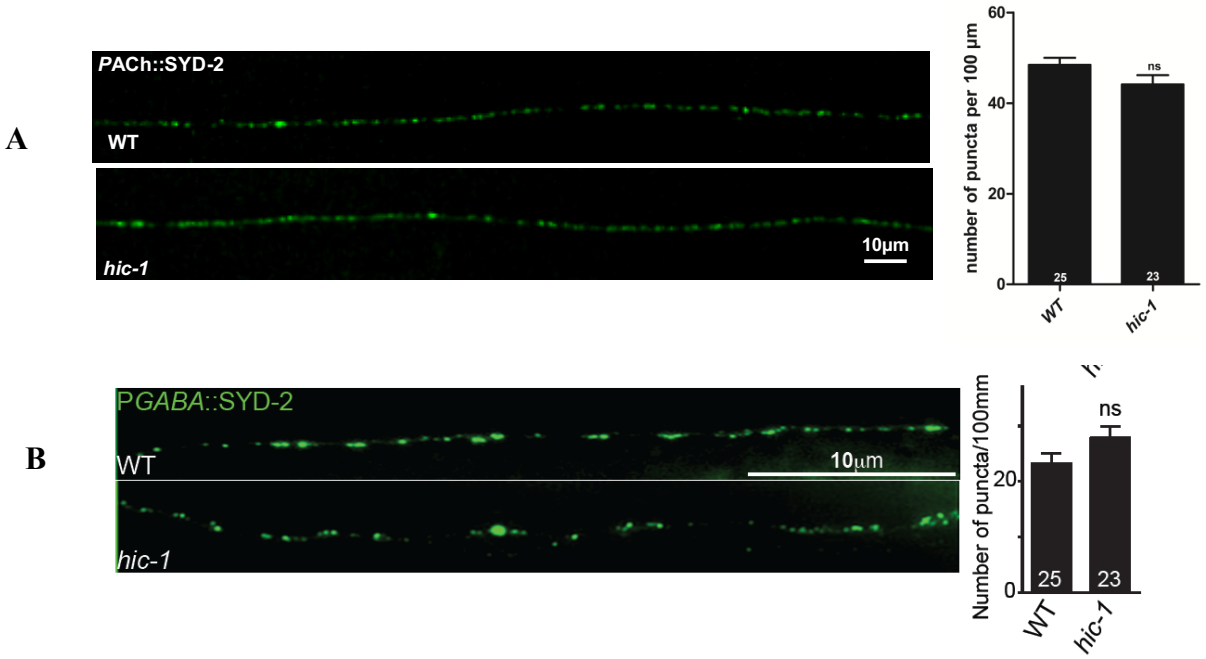

Figure 3.16 Synaptic density is unaltered in *hic-1* worms. Representative images of dorsal cords of WT and *hic-1* animals expressing SYD-2/α-LIPRIN as a transgene in (A) cholinergic (P*unc-17*::SYD-2::GFP), or (B) GABA neurons (P*unc-25*::SYD-2::GFP). The graph shows summary data of fluorescence intensity of SYD-2 punctual density.

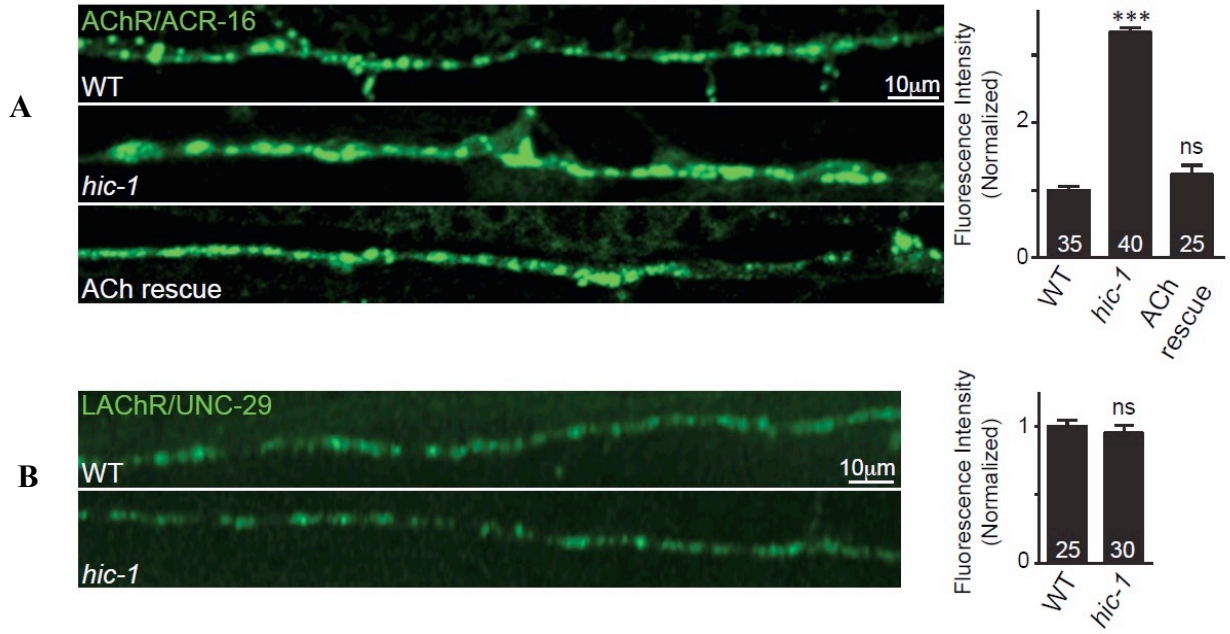

Figure 3.17 AChR/ACR-16 receptor levels are increased in *hic-1* worms. (A) Representative confocal images and summary data of fluorescence intensity of ACR-16::GFP receptors expressed in muscles (P*myo-3)* as a transgene in WT, *hic-1* animals expressing HIC-1 in cholinergic neurons. (B) Representative confocal images and summary data of fluorescence intensity of Levamisole-sensitive receptor subunit UNC-29 expressed in muscles (P*myo-3)* as a transgene in WT and *hic-1* worms.

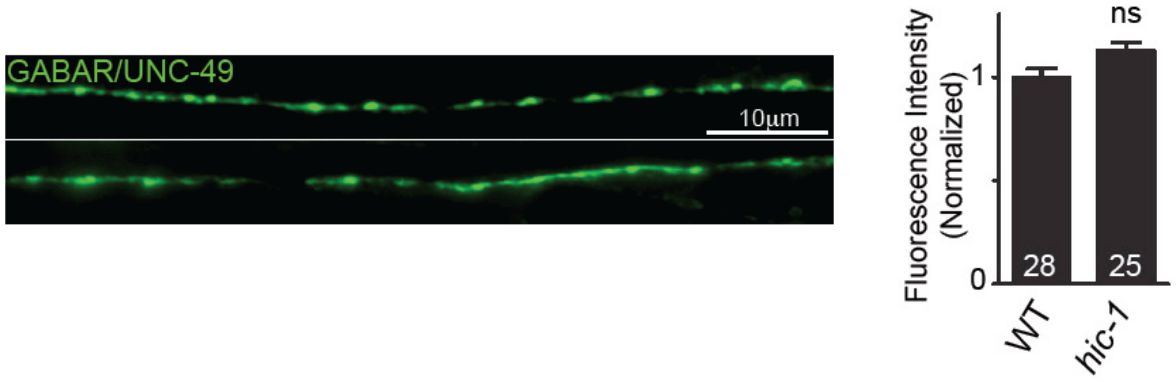

Figure 3.18 GABA receptors are not altered in *hic-1* mutants. Representative images and summary data of fluorescence intensity of GABA receptors tagged to GFP (*Pmyo-3*::UNC-49::GFP) in WT and *hic-1* worms.

AChR/acr-16 mutants appeared to completely suppress the hypersensitivity seen in the *hic-1* mutants (**Figure 3.20**).

So far, the data indicates that HIC-1 is required at the NMJ to specifically regulate AChR/ACR-16 levels. We next went on to test if the increased *AChR/acr-16* receptors in *hic-1* could contribute to increased muscle activity in these worms which is reflected by increased paralysis in the aldicarb assay.

3.4 Mutants in *hic-1* show aberrant muscle responsiveness:

So far, our results suggested that while there are no obvious presynaptic developmental defects in *hic-1* mutants, the postsynaptic AChR/ACR-16 levels are higher in these mutants. To further test if *hic-1* mutants show any defects in synaptic physiology, we went on to evaluate synaptic transmission in *hic-1* mutant animals. We first measured endogenous postsynaptic currents from NMJs, which reflects synaptic vesicles fusion evoked by the endogenous activity of the motor neurons. The electrophysiology recordings from the muscles showed that the frequency of the miniature excitatory postsynaptic current (mEPSC) was greater in the *hic-1* mutants when compared to WT controls (**Figure 3.21A**). This increase was rescued by expressing HIC-1 in cholinergic neurons (**Figure 3.21A**), however the average amplitude of mEPSCs was comparable to WT animals in *hic-1* mutant *C. elegans* (**Figure 3.21A**). We also measured evoked EPSCs in *hic-1* mutant animals, the peak amplitude of evoked EPSCs was not significantly different from the WT animals (**Figure 3.21B**). These data indicate that HIC-1 affects endogenous but not stimulus-evoked acetylcholine neurotransmitter release at the presynaptic nerve

terminals of the NMJ. In addition, the normal amplitudes of the mEPSCs and evoked EPSCs in *hic-1* mutants indicate that the number of functional AChR/ACR-16 receptors at the muscle membrane in *hic-1* is not altered. Since our data indicate that *hic-1* mutants show increased AChR/ACR-16 levels at the NMJ, this may suggest that the increased AChR/ACR-16 receptors in *hic-1* could be accumulating at non-synaptic or subsynaptic sites.

In order to test if there was any muscle activity defects caused by increased acetylcholine release or increased number of AChR/ACR-16 receptors, we analyzed calcium transients using GCaMP as a transgene expressed in the body-wall muscle of the animals (Schwarz et al., 2012). We measured the duration of the calcium transients in a complete cycle, which is the start of the calcium signals to the maximum peak and then maximum peak to the fall of the transients (Gong et al., 2016). The rise and fall time of the calcium transients in *hic-1* animals was not significantly different from WT animals (**Figure 3.21C**), however we observed a significant increase in the dwell time (**Figure 3.21C**). This phenotype were rescued upon expression of HIC-1 in cholinergic neurons. One possible explanation for this data could be that the increased acetylcholine release from the cholinergic NMJs in *hic-1* mutant animals (**Figure 3.21A**) could lead to increased calcium transients in the *hic-1* mutant animals. There is also a possibility that the increased subsynaptic fraction of AChR/ACR-16 receptors could also contribute to the increased Calcium response in *hic-1* animals (Brumwell et al., 2002).

We next wanted to investigate the mechanism of HIC-1 function in cholinergic neurons that allow for maintaining normal AChR/ACR-16 levels at the body-wall muscles. To further investigate how HIC-1 could be regulating AChR/ACR-16

receptors levels, we performed Fluorescence Recovery After photo-bleaching (FRAP) for ACR-16::GFP puncta in WT and *hic-1* mutant NMJs. FRAP measures diffusion of non-bleached fluorescent proteins to a bleached area (Reits and Neefjes, 2001). The speed and extent of the recovery of the fluorescent proteins depend on the movement of the protein. Synapses are thought to have two pools of receptors, one that is immobilized and does not recover after photo-bleaching and the other that is mobile and comes back to the region of interest (bleached area) with time (Dorsch et al., 2009). The percentage of fluorescence recovery and the rate of fluorescence recovery after photo-bleaching were significantly higher in *hic-1* mutants (**Figure 3.22**), indicating a higher percentage of a mobile fraction of AChR/ACR-16 receptors at the NMJ in *hic-1* mutants. Again, we were able to rescue this phenotype by specifically expressing HIC-1 in cholinergic neurons. These data indicate that HIC-1 could restrict the exchange between synaptic and mobile AChR/ACR-16 by controlling the mobile receptor fraction available for delivery at the synapse.

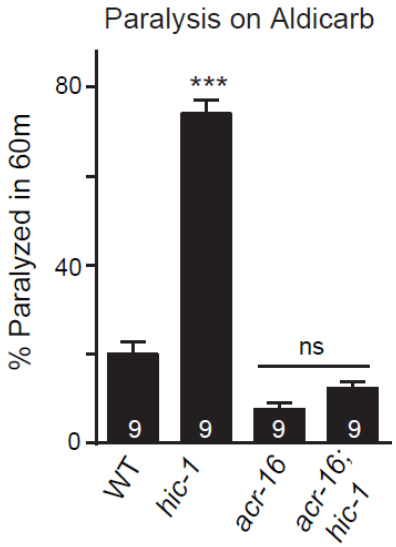

Figure 3.19 ACR-16 and HIC-1 are in the same signaling pathway. Percentage paralysis of different genotypes at 60 mins time point after aldicarb exposure.

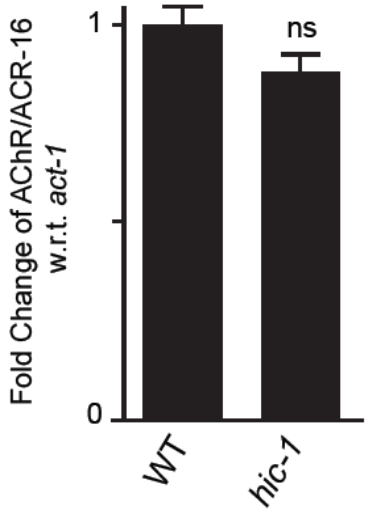

Figure 3.20 transcription level of AChR/ACR-16 is not altered in *hic-1* mutant worms. The bar graph of a quantitative real-time PCR experiment showing the fold change in the AChR/ACR-16 cDNA levels in WT and *hic-1* mutants with respect to the *act-1* gene as an internal control.

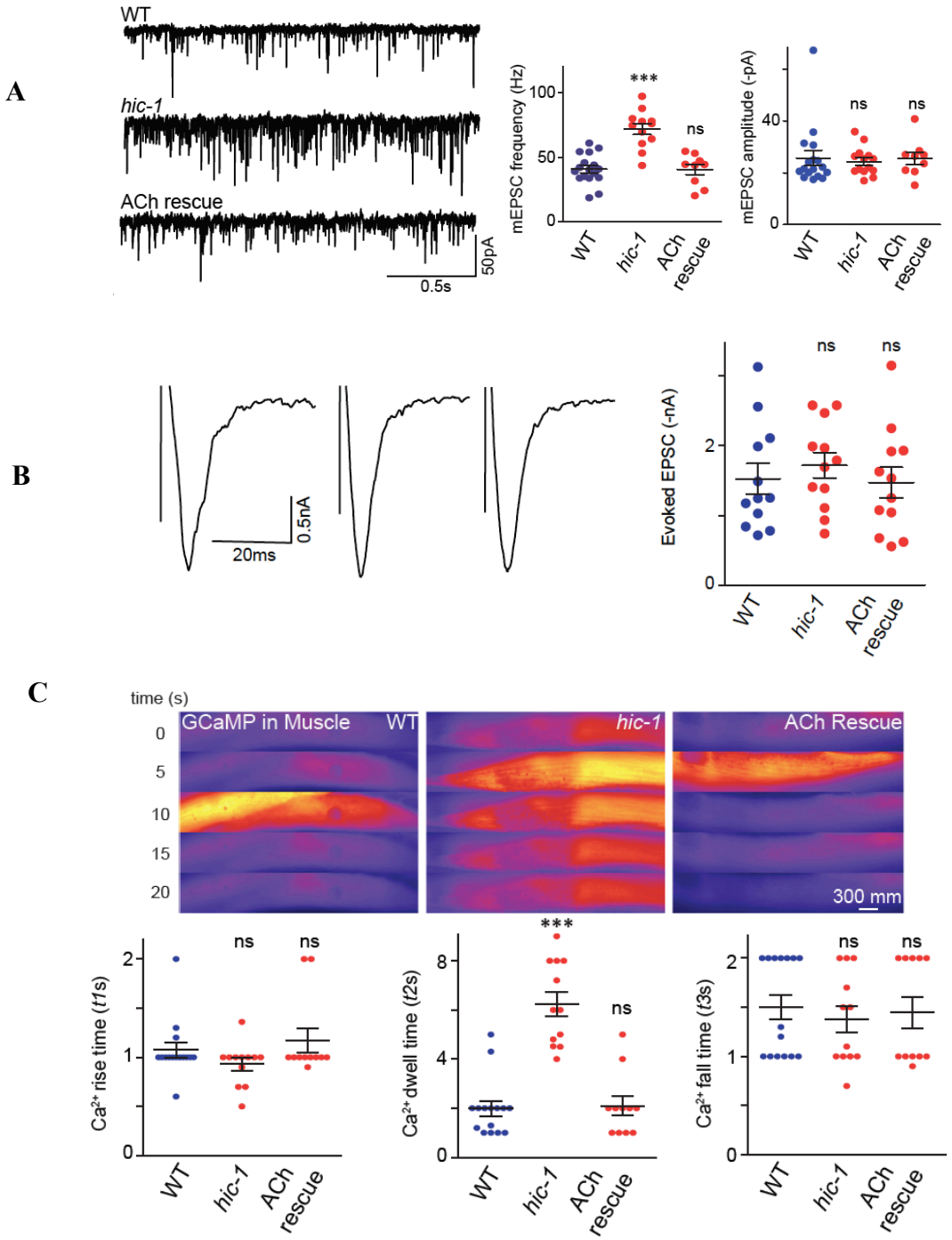
A
WT
hic-1
ACh rescue
50pA
0.5s
mEPSC frequency (Hz)
100
50
0
***
ns
WT
hic-1
ACh rescue
mEPSC amplitude (-pA)
40
0
ns
ns
B
0.5nA
20ms
Evoked EPSC (-nA)
2
0
ns
ns
C
time (s)
0
5
10
15
20
GCaMP in Muscle
WT
hic-1
ACh Rescue
300 mm
Ca2+ rise time (t1s)
Ca2+ dwell time (t2s)
Ca2+ fall time (t3s)

Figure 3.21 Muscle responsiveness is aberrant in *hic-1* mutant animals

A. Whole-cell recordings on the muscles were performed to record endogenous acetylcholine (ACh) release (mEPSCs) from WT, *hic-1*, and *hic-1*; P*ACh*::HIC-1 animals. The mEPSC frequency is greater in *hic-1* mutant *C. elegans* and is rescued by expressing HIC-1 in cholinergic neurons. The mEPSC amplitude was not significantly different across genotypes. The animals tested were: n=17 (WT), n=12 (*hic-1*) and n=9 (*hic-1*; P*ACh*::HIC-1).

B. Representative traces and summary data for evoked EPSCs peak amplitude in WT and *hic-1 C. elegans*. n=12 (WT), n=12 (*hic-1*), n=12 (*hic-1*; P*ACh*::HIC-1). The Data are represented as mean ± SEM and p values calculated using one-way ANOVA and Bonferroni's Multiple Comparison Test.

C. GCaMP is expressed in the body-wall muscles using a muscle-specific promoter. Representative time-lapse fluorescence images and data analysis of calcium transients in the *C.elegans* muscles are shown here. The *hic-1* mutants show increased calcium transients, which are rescued by expressing HIC-1 in cholinergic neurons. The dot plot graphs represent rise time (*t1*s), dwell time (*t2*s), and fall time (*t3*s) constants for calcium transients in different genotypes. p values calculated using one-way ANOVA and Bonferroni's Multiple Comparison Test. Animals tested: n=15 (WT), n=12 (*hic-1*) and n=11 (*hic-1*; P*ACh*::HIC-1).

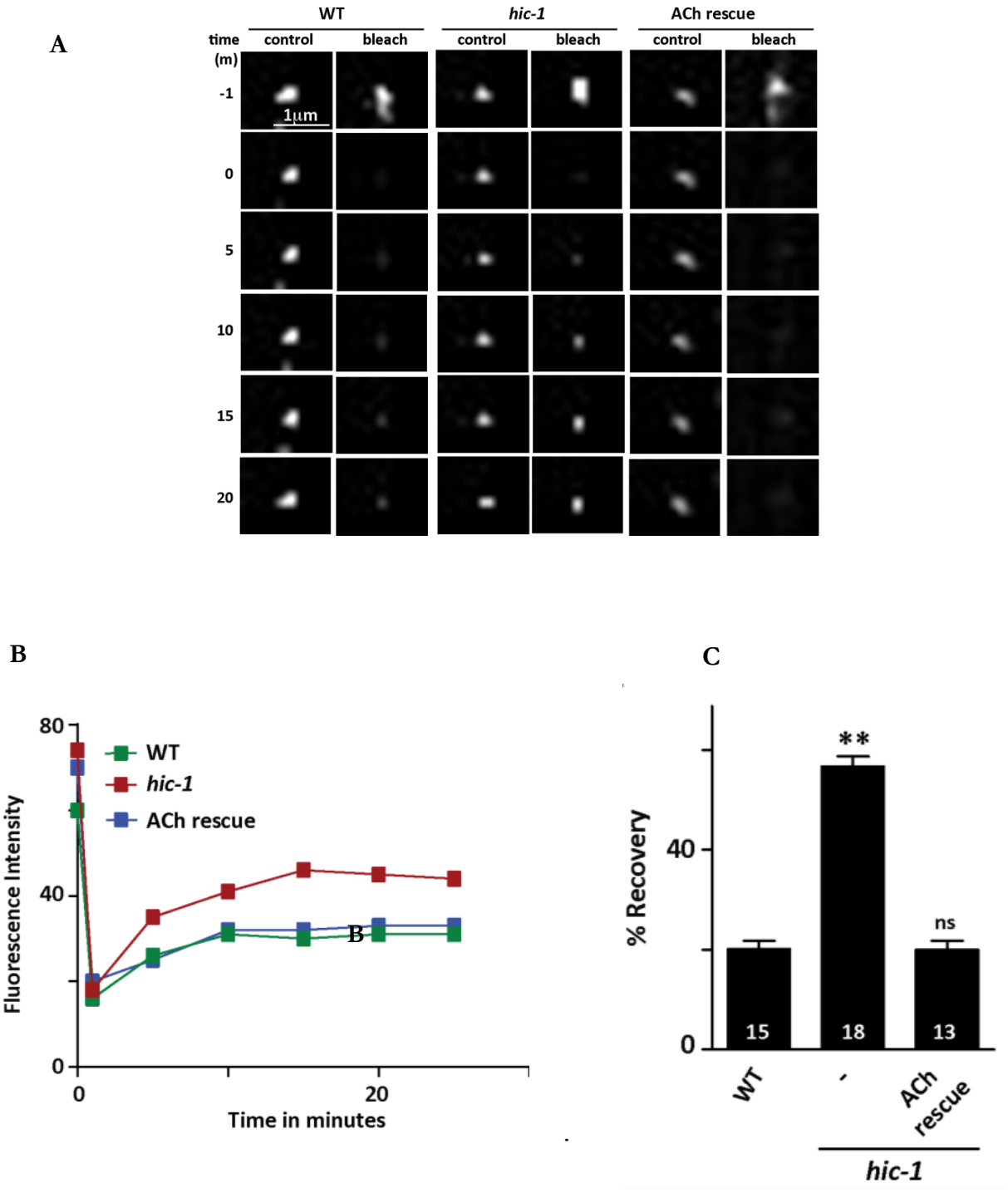
A
WT
hic-1
ACh rescue
time (m)
control
bleach
control
bleach
control
bleach
-1
0
5
10
15
20
1µm
B
Fluorescence Intensity
80
40
0
WT
hic-1
ACh rescue
B
0
20
Time in minutes
C
% Recovery
40
0
**
ns
15
18
13
WT
ACh rescue
hic-1

Figure 3.22 Mutants in *hic-1* show increased recovery rates of postsynaptic AChR/ACR-16

A. Representative time-lapse images at multiple time points of a single punctum of ACR-16::GFP that undergoes photobleaching for a FRAP experiment along with the non-bleached control puncta. -1m refers to the time before bleaching. The punctum was photobleached at the 0m time point, and the fluorescence intensity was measured at 5 m intervals. The fluorescence recovery and the percentage of recovery were calculated till the fluorescence intensity reached a plateau (at the 15 m time point).
B. The line graph shows the recovery rate of a single ACR-16::GFP puncta after photobleaching in WT, *hic-1* and *hic-1*; P*ACh*::HIC-1 animals.
C. The bar graph shows the percentage of recovery (fluorescence intensity of ACR-16::GFP puncta after photobleaching) at the 15m time point. The numbers at the base of the bar-graph indicate the number of puncta analyzed and the genotypes tested were WT, *hic-1,* and *hic-1*; P*ACh*::HIC-1.

3.5 Mutants in *hic-1* show increased locomotory behavior:

The *hic-1* mutants show increased paralysis in the presence of aldicarb drug (**Figure 3.1**). This increased hypersensitivity suggests an increased activity at the NMJs which could lead to fast movement of the worms (Niebur and Erdös, 1991; Thapliyal et al., 2018).

The locomotory behavior of the worms were analyzed in the absence of the food by counting total number of Body bends made by a single worm per minute and then taking an average for all the worms analyzed per genotype (Wu et al., 2012). We found that *hic-1* worms showed an increased rate

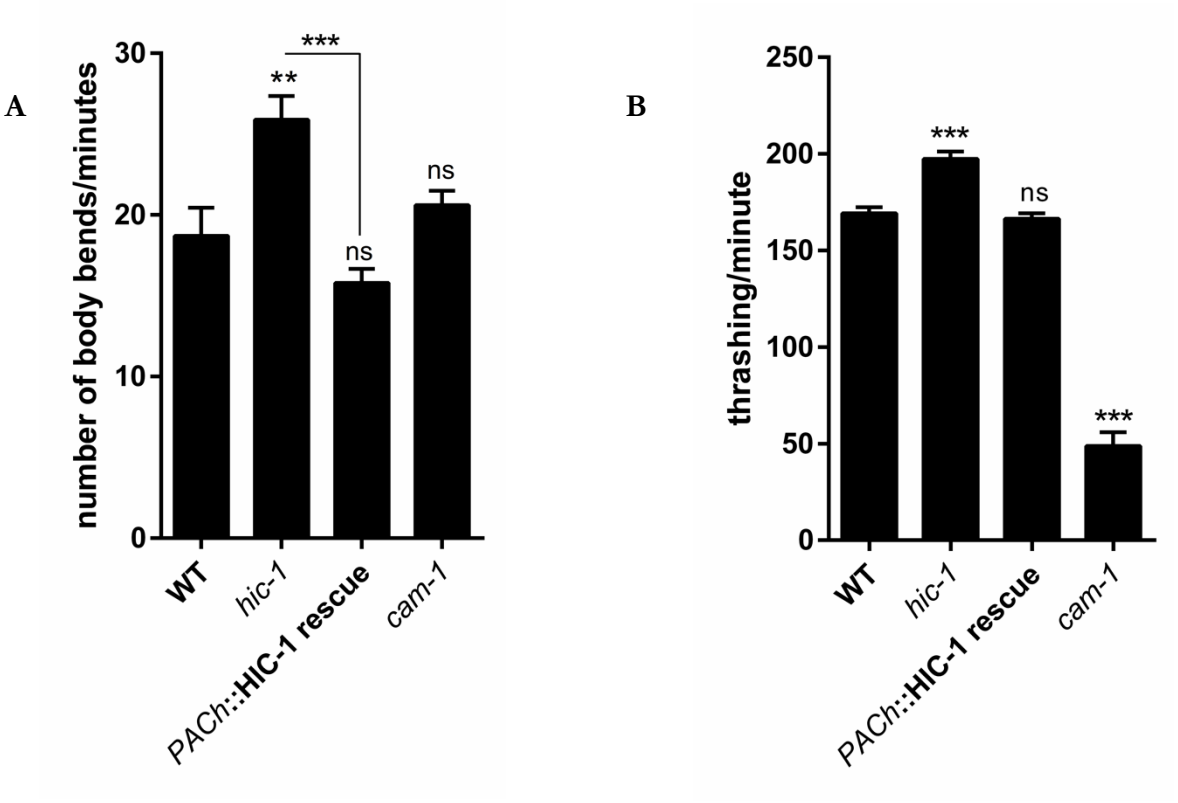

Figure 3.23 Mutants in *hic-1* show increased number of body bends and thrashing rates. Bar graphs showing rates of (A) body bends, and (B) thrashing for different genotypes. *cam-1* was used as a control. (N>25)

of body bends compared to WT worms (**Figure 3.23**). Also, thrashes of the worms per minute in the M9 buffer was calculated. One thrash corresponds to movement or swimming of the worm in one direction (Buckingham and Sattelle, 2009). We again found that thrashing rate was also significantly enhanced in the *hic-1* worms. The increased frequency of body bends and thrashing seen in *hic-1* mutants were rescued using the cholinergic rescue line of HIC-1. We next wanted to investigate

the mechanism of HIC-1 function in cholinergic neurons that allows for maintaining normal AChR/ACR-16 levels at the body-wall muscles.

Discussion

Although claudins are known to function in the epithelium (Gunzel and Yu, 2013), the present study characterizes synaptic functions of a novel yet uncharacterized claudin-like molecule, T28B4.4/HIC-1 in *C.elegans.* The aldicarb assay and co-localization studies revealed that HIC-1 is functioning at cholinergic synapses. ClaustalW multialignment analysis of different vertebrate and invertebrate claudins suggests that HIC-1 seems to be having a conserved PDZ binding motif at its C-terminus tail (**Figure 3.3**), which means it could have intracellular cell signaling functions similar to other claudins functioning at the epithelium. Although no obvious neuronal or synaptic developmental defects were seen in *hic-1* mutant worms, one class of acetylcholine receptors AChR/ACR-16 levels showed increased amounts on the muscle membrane in the *hic-1* mutants. To understand if the increased ACR-16 receptor phenotype could lead to increased muscles responsiveness in *hic-1* worms, calcium imaging and electrophysiology recording experiments were performed which suggested that there was a possibility that HIC-1 could be involved in increased muscle responsiveness. In the calcium imaging experiment, we could not detect any significant changes in the amplitude of the peak calcium transients in *hic-1* mutants (data not shown). However, the decay duration of the calcium transients was prolonged in these worms, indicating that there could be more functionally active ACR-16/α7 receptors on the muscle membrane in the *hic-1* mutants. Further, no change in the miniature EPSCs or

IPSCs from the *hic-1* NMJs suggest that the basal synaptic release is unaffected in these worms. Our data so far suggest that HIC-1, a presynaptic molecule is required for regulating postsynaptic acetylcholine receptors present at the muscle membrane. An obvious question one could ask is how HIC-1 is functions presynaptically to affect postsynaptic receptor levels. In the next chapter, we have tried to solve this mystery by using genetic and molecular approaches available in *C.elegans.*

Chapter 4:
HIC-1 regulates postsynaptic acetylcholine receptors (AChR/ACR-16) levels by controlling Wnt secretion from the cholinergic neurons

Introduction

A single neurotransmitter can activate multiple receptors, localized differentially on the pre- or postsynaptic membrane and the activation of different receptors can be distinguished on the basis of their pharmacological or electrophysiological responses (Jones and Sattelle, 2004). As mentioned earlier, most of the excitatory currents at the *C.elegans* NMJs are mediated by ACR-16/α7 receptors. Apart from acetylcholine and nicotine, the surface expression of these ACR-16/α7 receptors is regulated by the Wnt signaling pathway (Babu et al., 2011b; Barik et al., 2014b; Jensen et al., 2012b; Pandey et al., 2017; Wang et al., 2008a).Our results indicated a function of HIC-1 in maintaining the ACR-16/α7 receptors. Previous Studies suggest that a CAM-1/ ROR receptor tyrosine kinase receptor is functional at both pre and postsynaptic compartments of the *C.elegans* NMJs (Francis et al., 2005a) and Its postsynaptic expression on the muscle membrane contributes to the stabilization or trafficking of the ACR-16/α7 receptors on the muscle membrane (Francis et al., 2005a). Furthermore, Jensen et al. have elegantly dissected out the Wnt signaling pathway, which regulates the translocation of ACR-16/α7 receptors at the *C.elegans* NMJs. Their study shows that ACR-16/ α7 receptor translocation is mediated by members of the canonical Wnt signaling pathway pathway (Jensen et al., 2012a). Out of five Wnts LIN-44, EGL-20, CWN-1, CWN-2, and MOM-2 in *C.elegans* (Hilliard and Bargmann, 2006), CWN-2 is involved in this pathway. CWN-2 is released from the cholinergic neurons and binds to a heteromeric receptor; CAM-1/ROR-type receptor tyrosine kinase and LIN-17/Frizzled, which further activates its downstream effector Disheveled (DSH-1) to modulate surface

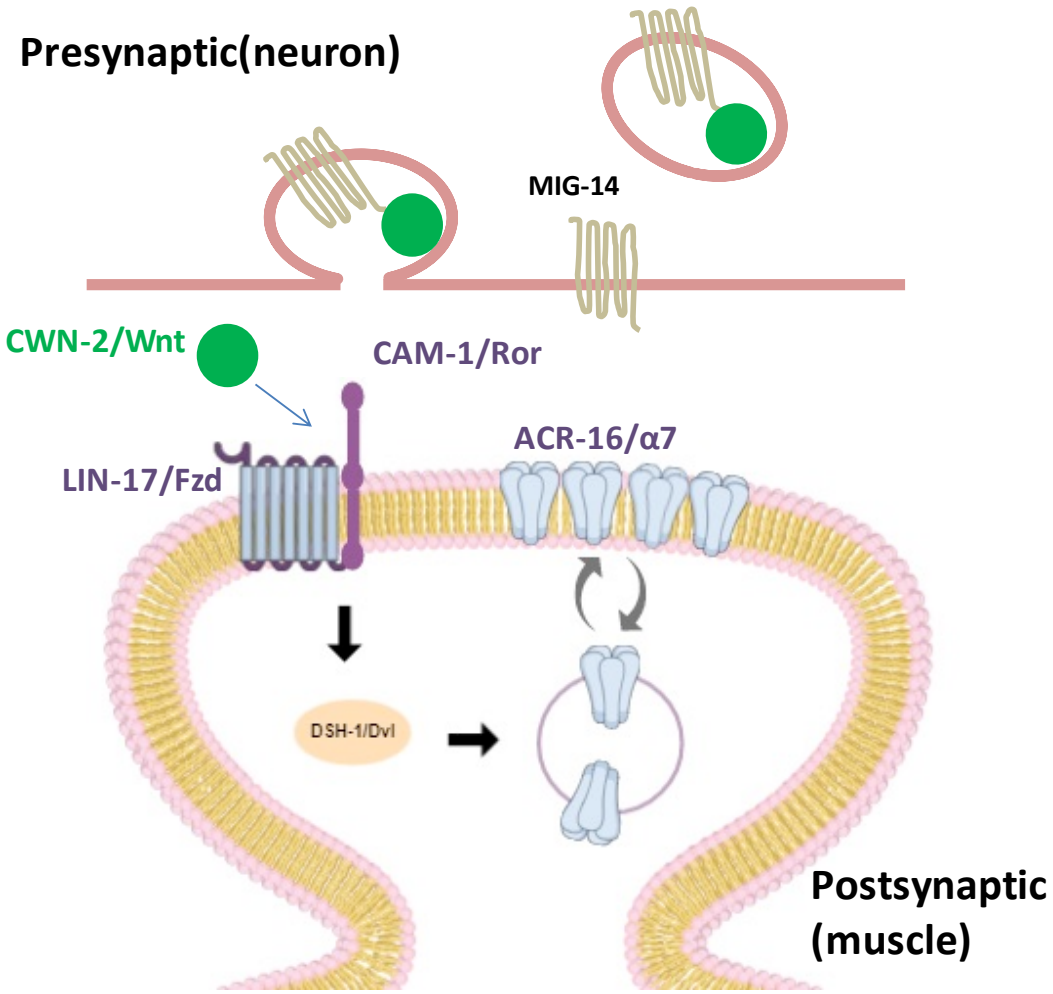

Figure 4.1. Regulation of ACR-16 receptors by Wnt signaling pathway: MIG-14/Wntless, a seven-pass transmembrane protein is required for the secretion of all the Wnts. CWN-2/Wnt is secreted from the motor neurons and binds to a heteromeric receptor LIN-17/Fzd and CAM-1/Ror present at the postsynaptic muscle membrane. The activated receptor then triggers downstream signaling involving DSH-1/Dvl and regulates ACR-16/α7 receptor trafficking on the muscle membrane (Image modified from Jensen et al., 2012).

expression of ACR-16/α7 receptors (Jensen et al., 2012b). Their studies also revealed that ACR-16/ α7 receptors are involved in the activity-dependent synaptic plasticity, which is also mediated by heteromeric CAM-1 and LIN-17 receptors. A schematic of the Wnt signaling which regulates ACR-16/α7 translocation on the muscle membrane is illustrated above (**Figure 4.1**). Previous work has shown that a GPI anchored immunoglobulin (Ig) superfamily protein, RIG-3 acts as an antipotentiation molecule at the *C.elegans* NMJ. RIG-3 is involved in the Wnt Signaling pathway to modulate the levels of ACR-16/ α7 receptors (Babu et al., 2011a). RIG-3 functions at the presynaptic motor neurons where it directly interacts with immunoglobulin domain of a nonconventional Wnt receptor, CAM-1 and inhibits the function of LIN-44/WNT in the Wnt signaling pathway which in turn regulates ACR-16/α7 receptors levels on the postsynaptic muscle membrane (Pandey et al., 2017). Using genetic and molecular approaches, we found that HIC-1 is also a component of the Wnt signaling pathway that regulate ACR-16/α7 receptor levels and it does so by regulating the secretion of Wnt ligands from cholinergic motor neurons.

A lot of previous work has shown that claudins interact with the actin cytoskeleton through their PDZ binding motif (Nomme et al., 2015; Turksen, 2004). Here also we have discovered that HIC-1, a claudin homolog, is required to maintain a normal actin cytoskeleton. Our data shows that changes in the actin cytoskeleton by loss of *hic-1* causes increased release of Wnt vesicles from motor neurons. We also see a similar phenotype of enhanced Wnt secretion when the actin cytoskeleton is disrupted using an actin depolymerizing drug, Latrunculin A.

Results

4.1 HIC-1 is required to maintain normal Wnt release from cholinergic neurons

The data so far suggests that HIC-1 is functional in cholinergic motor neurons to regulate the levels of postsynaptic ACR-16/ α7 receptors; we wondered how HIC-1 being a presynaptic molecule could be affecting ACR-16/α7 levels through the Wnt signaling pathway. To address the possibility that HIC-1 could be functioning through the Wnt signaling pathway to regulate ACR-16/α7 delivery at the body-wall muscle surface; we first performed aldicarb assays for different Wnt pathway mutants involved in ACR-16/α7 receptor regulation in the *hic-1* mutant background. MIG-14/Wntless, a conserved seven-pass transmembrane receptor is required for the secretion of Wnt vesicles from Wnt-producing cells

The *C.elegans mig-14* mutants are resistant to aldicarb in comparison to WT animals, while the *mig-14; hic-1* double mutants were able to suppress the hypersensitivity of *hic-1* mutants and show a phenotype indistinguishable from the *mig-14* mutant phenotype **(Figure 4.2A**), suggesting that MIG-14 could function downstream of HIC-1. Previous studies have shown that the canonical Wnt receptor, LIN-17/Frizzled, is required for maintaining ACR-16/α7 on the body-wall muscles (Jensen et al., 2012a). We went on to further understand the role of HIC-1 in the Wnt signaling pathway and to test if HIC-1 is functioning through Frizzled /LIN-17, we made double mutants *frizzled/lin-17; hic-1* and performed the aldicarb assay with the double mutants. We found that the

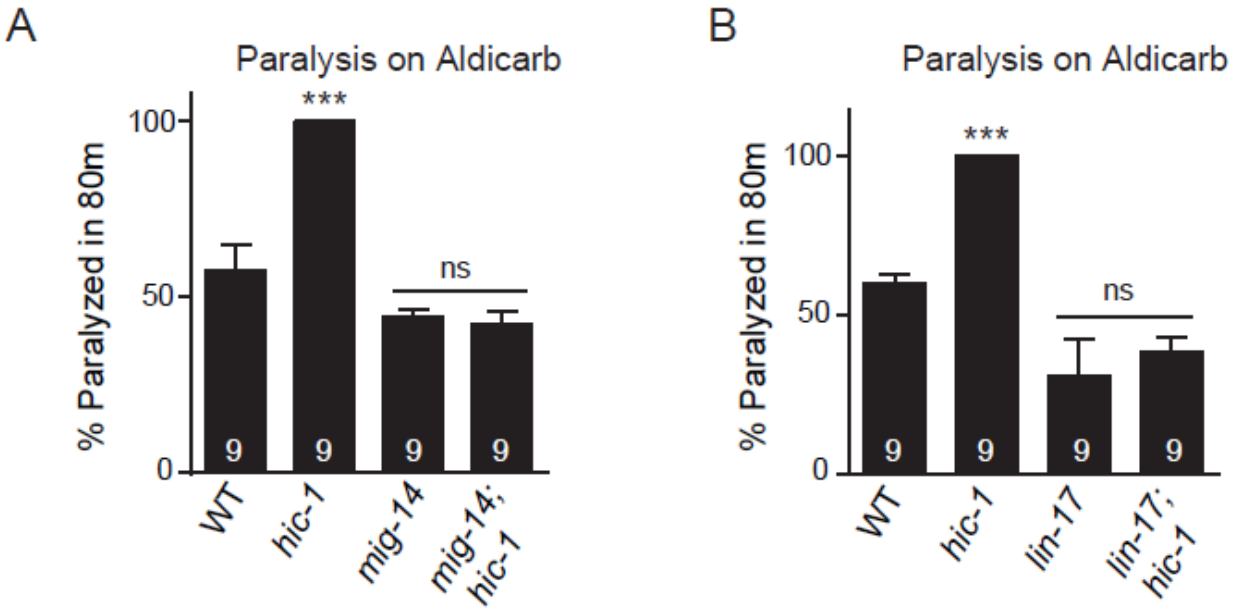

Figure 4.2 HIC-1 is involved in the Wnt signaling pathway and is upstream to MIG-14 and LIN-17.

(A) Indicates a bar-graph of aldicarb assays for double mutants containing *wntless/mig-14* and *hic-1* along with control animals.

(B) Indicates the paralysis of *C. elegans* on aldicarb for *frizzled/lin-17; hic-1* mutants along with control strains.

hypersensitivity to aldicarb that was seen in *hic-1* mutants was completely suppressed by mutants in *frizzled/lin-17* (**Figure 4.2B**) indicating that HIC-1 might be functioning through the LIN-17 Wnt receptor and more generally through the Wnt signaling pathway. We next wanted to understand how HIC-1 could be affecting the Wnt pathway through its expression in presynaptic neurons. One

possible function for HIC-1 could be to regulate Wnt vesicle release from cholinergic synapses that are known to express Wnt (Koles and Budnik, 2012b). To address the role of HIC-1 in Wnt secretion, we went on to visualize Wnt secretion in *hic-1* mutants. To visualize Wnt secretion, we took advantage of the well-established coelomocyte assay in *C. elegans.* Coelomocyte are specialized scavenger cells in *C. elegans*, which take up molecules that are secreted in the body cavity/pseudocoelom (Fares and Greenwald, 2001; Sieburth et al., 2006). Previous reports have also used this assay to study Wnt/CWN-2 and Wnt/LIN-44 secretion (Jensen et al., 2012a; Pandey, 2017) and illustrated in **Figure 4.3A**)). Since both Wnt/CWN-2 and Wnt/LIN-44 have been reported to be required for maintaining ACR-16/α7 levels at the NMJ, we assayed the secretion of these two Wnts.

Wnts tagged with mCherry were expressed exclusively in cholinergic neurons, and imaged for fluorescence intensity in the dorsal cord as well as in coelomocytes (**Figures 4.3B-D**).

The dorsal cord punctal fluorescence corresponds to secretory vesicles containing Wnts in the axons, and the coelomocyte fluorescence indicates Wnts that are secreted from the neurons and accumulate in the coelomocytes (Fares and Greenwald, 2001; Sieburth et al., 2007). We observed that in *hic-1* mutants, coelomocyte fluorescence was significantly increased whereas the punctal axonal fluorescence intensity of CWN-2 was significantly reduced (**Figure 4.3B and C**). To further confirm that we were indeed looking at Wnt secretion, we injected a coelomocyte specific marker P*unc-122*::GFP (Frøkjær-Jensen et al., 2008) in

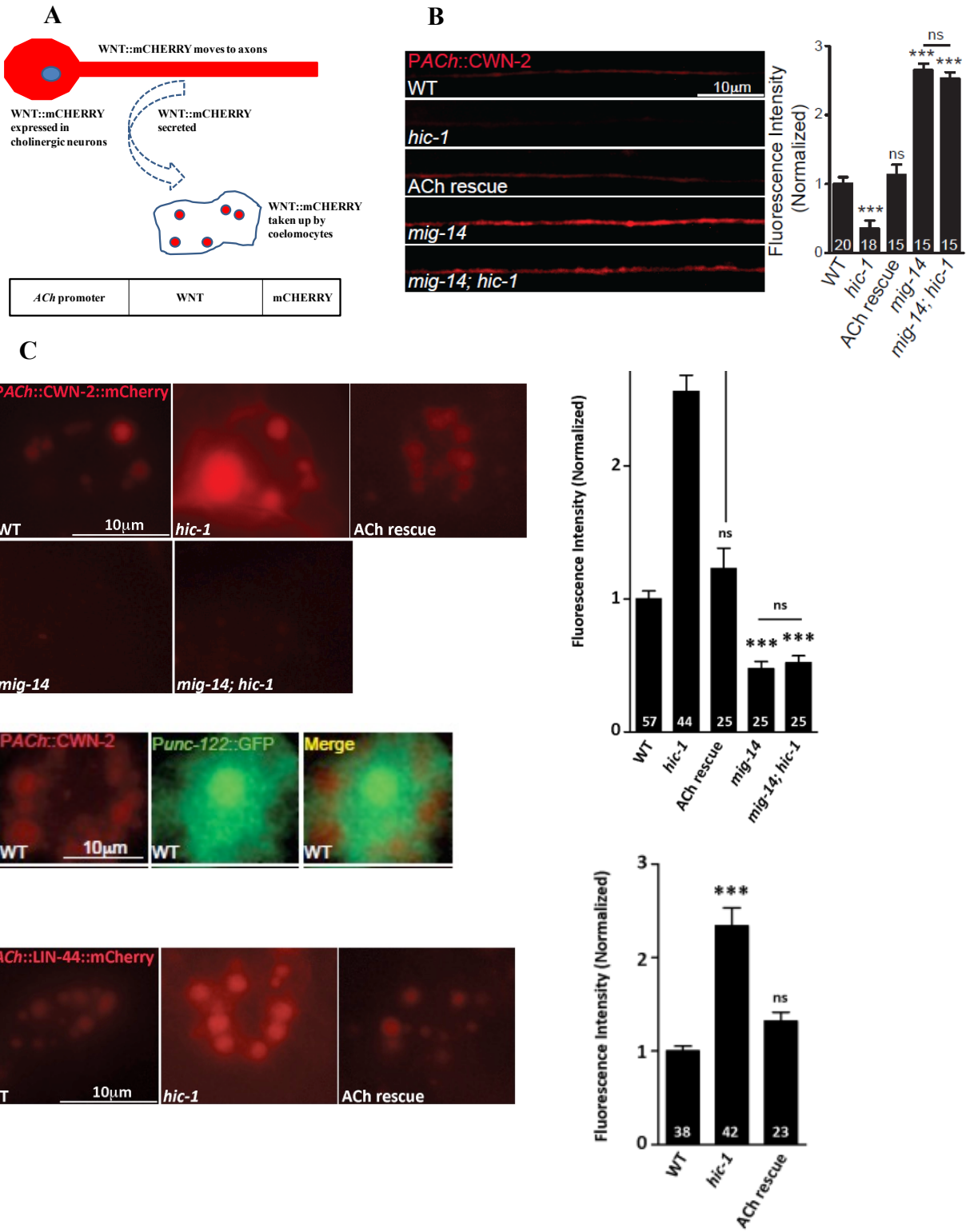
A
WNT::mCHERRY moves to axons
WNT::mCHERRY expressed in cholinergic neurons
WNT::mCHERRY secreted
WNT::mCHERRY taken up by coelomocytes
ACh promoter
WNT
mCHERRY
B
PACh::CWN-2
WT
10µm
hic-1
ACh rescue
mig-14
mig-14; hic-1
Fluorescence Intensity (Normalized)
ns
***
20
18
15
15
15
WT
hic-1
ACh rescue
mig-14
mig-14; hic-1
C
PACh::CWN-2::mCherry
WT
10µm
hic-1
ACh rescue
mig-14
mig-14; hic-1
Fluorescence Intensity (Normalized)
57
44
25
25
25
D
PACh::CWN-2
Punc-122::GFP
Merge
WT
10µm
E
PACh::LIN-44::mCherry
38
42
23

Figure 4.3 Wnt secretion is enhanced in *hic-1* mutant worms – (A) Illustration of the Coelomocyte uptake assay for Wnts (based on previously described assays from (Fares and Greenwald, 2001; Jensen et al., 2012a; Sieburth et al., 2006). The Wnt Ligand is tagged with mCherry, and the fluorescence is quantitated along the DNC and in the coelomocytes. The fluorescence in the coelomocytes represents secreted Wnt.
(B) Wnt/CWN-2 fluorescence along the DNC and quantitation of intensity of fluorescence (normalized) from WT, *hic-1*, HIC-1 rescue in ACh neurons, *mig-14* and *mig-14; hic-1* animals.
(C) Representative images and quantitation of coelomocyte fluorescence (normalized) in animals expressing mCherry tagged Wnt/CWN-2 in cholinergic neurons from WT, *hic-1*, HIC-1 rescue in ACh neurons, *mig-14* and *mig-14; hic-1* animals.
(D) Coelomocyte form a Wild type worm expressing CWN-2::mCherry and a coelomocyte-specific marker P*unc-122*::GFP.
(E) Representative images and quantitation of coelomocyte fluorescence (normalized) in animals expressing mCherry tagged Wnt/LIN-44 in cholinergic neurons. The following *C. elegans* strains are indicated; WT, *hic-1,* and *hic-1*; P*ACh*::HIC-1.

worms expressing (representative image is shown in **Figure 4.3D**) and we also analyzedWnt secretion in the *Wntless*/*mig-14* background. Wntless/MIG-14 has been previously shown to be required for the binding and secretion of Wnt ligands from Wnt-producing cells and loss of *Wntless/mig-14* causes a decrease in Wnt secretion (Eisenmann and Kim, 2000). We observed a significant reduction of Wnt secretion in the coelomocytes and a concomitant increase in the axonal punctal fluorescence in the *Wntless/mig-14*mutants (**Figure 4.3B and C**). Also, we observed that *Wntless/mig-14* was completely able to suppress both the increased coelomocyte fluorescence and decreased axonal punctal fluorescence defects of *hic-1* mutants (**Figure 4.3B and C**). To test if HIC-1 could be affecting the

expression of Wnt ligands, we performed quantitative real-time PCR experiments for the Wnt ligands CWN-2 and LIN-44 in WT, *hic-1,* and *Wntless*/*mig-14* mutant animals. No significant differences in the RNA levels of *cwn-2* and *lin-44* were detected in any of the two mutants in comparison with WT animals (**Figure 4.4**), indicating that HIC-1 does not appear to affect the expression of Wnt genes.

Since HIC-1 appeared to be affecting Wnt release from cholinergic neurons, we next asked if HIC-1 could function as a more general molecule involved in the release of small proteins from cholinergic neurons. To this end we performed two experiments; first, we performed an aldicarb assay to see if mutants in *hic-1* could function in the same pathway as neuropeptides. We tested the aldicarb phenotype of *egl-21* (a carboxypeptidase, required for the normal synthesis of neuropeptides) (Trent et al., 1983), similar to previous reports, we also found that *egl-21* mutants were resistant to aldicarb (Sieburth et al., 2005b) while the *egl-21;hic-1*double mutants showed a phenotype that was intermediate between the resistance seen in *egl-21* mutants and the hypersensitivity to aldicarb seen in *hic-1* mutants (**Figure 4.5A**). These data indicate that HIC-1 may not be functioning through neuropeptides. Next, we went on to look at the expression of the neuropeptide NLP-21 tagged with YFP and expressed in cholinergic neurons (Staab et al., 2013) in WT and *hic-1* mutants. On imaging the dorsal cord and the coelomocyte in these mutants, we found no significant differences in the fluorescence intensity in either the cord or the coelomocytes (**Figure 4.5B and C**).

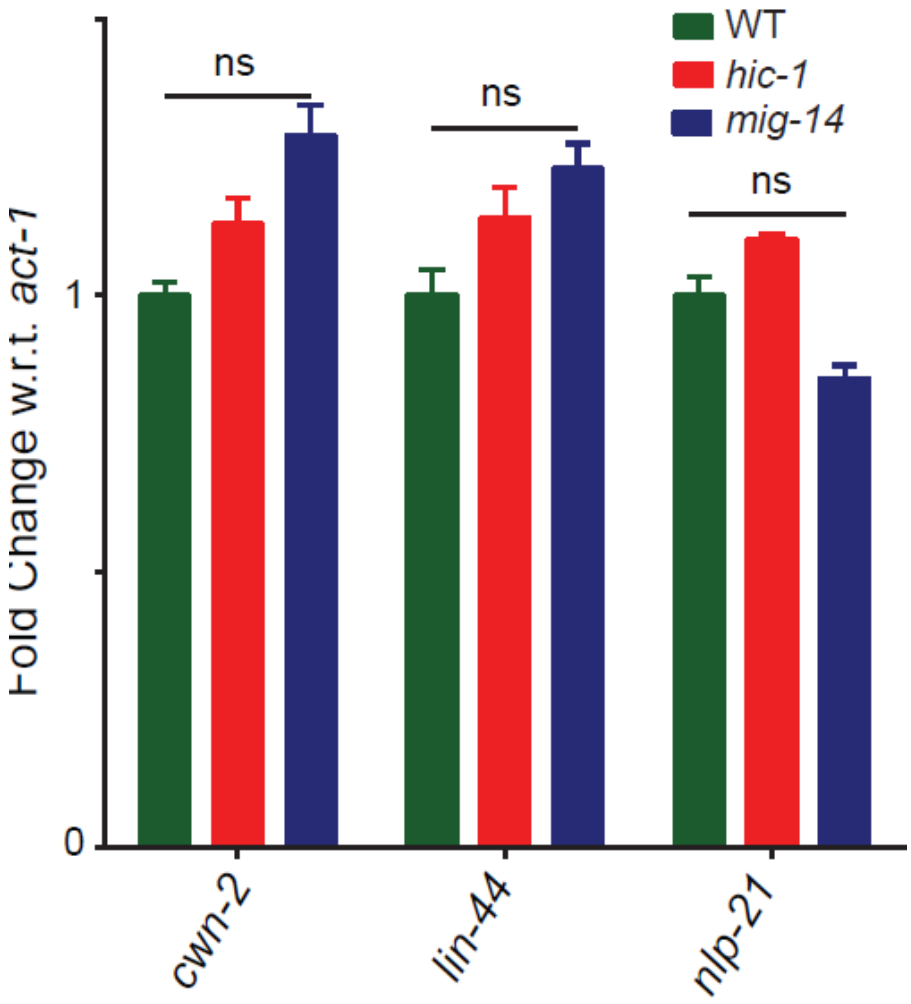

Figure 4.4 Quantitative real-time PCR graph for Wnt ligands *cwn-2*, *lin-44*, and the neuropeptide *nlp-21* in the following genotypes; WT*, hic-1*, and *mig-14.*

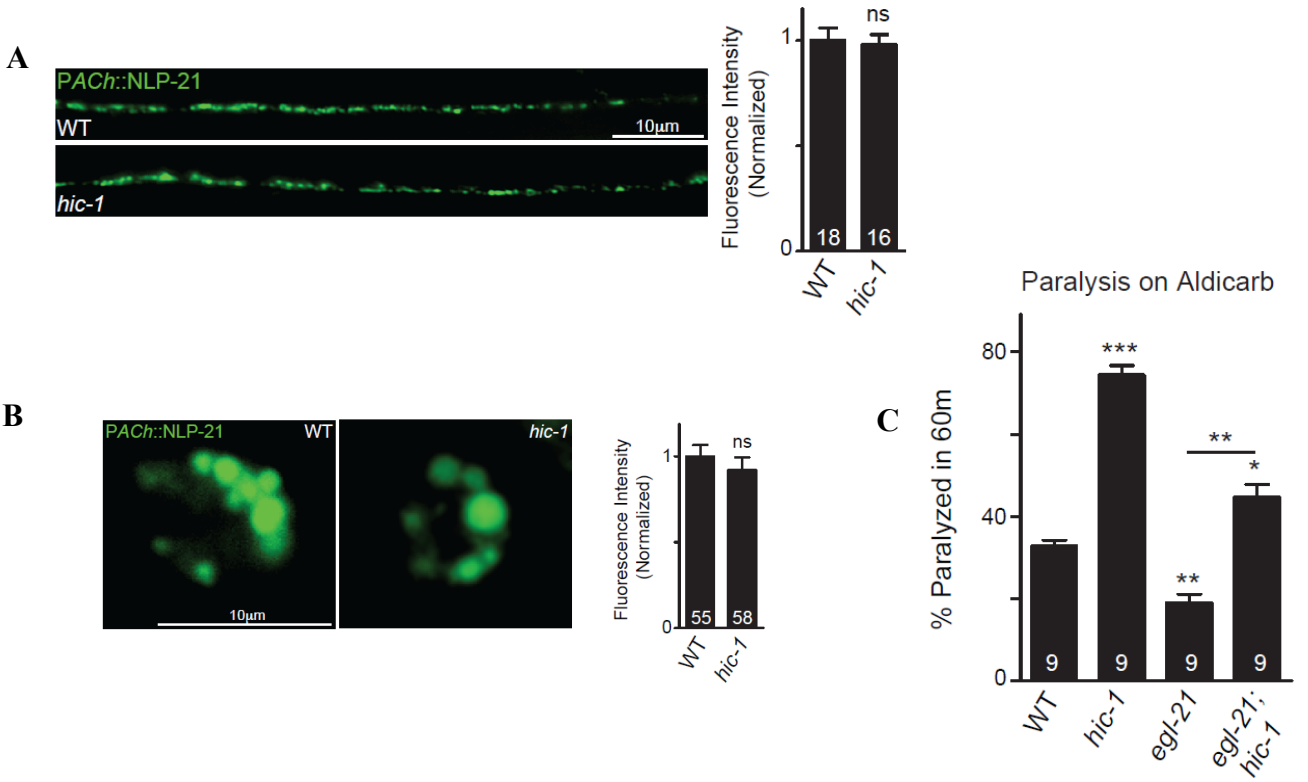

Figure 4.5 HIC-1 is not involved in Neuropeptide signaling or secretion

(A) Bar-graph indicating the paralysis of *C. elegans* at the 60m time point. The genotypes assayed were; WT, *hic-1*, *egl-2,* and *egl-21; hic-1*.

(B) Representative images and quantitation of fluorescence intensity (normalized) along the DNC in animals expressing fluorescently tagged NLP-21 in cholinergic motor neurons. WT and *hic-1*mutant animals were analyzed.

(C) Representative images and quantitation of fluorescence intensity (normalized) in the coelomocytes of WT and *hic-1* mutant animals, expressing fluorescently tagged NLP-21 in cholinergic motor neurons.

These data indicate that *hic-1* does not appear to affect neuropeptide secretion from cholinergic synapses indicating that HIC-1 is not a general factor affecting constitutive secretion of small molecules. Taken together, these data indicate that the HIC-1 is required for normal Wnt secretion from cholinergic neurons and that HIC-1 functions upstream of the Wnt signaling pathway to regulate AChR/ACR-16 levels at the NMJ. We next wanted to understand how HIC-1 could be affecting Wnt secretion.

4.2 HIC-1 is required to maintain the actin cytoskeleton in cholinergic neurons

Claudins interact with the actin cytoskeleton via mediator proteins, which in turn allows them to participate in intracellular cell signaling (Kojima et al., 2013). Further, it is known that the actin cytoskeleton undergoes changes at the synapse during increased synaptic activity and could play a role in ACh neurotransmitter release (reviewed in (Dillon and Goda, 2005)).We were interested in testing if HIC-1, being a claudin homolog, could be involved in maintaining the actin cytoskeleton. We performed imaging experiments to visualize the actin network at the cholinergic synapses by initially using an actin-binding protein Gelsolin (GSLN-1) tagged with GFP and expressed in cholinergic synapses (Sieburth et al., 2005b). We observed that the GSLN-1::GFP fluorescence intensity was significantly reduced in the *hic-1* mutants in comparison to WT controls (**Figure 4.6A**). The decreased levels of Gelsolin in *hic-1* was completely rescued by expressing HIC-1 in cholinergic neurons (**Figure 4.6A**). These results suggest that the actin cytoskeleton could be disrupted in the absence of *hic-1*.

A

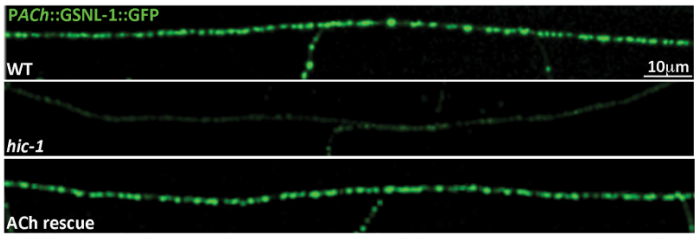
PACh::GSNL-1::GFP
WT
10μm
hic-1
ACh rescue

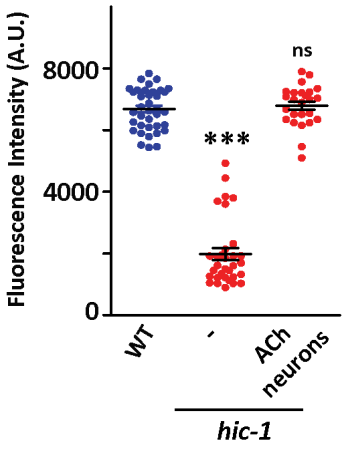
Fluorescence Intensity (A.U.)
8000
4000
0
ns
***
WT
-
ACh neurons
hic-1

B

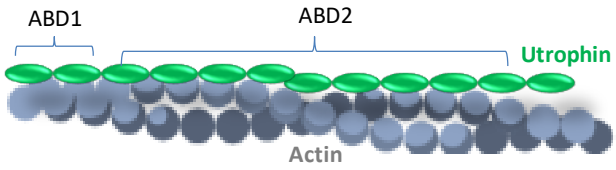
ABD1
ABD2
Utrophin
Actin

C

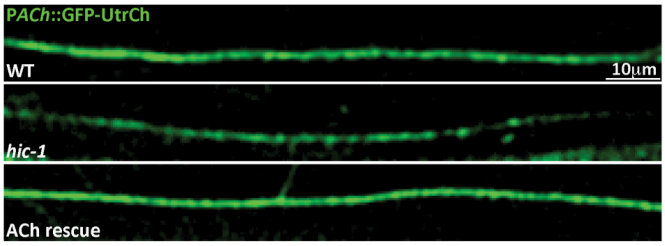
PACh::GFP-UtrCh
WT
10μm
hic-1
ACh rescue

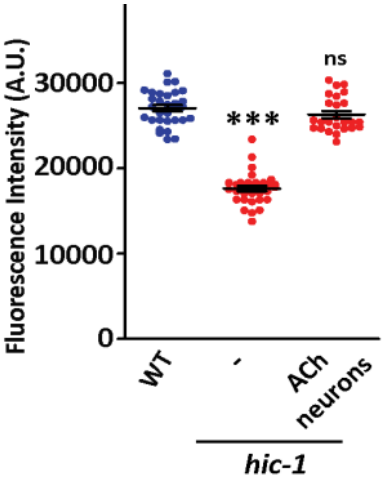
Fluorescence Intensity (A.U.)
30000
20000
10000
0
ns
***
WT
-
ACh neurons
hic-1

D

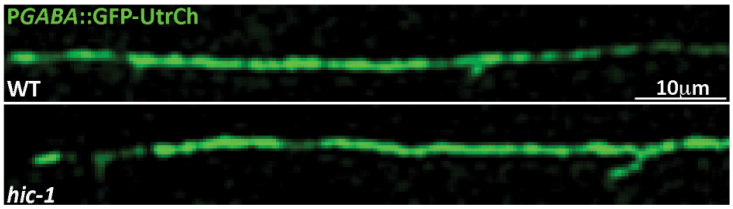
PGABA::GFP-UtrCh
WT
10μm
hic-1

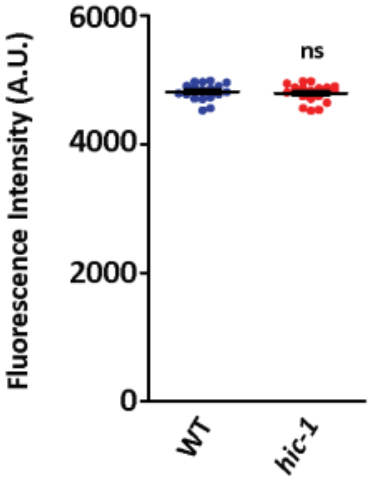
Fluorescence Intensity (A.U.)
6000
4000
2000
0
ns
WT
hic-1

Figure 4.6 HIC-1 is required to maintain normal actin cytoskeleton in cholinergic neurons.

A. Representative images and quantitation of Gelsolin/GSNL-1 fluorescence along the DNC of *C. elegans* expressing the actin-binding protein Gelsolin (GSLN-1) tagged with GFP in a subset of cholinergic neurons. The strains tested are WT (n=35), *hic-1* (n=28) and *hic-1* mutants expressing HIC-1 in cholinergic neurons (n=25).

B. Schematic of Utrophin(UtrCH) binding to stable F-actin (image modified from (Burkel et al., 2007)).

C. Representative images and quantitation of GFP-UtrCH fluorescence (along the DNC of *C. elegans* expressing GFP-UtrCH in cholinergic neurons. The strains tested are WT (n=30), *hic-1* (n=27), and *hic-1* mutants expressing HIC-1in cholinergic neurons (n=23).

D. Representative images of the DNC and Quantitation for GFP-UtrCH expressed in GABA neurons using the *unc-25* promoter in WT (n=15) and *hic-1* (n=17) mutant animals.

Next, we visualized the F-actin cytoskeleton in cholinergic synapses using an actin-binding probe Utrophin tagged with GFP to it's N-terminal (GFP-UtrCH) expressed in the cholinergic neurons. Utrophin is the calponin-homology domain of dystrophin and is known to strongly bind to stable F-actin (Burkel et al., 2007) and shown in **Figure 4.6B**)). A decrease in GFP-UtrCH intensity was observed with cholinergic GFP-UtrCH in *hic-1* mutants, and this phenotype was rescued by expressing HIC-1 in cholinergic synapses (**Figure 4.6B**). As a control experiment, we examined GFP-UtrCH fluorescence in GABA synapses and found this fluorescence to be unaltered (**Figure 4.6C**). These data indicate that HIC-1 is involved in maintaining the actin cytoskeletal network. We next wondered if HIC-1 could be affecting Wnt release by regulating the actin cytoskeleton. Although there are no experimental evidence so far for actin's involvement in the Wnt secretion but it is proposed that actin is a part

of the Wnt secretory machinery which involves SyntaxinA1, Rab-11 and Myo-5 operated at the periactive zone of the *Drosophila* synapses (reviewed in (Koles and Budnik, 2012a), image modified and shown in (**Figure 4.7**)). If this were indeed the case, then we would expect that disrupting the F-actin cytoskeleton would show increased Wnt secretion similar to that seen in *hic-1* mutants. To address this possibility, we disrupted the F-actin cytoskeleton by injecting WT animals with a pharmacological agent Latrunculin A (LAT-A) (Coue et al., 1987). First, we tested that LAT-A indeed disrupted the F-actin cytoskeleton, as was visualized using GFP-UtrCH (**Figure 4.8A**). Next, we imaged the Wnt ligand, CWN-2 tagged with mCherry in the coelomocytes. The Lat-A drug was dissolved in DMSO so we checked whether the DMSO has any effect on the Wnt release. We found a significant increase in CWN-2::mCherry fluorescence in the coelomocytes of LAT-A treated animals in comparison to mock-treated (only DMSO) *C. elegans* (**Figure 4.8B**). Further, the coelomocyte fluorescence was significantly reduced in *mig-14* animals after LAT-A treatment (**Figure 4.8B**). Together, these data suggest that depolymerization of the F-actin cytoskeleton causes increased Wnt release, indicating that the F-actin cytoskeleton is acting as a 'brake' for Wnt vesicle release and disrupting F-actin could cause an uncontrolled release of Wnt ligands.

These findings reveal a possible mechanism for HIC-1 function in cholinergic neurons and synapses, where HIC-1 could be participating in maintaining a stable F-actin network which in turn is required for sequestering the Wnt ligand containing vesicles.

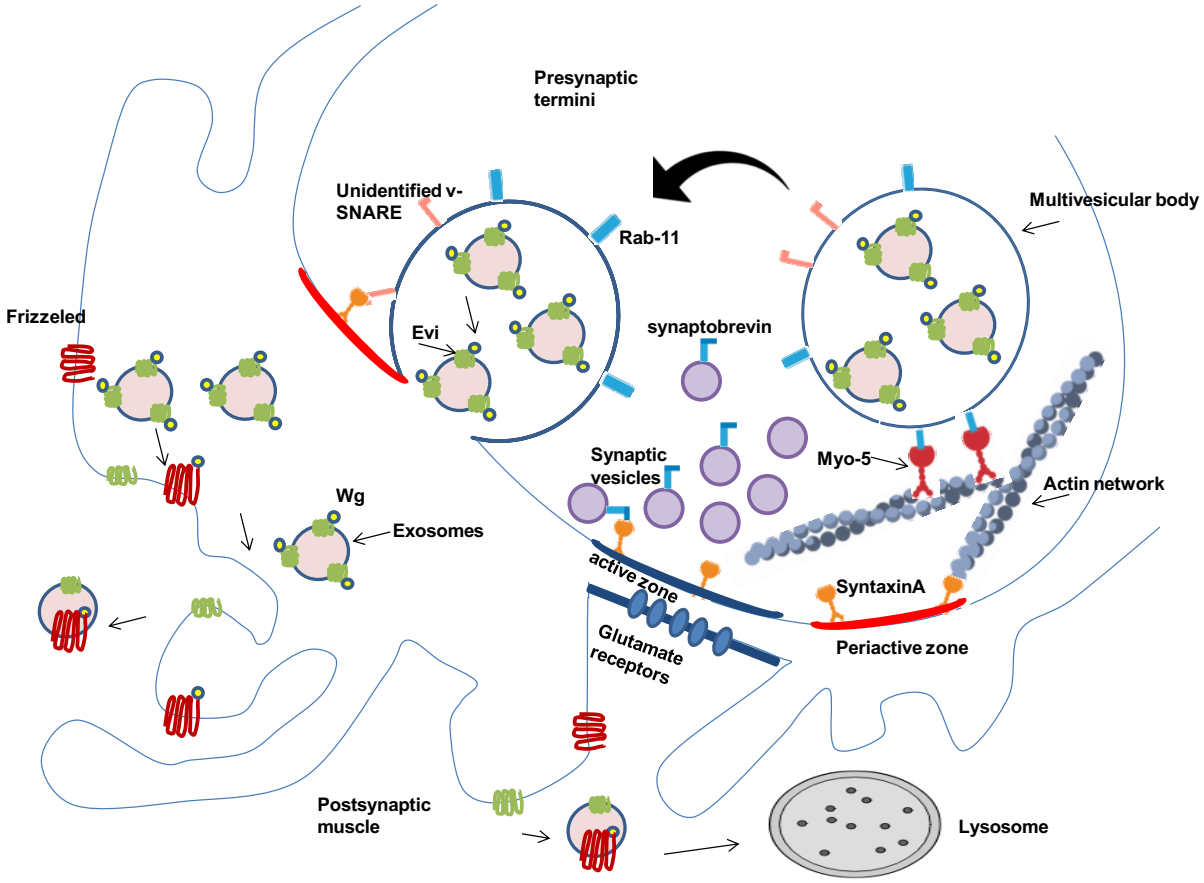

Figure 4.7 Wnts are secreted in the form of exosomes from the Periactive zone (image modified from (Koles and Budnik, 2012a)). Based on their studies Koles and Budnik have highlighted elegantly in this review the key molecular signaling during Wnt release at the *Drosophila* NMJs. They mentioned that the Wnts are released in the form of multivesicular bodies or exosomes. The pathway for Wnt exosomes release is highly conserved. Syntaxin1A, Rab11, actin, and myosin5 are key players in the exosome release machinery in the motor neuron.

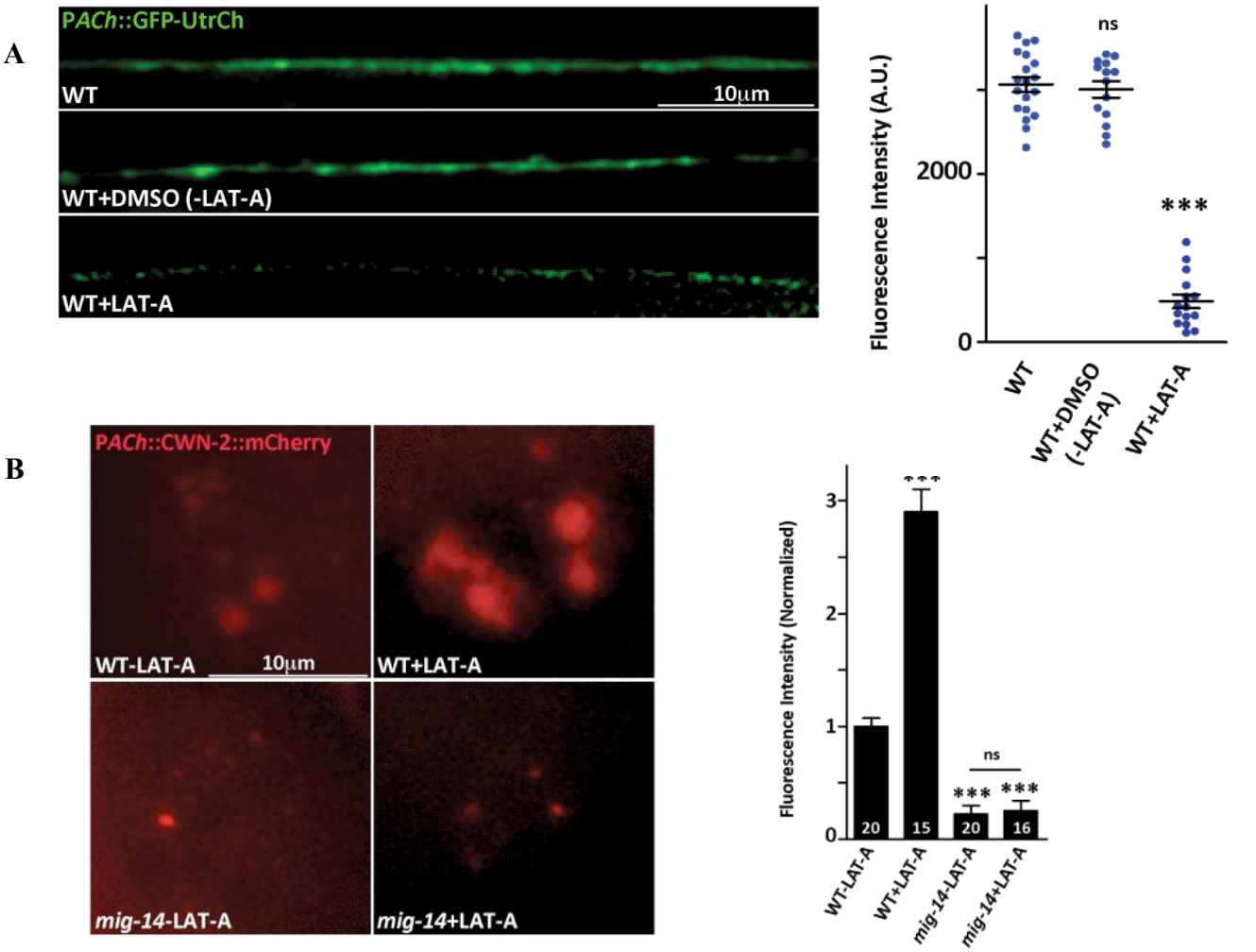

Figure 4.8 Wnt secretion is increased upon actin disruption by Lat A treatment

A. Representative images and Quantitation of the DNC of animals expressing GFP-UtrCH in cholinergic neurons. WT (n=19) animals and WT animals injected with DMSO (n=14) or DMSO and LAT-A (n=15) were imaged for this experiment.

B. Representative images and quantitation of coelomocytes fluorescence (normalized) in WT and *mig-14* strains that express Wnt/CWN-2::mCherry in cholinergic neurons. The panels on the left indicate mock-treated animals and the panels on the right show Latrunculin-A (LAT-A) treated *C. elegans*.

Discussion

Results from the current chapter demonstrate that HIC-1 is required for the controlled release of Wnts from the motor neurons. Out of five Wnts reported in *C.elegans* (Hilliard and Bargmann, 2006), we have tested two Wnts (CWN-2 and LIN-44) that are known to maintain ACR-16/α7 receptors level. The CWN-2 and LIN-44 were secreted in an uncontrolled manner in the *hic-1* mutant worm. There are possibilities that HIC-1 might be regulating secretion of all the Wnts from the motor neurons. Neither neurotransmitter release (**Figure 3.21A and Figure 3.22A**) nor Neuropeptide secretion (**Figure 4.5B C**) was altered in *hic*-1 mutants, suggesting HIC-1 is not a general molecule which controls constitutive release from the motor neurons, but the mode of action of HIC-1 is selective for Wnt release. Further, HIC-1 maintains a normal actin cytoskeleton in the cholinergic neurons. We found that upon actin disruption by using Lat A drug, Wnt secretion was upregulated in WT worms (**Figure 4.8**) but Neuropeptide secretion remained unaltered **(data not shown).** However, we cannot rule out the possibility that other small molecules secreted from the motor neurons are not being deregulated by disrupting actin network, but still the above-mentioned experiment sheds light on a correlation between actin network and Wnt secretion in the cholinergic neuron and is an indication of HIC-1 function in these neurons, where HIC-1 maintains a normal F-actin architecture which in turn maintains controlled release of Wnts from the motor neurons. In our next study, we went on to explore interacting partner(s) for HIC-1 by which it could participate in the Wnt signaling and actin network maintenance in *C.elegans* motor neurons.

Chapter 5:

HIC-1 interacts with NAB-1 to maintain normal Wnt release in the cholinergic neurons

Introduction

After establishing that HIC-1 regulates Wnt secretion through maintaining a normal actin cytoskeleton in the motor neurons, next, we wanted to further understand how HIC-1 interacts with the actin cytoskeleton by elucidating the interacting partner(s) for HIC-1 at the cholinergic synapse. Previous work has shown that claudins have a PDZ-binding motif (bm) at their C-terminus that allows claudins to interact directly with cytoplasmic PDZ domain-containing scaffolding proteins; TJ-associated proteins MUPP1, PATJ, ZO-1, ZO-2 and ZO-3, and MAGUKs (reviewed in (Lal-Nag and Morin, 2009)). As mentioned earlier, HIC-1 also contains a putative PDZ(bm) at its C-terminus tail. Through genetic and imaging experiments, we found that HIC-1 interacts to an actin-binding protein, NAB-1 through its PDZ binding motif. Genetic and molecular experiments suggested that HIC-1 and NAB-1 are in the same signaling pathway and that the actin-binding domain of NAB-1 anchored to HIC-1(ΔPDZbm) is sufficient enough to rescue synaptic functions of NAB-1 in *nab-1;hic-1* double mutant worms.

Results

5.1 HIC-1 interacts with an actin-binding protein, Neurabin

To test if the PDZ binding motif of HIC-1 is involved in the function of HIC-1 at the NMJ, we deleted the last four amino acids of the HIC-1 protein which is the putative PDZ(bm) and expressed this protein (HIC-1ΔC(4aa)) under the cholinergic promoter in *hic-1* mutants.

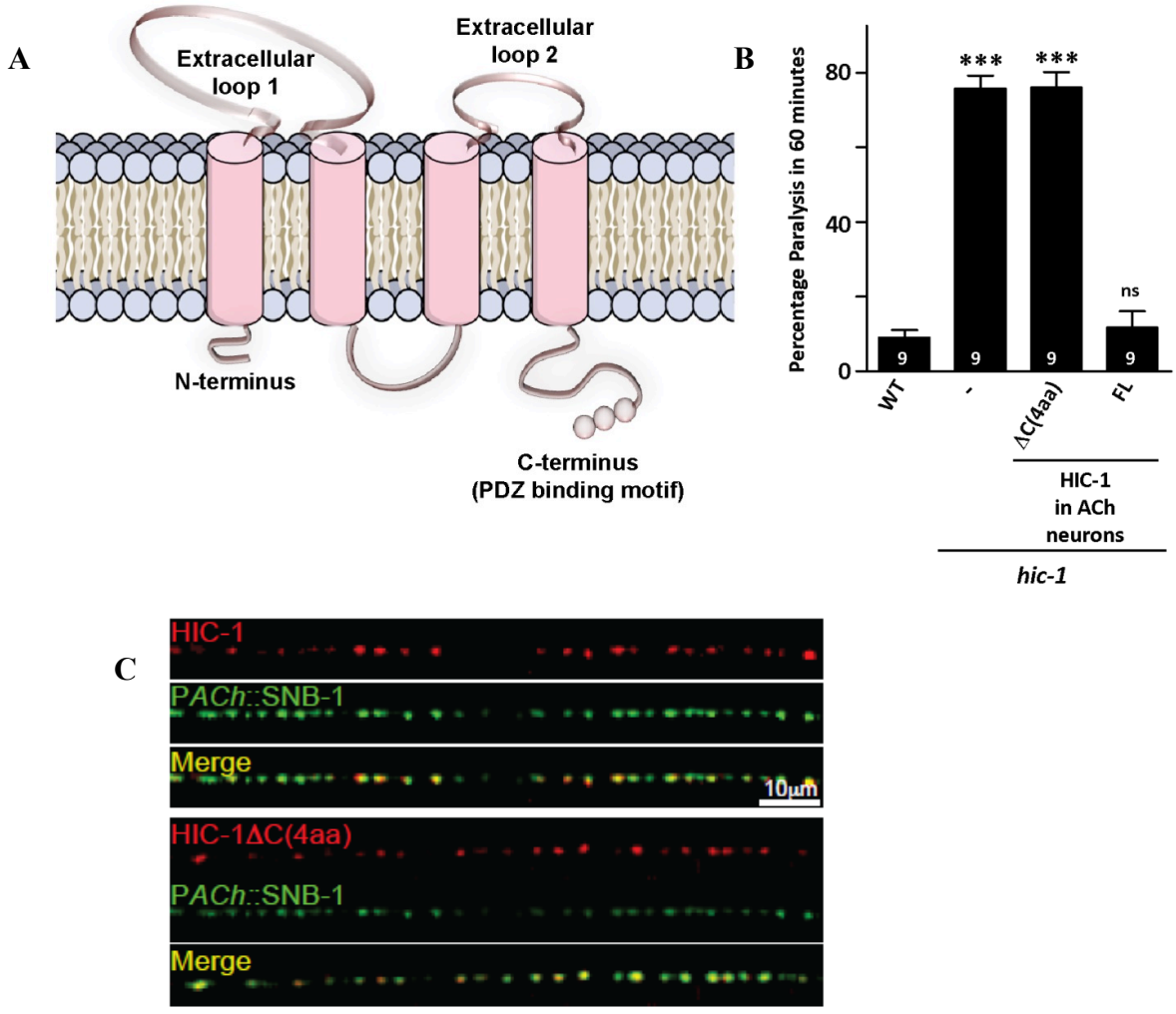

Figure 5.1 putative PDZ binding motif of HIC-1 is critical for its synaptic functions.

(A) Putative structure of HIC-1 highlighting different domains including PDZ binding motif at C-terminus. (B) The bar graph showing percentage paralysis of WT, *hic-1,* P*ACh::*HIC-1ΔC(4aa) rescue and P*ACh::*HIC-1 rescue at 60 min. time point. ΔC(4aa) represents deletion of the last 4 amino acids(aa) from C terminus of HIC-1. (C) Expression of HIC-1 and HIC-1ΔC(4aa) in cholinergic synapses that are labeled with SNB-1. The number of animals imaged of each genotype is HIC-1 (n=12) and HIC-1ΔC (4aa) (n=15).

The truncated protein failed to rescue the hypersensitivity phenotype seen in the *hic-1* mutant animals (**Figure 5.1B**), suggesting that the putative PDZ(bm) made up of the last four amino acids is likely to be required for HIC-1's binding to mediator protein(s) that may help the association of HIC-1 to the actin cytoskeleton. To test if the putative PDZ(bm) of HIC-1 is required for the synaptic localization of the protein, we visualized the HIC-1ΔC(4aa) truncated protein at the synapse by tagging this deleted protein with mCherry, the HIC-1ΔC(4aa) was co-localized with SNB-1 in the cholinergic neurons, indicating that the deleted protein showed normal localization at the synapse, similar to that seen in the control Full length (FL) HIC-1 that was also tagged with mCherry (**Figure 5.1C**).

Next, we went on to find a possible interactor of HIC-1. Since HIC-1 does not have an actin-binding domain, we decided to search for putative HIC-1 interacting proteins by searching for proteins which satisfied the following criteria; (1) the molecule should be present at the synapse, (2) it should have an actin-binding domain, and (3) it should also have a PDZ domain. While searching through literature and wormbase, we found one such protein Neurabin/NAB-1, which qualified all the three criteria. Previous work has shown that NAB-1 is required for instructing synapse assembly by linking adhesion molecules and F-actin to active zone proteins (Chia et al., 2012a). We asked if NAB-1 could interact with HIC-1 and thus act as an adaptor to link HIC-1 with F-actin.

Before testing for an interaction between HIC-1 and NAB-1, we first performed aldicarb assays for *nab-1* and found that *nab-1* animals were hypersensitive to aldicarb. The hypersensitivity seen in *nab-1* mutants was rescued by expressing NAB-1 specifically in cholinergic neurons **(Figure 5.2B**) or under its own

promoter in a translational reporter line tagged to GFP **(Figure 5.2C**). The mutants of *nab-1; hic-1* also showed hypersensitivity towards aldicarb similar to that seen in *nab-1* or *hic-1* single mutants (**Figure 5.2B**). These data suggest that *nab-1* genetically interacts with *hic-1*. Next, we performed a split YFP/BiFC experiment to find if there was a direct interaction between HIC-1 and NAB-1. Bimolecular Fluorescence complementation (BiFC) analysis enables direct visualization of protein interactions by measuring the association of two non-fluorescent fragments of a fluorescent protein fused to putative interacting partners (Kerppola, 2013).

A bright YFP fluorescence was detected at the cholinergic synapses labeled with RAB-3::mCherry, when HIC-1 tagged with the C-terminus half of YFP and NAB-1 tagged with the N-terminus half of YFP were coinjected in the animals (**Figure 5.3B**), whereas the YFP fluorescence intensity was significantly reduced when the HIC-1ΔC(4aa)::SpYFP and NAB-1::SpYFP were used in the above experiment (**Figure 5.3B**). The controls; HIC-1::SpYFP, HIC-1ΔC(4aa) ::SpYFP and NAB-1::SpYFP also showed a significantly reduced YFP signal at the cholinergic synapse (**Figure 5.4**), indicating that the interaction/YFP signal that was seen with HIC-1::SpYFP and NAB-1::SpYFP was likely because of an interaction between HIC-1 and NAB-1. Further, the HIC-1::SpYFP but not the HIC-1ΔC(4aa)::SpYFP was able to rescue the aldicarb hypersensitivity defect of *hic-1* mutant animals and the NAB-1::SpYFP also rescued the hypersensitivity to aldicarb seen in the *nab-1* mutants (**Figure 5.5**), We next wanted to explore the possibility that mutants in *nab-1* could show a phenotype similar to that seen in *hic-1* mutants.

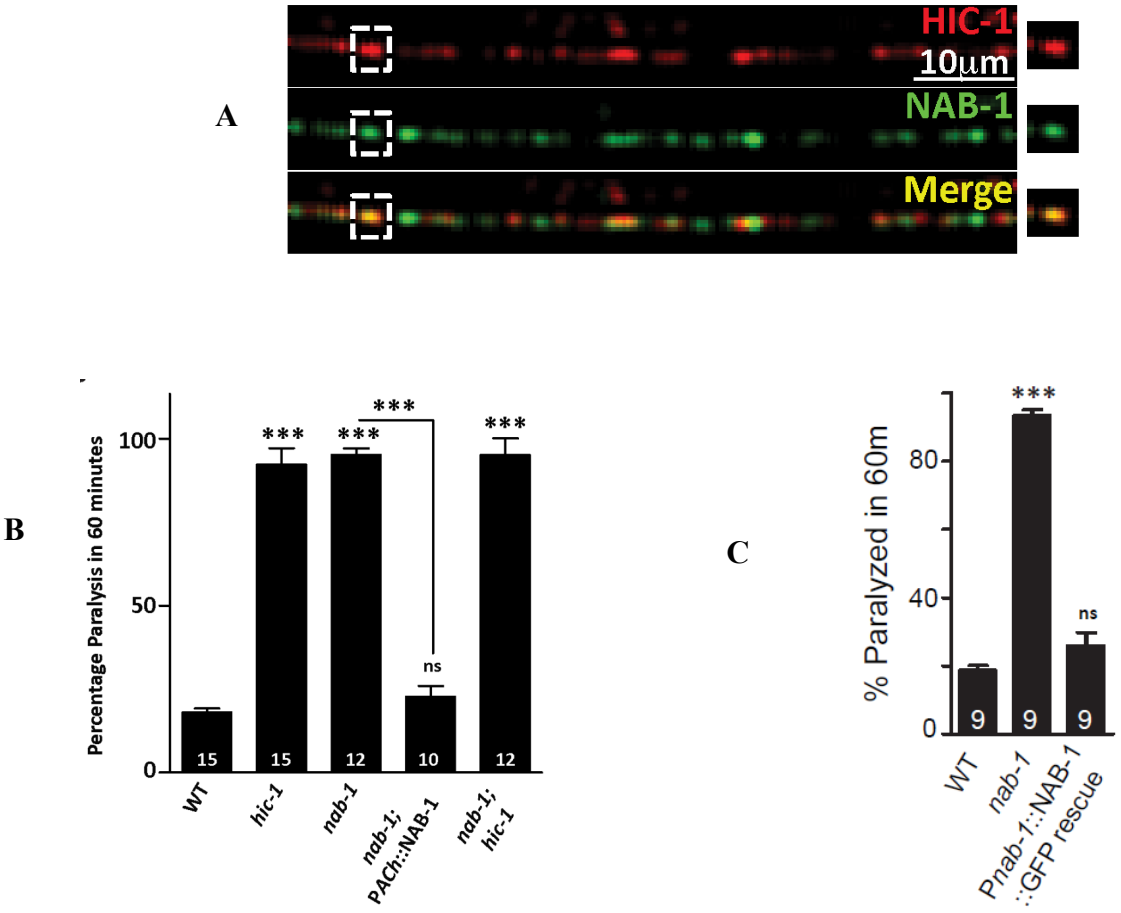

Figure 5.2 HIC-1 genetically interacts with NAB-1.

A. DNC of *C.elegans* expressing translational reporter constructs of both HIC-1::mCherry and NAB-1::GFP. Co-localization was seen for HIC-1 and NAB-1 at the synapses.

B. Graph showing the percentage of *C. elegans* paralyzed at 60m after aldicarb exposure. The experiment was done with WT, *hic-1*, *hic-1*; nab-1, P*ACh*::NAB-1 and *nab-1; hic-1* animals.

C. Bar-graph illustrating paralysis on aldicarb at the 60m time point for the following strains; WT, *nab-1,* and *nab-1*; P*nab-1*::NAB-1::GFP.

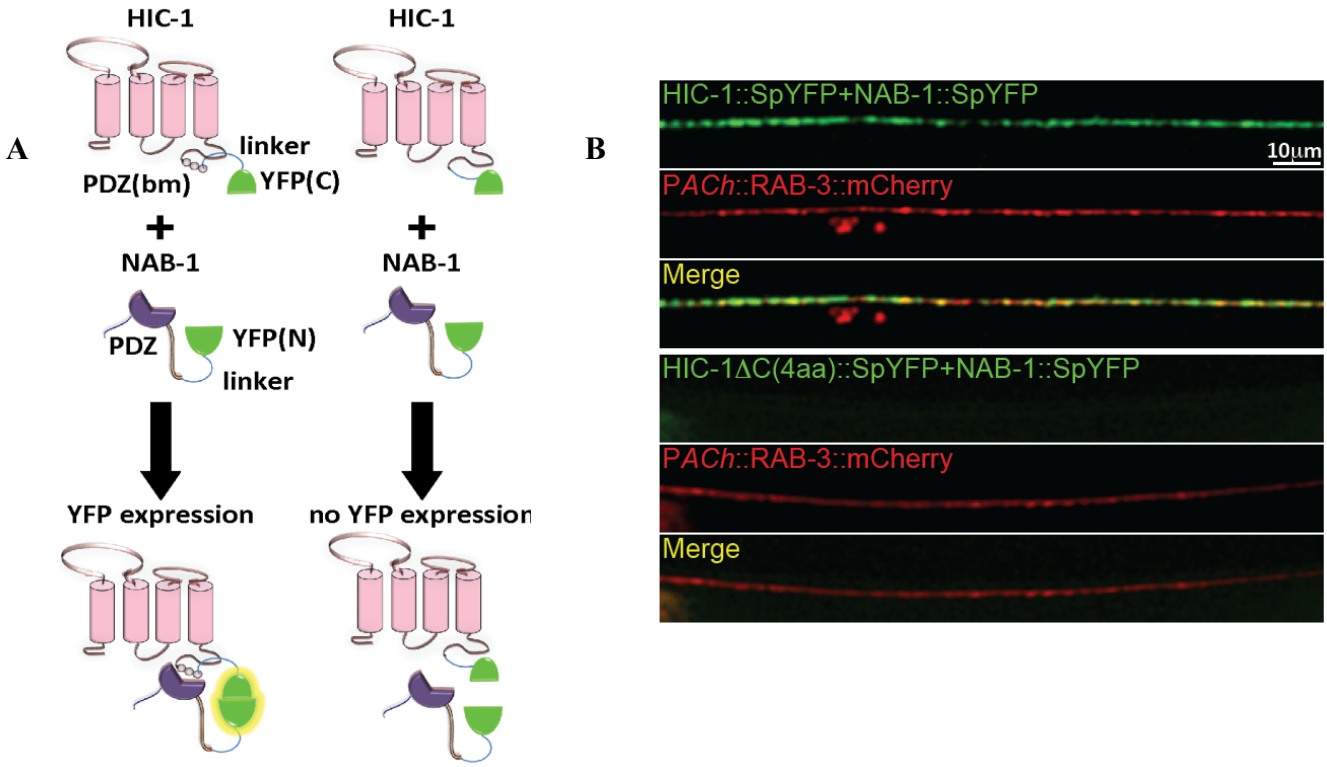

Figure 5.3 HIC-1 directly interacts with NAB-1 through its PDZ binding motif.

A.Schematic indicating the BiFluorescence Complementation (BiFC) assay between HIC-1 and NAB-1. HIC-1 (pink) is tagged with C-terminal half of YFP (green) via a linker sequence (blue), the PDZ binding motif (bm) is indicated as circles. The C-terminus of NAB-1 is tagged to N-terminal half of YFP (green) via a linker sequence (blue). The interaction between NAB-1 and HIC-1 leads to reconstitution of YFP fluorescence (yellow glow) while no fluorescence is detected in the absence of the PDZ(bm) of HIC-1.

B. Representative images and quantification of the DNC of WT animals expressing either HIC-1::SpYFP and NAB-1::SpYFP together or HIC-1ΔC(4aa) and NAB-1:: SpYFP together in the cholinergic neurons. The cholinergic synapses are labeled with RAB-3::mCherry.

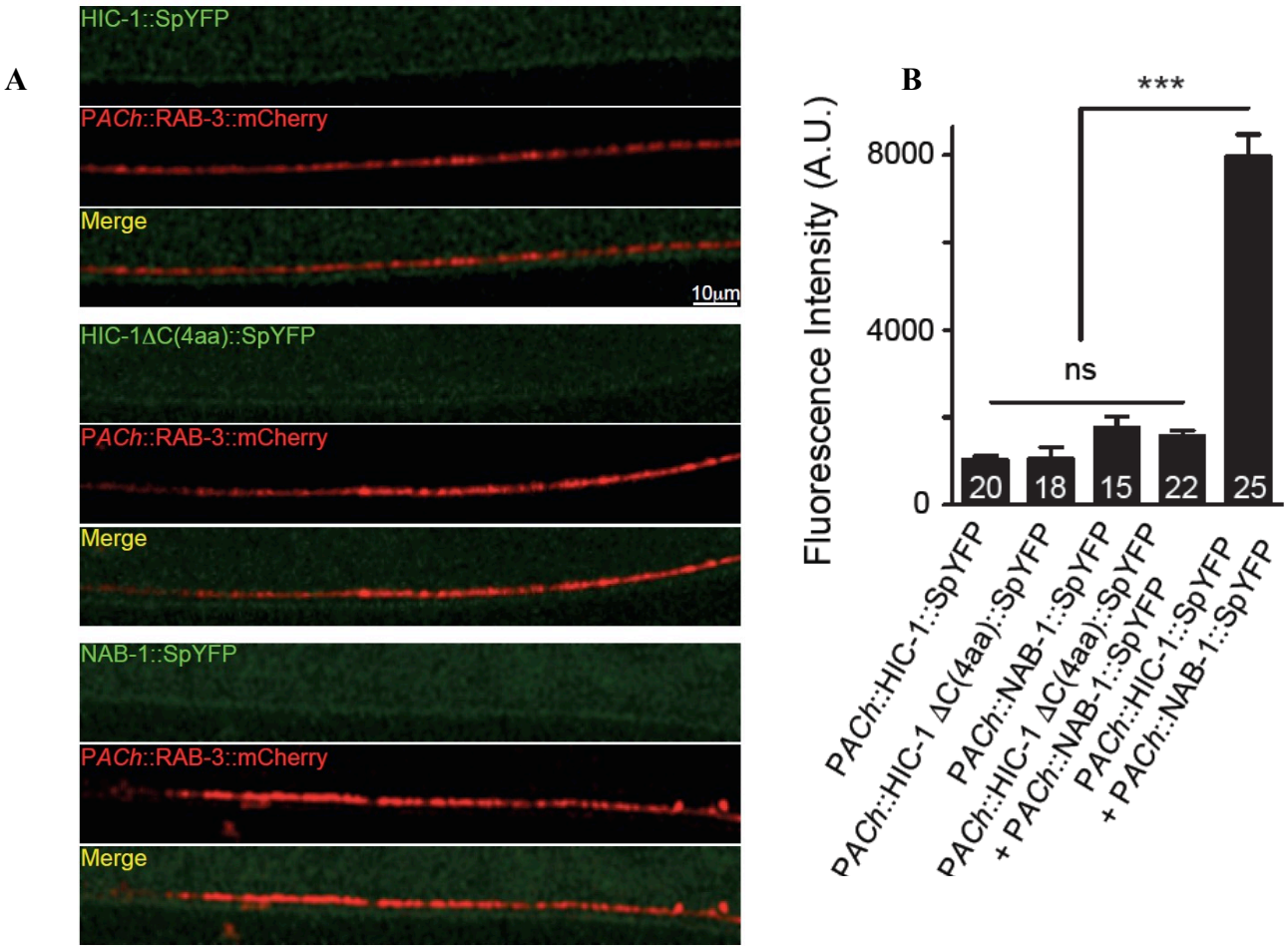

Figure 5.4 controls for BiFC experiment

A. Representative images and quantitation of the DNC in transgenics expressing RAB-3::mCherry along with each of the following constructs; HIC-1::SpYFP, HIC-1ΔC(4aa)::SpYFP and NAB-1::SpYFP all of which were expressed in cholinergic neurons.

B. The panel on the right shows the quantification of the YFP reconstitution between HIC-1 and NAB-1 along with multiple controls.

5.2 HIC-1 and NAB-1 function in the same signaling pathway:

To further validate the interaction between NAB-1 and HIC-1, we performed experiments to see if *nab-1* mutants showed phenotypes similar to *hic-1*. Firstly, we looked at the postsynaptic acetylcholine receptor (ACR-16::GFP) levels in *nab-1* mutants. The fluorescence intensity of ACR-16:: GFP was significantly enhanced in *nab-1* mutants and the increased ACR-16::GFP intensity was rescued by expressing NAB-1 in cholinergic neurons. The *nab-1; hic-1* double mutants showed significantly increased levels of postsynaptic acetylcholine receptors similar to *hic-1* and *nab-1* single mutants (**Figure 5.6A**), indicating HIC-1 and NAB-1 are in the same signaling pathway which regulates ACR-16/α7 receptors levels at the postsynaptic muscle membrane. We were also interested in deciphering if Wnt secretion is altered in *nab-1* mutants. We observed that this was indeed the case, the CWN-2::mCherry fluorescence intensity was significantly enhanced in the coelomocytes of *nab-1* mutants, again the increased coelomocyte fluorescent phenotype was rescued by expressing NAB-1 in the cholinergic neurons. The *nab-1; hic-1* mutant animals showed increased levels of CWN-2 secretion similar to either of the single mutant (**Figure 5.6B**). A similar experiment was performed for another Wnt ligand, LIN-44, which also showed increased release from the cholinergic neurons in *nab-1* and *nab-1; hic-1* mutants (**Figure 5.6C**), suggesting that similar to HIC-1, NAB-1 could be functioning in the same signaling pathway which is regulating the secretion of Wnt ligands from the cholinergic neurons. Next, we wanted to ascertain the status of the actin cytoskeleton in the *nab-1* animals. Similar to previous reports for NAB-1 acting as

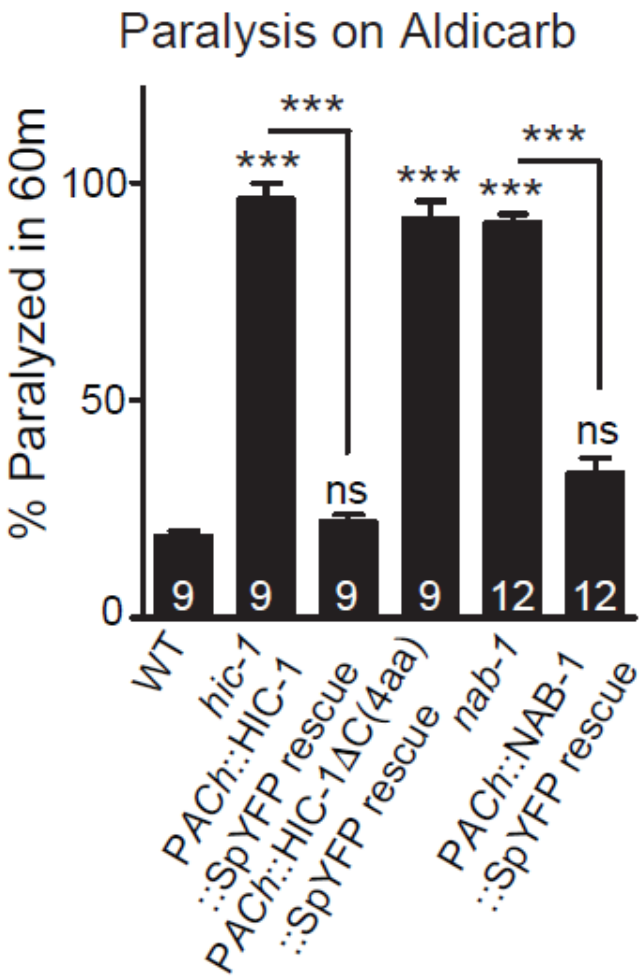

.

Figure 5.5 Aldicarb assay for BiFC constructs

Bar-graph illustrating paralysis on aldicarb at the 60m time point for the BiFC constructs used in Fig. 6. The genotypes analyzed were; WT, *hic-1*, *hic-1*; P*ACh*::HIC-1::SpYFP, *hic-1*; P*ACh*::HIC-1ΔC(4aa)::SpYFP, *nab-1* and *nab-1*; P*ACh*::NAB-1::SpYFP.

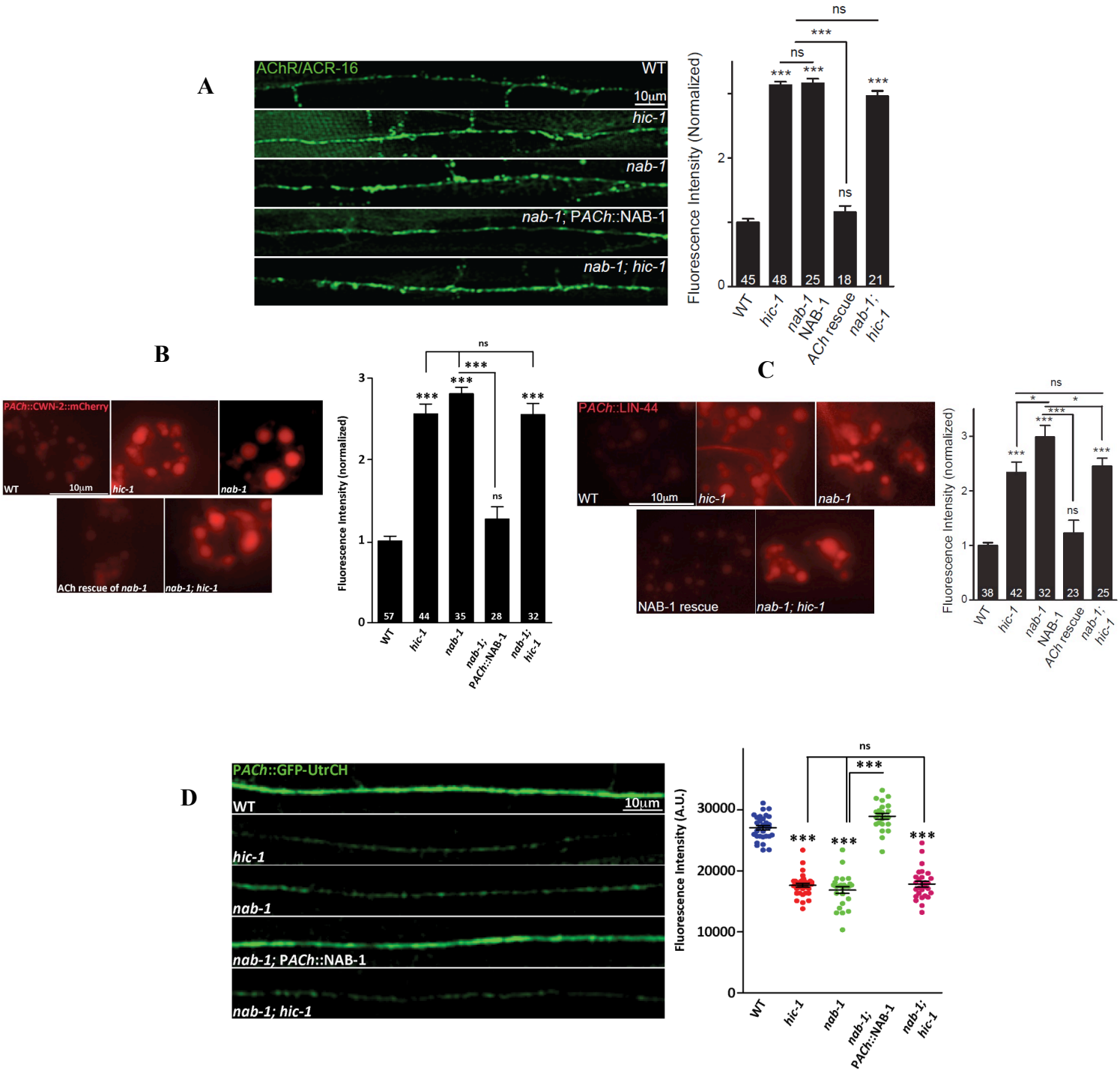
A
AChR/ACR-16
WT
10µm
hic-1
nab-1
nab-1; PACh::NAB-1
nab-1; hic-1
Fluorescence Intensity (Normalized)
ns
***
45
48
25
18
21
WT
hic-1
nab-1
NAB-1
ACh rescue
nab-1; hic-1
B
PACh::CWN-2::mCherry
WT
10µm
hic-1
nab-1
ACh rescue of nab-1
nab-1; hic-1
Fluorescence Intensity (normalized)
57
44
35
28
32
nab-1; PACh::NAB-1
C
PACh::LIN-44
NAB-1 rescue
38
42
23
25
D
PACh::GFP-UtrCH
Fluorescence Intensity (A.U.)
30000
20000
10000
0

Figure 5.6 HIC-1 and Neurabin function together for normal Wnt release.

A. Representative images and quantitation of fluorescence intensity (normalized) along the DNC in animals expressing ACR-16::GFP under the body-wall muscle *(myo-3)* promoter. The genotypes imaged are WT, *hic-1*, *nab-1*, *nab-1*; PACh::NAB-1 and *nab-1; hic-1*.

B. Representative images and quantitation of coelomocyte fluorescence intensity (normalized) from Wnt/CWN-2::mCherry tagged line expressed in cholinergic neurons. The genotypes used in this experiment were WT, *hic-1*, *nab-1*, *nab-1*; P*ACh*::NAB-1 and *nab-1; hic-1*.

C. Representative images and quantitation of fluorescence intensity (normalized) in coelomocytes of animals expressing Wnt/LIN-44 tagged to mCherry in cholinergic neurons. The genotypes imaged were WT, *hic-1*, *nab-1*, *nab-1*; P*ACh*::NAB-1 and *nab-1; hic-1*.

D. Representative images and quantitation of DNC fluorescence from a GFP-UtrCH line expressed in cholinergic neurons. The genotypes used in this experiment were WT (n=25), *hic-1* (n=20), *nab-1* (n=20), *nab-1*; P*ACh*::NAB-1 (n=21) and *nab-1; hic-1* (n=25).

an actin-binding protein (Chia et al., 2012a), we also found that NAB-1 is required for the maintenance of presynaptic F-actin as mutants for *nab-1* showed a significantly decreased level of the F-actin binding probe in the cholinergic neurons, GFP-UtrCH. Further GFP-UtrCH levels were restored by expressing NAB-1 in cholinergic neurons. The *nab-1; hic-1* animals again showed a similar reduction of GFP-UtrCH fluorescence intensity similar to the single mutants (**Figure 5.6D**), supporting the previous experiments that suggested that NAB-1 and HIC-1 are both required to maintain the actin cytoskeleton

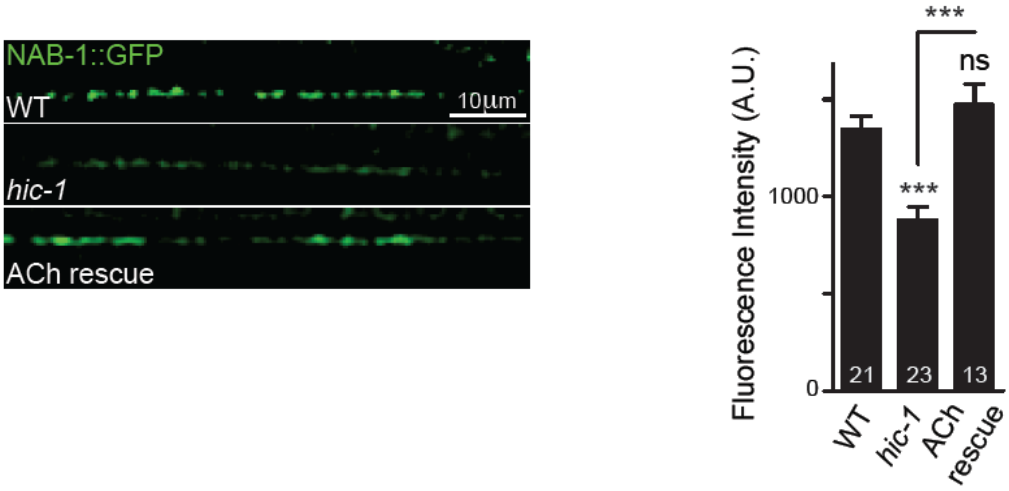

Figure 5.7 NAB-1 localization is affected in *hic-1* mutant worms. Representative images and quantitation of NAB-1::GFP fluorescence intensity along the DNC in WT, *hic-1 and hic-1;*P*ACh::*HIC-1 animals.

in the cholinergic neurons. To further investigate the interaction between NAB-1 and HIC-1, we looked at the localization of NAB-1 and HIC-1 and found a significant co-localization between the translational reporters at the synapse (**Figure 5.2A**). If HIC-1 is modulating the F-actin cytoskeleton via NAB-1, we hypothesized that NAB-1 expression at the synapse could be dependent on HIC-1. In order to test this, we analyzed the localization of NAB-1 in *hic-1* animals and found that the NAB-1::GFP fluorescence intensity was significantly reduced in *hic-1* mutants which was rescued by expressing HIC-1 in cholinergic neurons in these *C. elegans* (**Figure 5.7**).

Taken together, these data suggest that HIC-1 interacts with NAB-1 through its PDZ binding motif and that NAB-1 localization is dependent on HIC-1 expression. Taken together, these experiments signify that there could be a direct interaction between HIC-1 and NAB-1 and that they are both involved in a signaling pathway to mediate normal Wnt secretion and maintenance of the actin cytoskeleton at cholinergic synapses. We next wanted to test if the actin-binding domain (ABD) of NAB-1 linked to the C-terminal of HIC-1 was sufficient to replace the function of NAB-1 in Wnt release and maintenance of the actin cytoskeleton at the NMJ.

5.3 HIC-1 with a C-terminal NAB-1(ABD) is sufficient to rescue the Wnt release defects associated with *nab-1; hic-1* double mutants

To further assert the role of HIC-1 through the NAB-1(ABD) in maintaining Wnt release and a normal F-actin cytoskeleton at the NMJ, we made a construct that removed the last PDZ interacting amino acids of HIC-1 and replaced it with the actin-binding domain (ABD) of NAB-1 (HIC-1ΔC(4aa)+NAB-1(ABD), (**illustrated in Figure 5.8A**). We then went on to test the rescue of this construct in the *nab-1; hic-1* double mutants. We found that in comparison to HIC-1ΔC(4aa) that did not rescue the hypersensitivity to aldicarb seen in the *nab-1; hic-1* mutant animals, the HIC-1ΔC (4aa)+NAB-1(ABD) expressing *C. elegans* largely rescued the hypersensitivity to aldicarb seen in these animals (**Figure 5.8B**). These data indicate that the function of HIC-1 in maintaining normal aldicarb sensitivity could be largely due to HIC-1 interacting with NAB-1 and allowing for maintenance of a normal actin cytoskeleton and hence normal Wnt release.

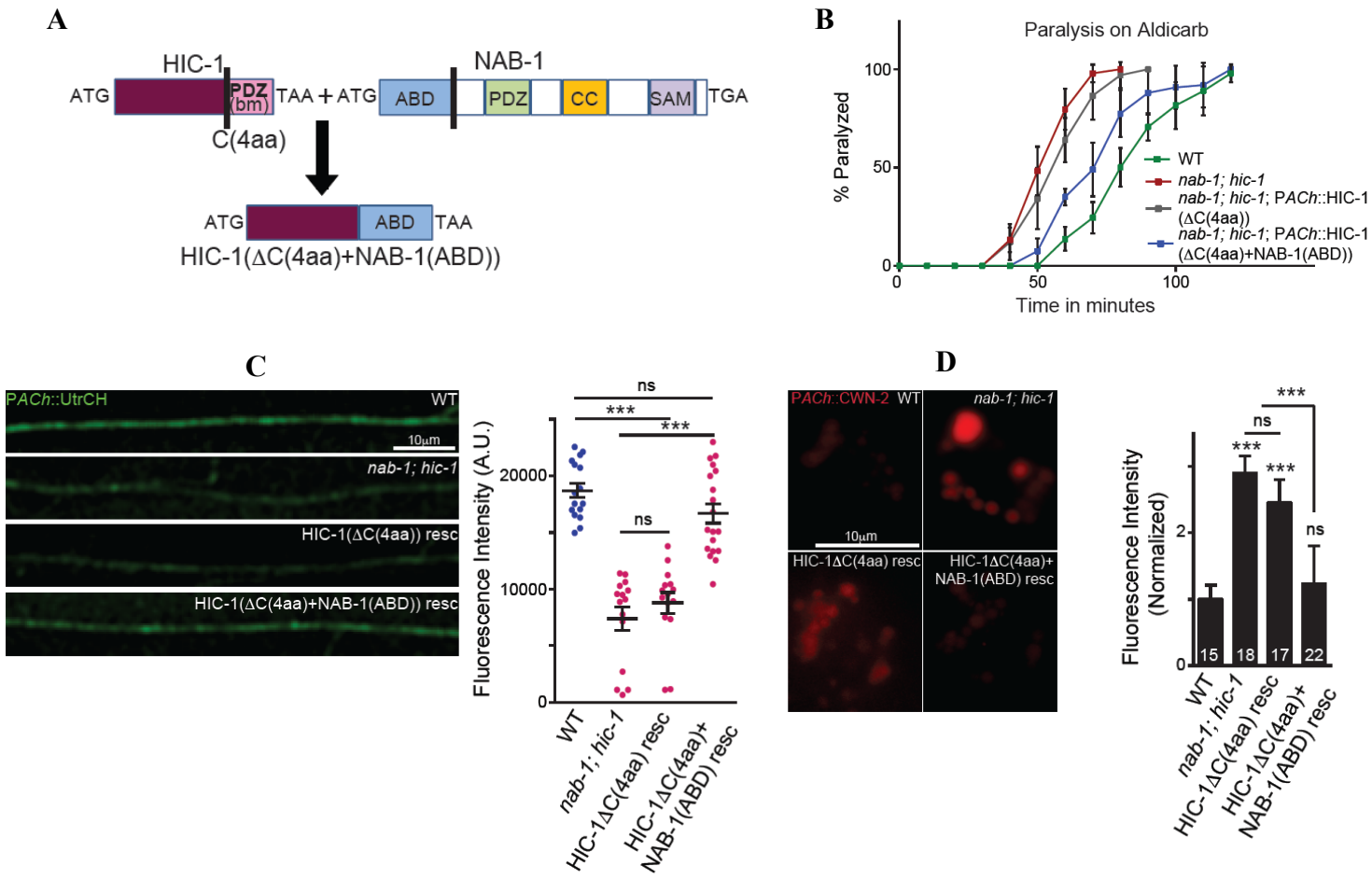

Figure 5.8 Neurabin linked to HIC-1 is sufficient to rescue the NMJ defects of the *nab-1; hic-1* double mutants

A. Illustrates a schematic of the fusion construct HIC-1(ΔC(4aa)+NAB-1(ABD)). The C-terminal 4 amino acids were deleted from HIC-1, and the Actin-Binding Domain (ABD) of NAB-1 was added in frame with the above HIC-1 construct. The domains of NAB-1 are shown in accordance with previously published data (Chia et al., 2012a)

B. A time-course paralysis on aldicarb for the following strains; WT, *nab-1; hic-1*, *nab-1; hic-1*; P*ACh*::HIC-1(ΔC(4aa)) and *nab-1; hic-1*; P*ACh*::HIC-1(ΔC(4aa)+NAB-1(ABD)).

C. Representative images and quantitation of coelomocyte fluorescence intensity (normalized) from Wnt/CWN-2::mCherry expressed in cholinergic neurons. The

genotypes used in this experiment are; WT, *nab-1; hic-1*, *nab-1; hic-1*; P*ACh*::HIC-1(ΔC(4aa)) and *nab-1; hic-1*; P*ACh*::HIC-1(ΔC(4aa)+NAB-1(ABD)).

D. Representative images and quantitation of the DNC of animals expressing GFP-UtrCH as a transgene in cholinergic neurons. The genotypes used in this experiment were; WT (n=16), *nab-1; hic-1* (n=15), *nab-1; hic-1*; P*ACh*::HIC-1(ΔC(4aa)) (n=15) and *nab-1; hic-1*; P*ACh*::HIC-1(ΔC(4aa)+NAB-1(ABD)) (n=19).

We next went on to test the rescue of defects in Wnt release and the F-actin cytoskeleton in the *nab-1; hic-1* double mutant animals. We found that again while the HIC-1ΔC(4aa) expressing line could not rescue the Wnt/CWN-2 release defects associated with the *nab-1; hic-1* mutants, the HIC-1ΔC(4aa)+NAB-1(ABD) expressing animals could largely rescue the Wnt/CWN-2 release defects seen in the mutants (**Figure 5.8C**). Finally, we visualized the actin cytoskeleton using GFP-UtrCH expressed in cholinergic neurons in *nab-1; hic-1* animals and the double mutant animals expressing the chimeric protein HIC-1(ΔC(4aa)+NAB-1(ABD)) or the deletion HIC-1ΔC(4aa) in cholinergic neurons. Consistent with our previous results, we again found that only the chimera of HIC-1 and NAB-1(ABD) could rescue the F-actin defect in the *nab-1; hic-1* mutants (**Figure 5.8D)**. Together, these data indicate that the actin-binding domain of NAB-1 anchored to HIC-1 is sufficient to rescue the NMJ defects of increased Wnt secretion seen in the single and double mutants of *hic-1* and *nab-1*.

Discussion

Insights from the current chapter suggests that the claudin homolog, HIC-1 interacts with an actin-binding protein, NAB-1 through its PDZ binding motif and this actin-binding domain of NAB-1 anchored onto HIC-1 is able to rescue synaptic functions of NAB-1. It supports the idea that NAB-1 is acting as an adaptor protein to link HIC-1 to actin cytoskeleton. NAB-1, being an actin-binding protein, could be a part of a protein complex to recruit other actin binding/modulating protein(s) and this whole complex could be involved in maintaining a normal actin cytoskeleton. More biochemical experiments and their analysis are needed to pinpoint what other proteins are involved in maintaining the complex including HIC-1 and NAB-1 at the synapses to recruit the actin cytoskeleton.

Summary

The findings from the current thesis work reveal the functioning of a novel claudin-like molecule, HIC-1, at the *C.elegans* NMJs. Chapter three demonstrates that HIC-1 is functioning at the cholinergic synapses and is required to maintain normal levels of ACR-16/α7 receptors at the muscle membrane. Chapter four deals with how HIC-1 regulates these ACR-16/α7 receptor levels at the postsynaptic muscle membrane. The current study shows that HIC-1 is also part of the Wnt signaling pathway which maintains translocation of ACR-16/α7 receptor levels (Jensen et al., 2012b) and it does so by regulating Wnt secretion from the cholinergic neurons and HIC-1 maintains a normal F-actin cytoskeleton at the level of cholinergic motor neurons. Chapter five goes on to describe HIC-1 function more elaborately. It deals with mainly; how HIC-1 functions intracellularly like a claudin, and interacts via its PDZ binding motif to an actin-binding protein, NAB-1 and how through NAB-1, it is maintaining a normal F-actin cytoskeleton. The proposed model for HIC-1 function at the *C.elegans* cholinergic neuron is shown (**Figure 6.1**). Collectively, these results not only shed light on the functioning of a claudin-like molecule at the NMJ, but they also allow one to think of how Wnt secretion could be regulated in neurons.

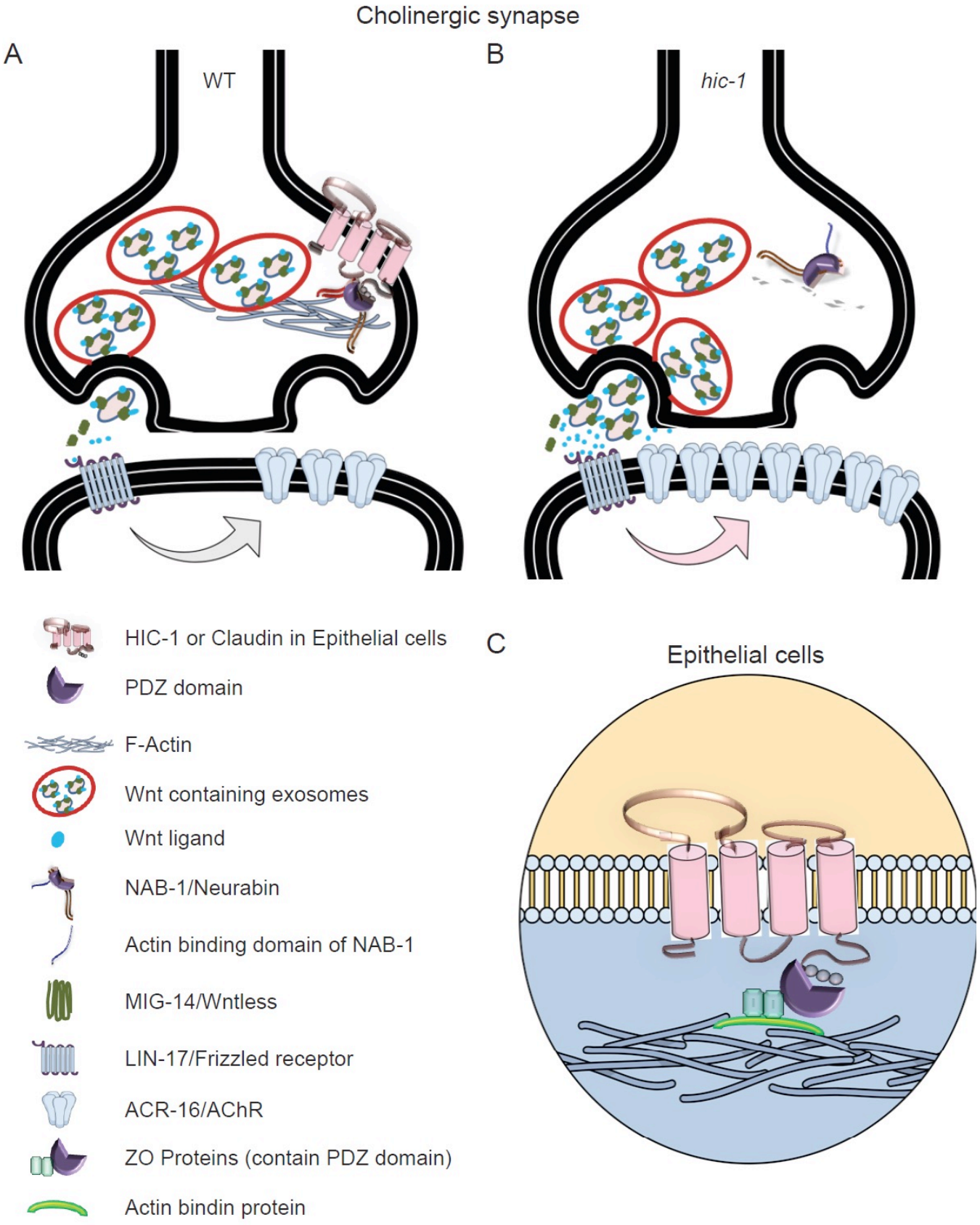
Cholinergic synapse
A
WT
B
hic-1
HIC-1 or Claudin in Epithelial cells
PDZ domain
F-Actin
Wnt containing exosomes
Wnt ligand
NAB-1/Neurabin
Actin binding domain of NAB-1
MIG-14/Wntless
LIN-17/Frizzled receptor
ACR-16/AChR
ZO Proteins (contain PDZ domain)
Actin bindin protein
C
Epithelial cells

Figure 6.1 Possible Model

The illustrations in A and B depict the possible function of HIC-1 at the NMJ of *C.elegans.* This model is based on previously published results from (Jensen et al., 2012a; Pandey, 2017) and the results presented in this manuscript.

A. Illustrates the WT scenario where HIC-1 is expressed in cholinergic neurons and allows for normal Wnt release and hence normal ACR-16/α7 levels at the NMJ.

B. Indicates hic-1 mutants that show increased Wnt release from cholinergic neurons and a causative increase in ACR-16/α7 levels at the NMJ.

C. Indicates the similarity between HIC-1 function at the NMJ and claudin function in epithelial cells. The intracellular region of HIC-1 functions like a claudin by affecting the actin cytoskeleton through a PDZ domain molecule NAB-1, similar to the intracellular functioning of claudins in epithelial cells (reviewed in (Gunzel and Yu, 2013).

Chapter 6:
Conclusions and future directions

6.1 HIC-1 and NAB-1 are novel regulators of Wnt secretion:

At the *C. elegans* NMJ, the Wnt signaling pathway modulates postsynaptic acetylcholine receptor levels allowing activity-dependent synaptic plasticity (Babu et al., 2011b; Jensen et al., 2012a; Jensen et al., 2012c; Pandey et al., 2017). Jensen *et al.* have elegantly dissected out the role of the presynaptic Wnt/CWN-2, and it's receptor Frizzled/LIN-17 in the translocation of ACR-16/α7 receptors on to the muscle membrane at the *C.elegans* NMJ (Jensen et al., 2012c). Consistent with these previous findings, we demonstrate through imaging and behavioral analysis that HIC-1 regulates postsynaptic ACR-16/α7 receptors by controlling Wnt secretion from the presynaptic cholinergic motor neurons (illustrated in **Figure 6.1**). Data from the coelomocyte uptake assay, indicate that the release of Wnt/CWN-2 and Wnt/LIN-44 ligands from the motor neurons in *hic-1*, *nab-1,* and *nab-1; hic-1* mutant animals occurs in an uncontrolled manner in comparison to WT control animals, although the initial levels of Wnts were likely the same as indicated by no change in RNA levels in these mutants. To our knowledge, these data potentially indicate the first characterization of a loss of function mutant that causes an increase in Wnt secretion. More comprehensive studies on how Wnt secretion is deregulated in such mutants could be helpful in treating illnesses where blocking Wnt secretion or designing therapeutic targets against Wnt signaling have been proven to be helpful (Wang et al., 2016a; Wang et al., 2016b) and reviewed in (Gregorieff and Clevers, 2005; Inestrosa et al., 2007)).

We have shown that HIC-1 interacts with Neurabin (NEURal tissue-specific Actin-filament BINding protein) and this interaction allows for a normal actin cytoskeleton and hence normal Wnt release from cholinergic motor neurons. Neurabin/NAB-1 is

a multidomain protein which plays diverse functions in the nervous system. It has an F-actin binding domain at the N- terminus, a PDZ domain which is reported to bind to transmembrane proteins and a coiled-coil domain at C-terminus (Nakanishi et al., 1997a). Previous studies on the *C.elegans* HSN neurons have shown that the specificity determining cell adhesion molecules, SYG-1 and SYG-2 (Shen and Bargmann, 2003; Shen et al., 2004), locally assemble F-actin in HSN neurons and NAB-1 then binds to F-actin and goes on to recruit active zone proteins SYD-1 and SYD-2 (Chia et al., 2012b). Furthermore, Hung *et al.* have shown that NAB-1 is also required for neuronal polarity (Hung et al., 2007). These data point to the fact that NAB-1 could have multiple roles in the nervous system and it's interaction with HIC-1 to allow for normal Wnt secretion is probably just one of the many processes that it could be involved in. One could imagine that it may function as an adapter for multiple proteins to allow interaction of different proteins with F-actin and hence regulate different processes in the nervous system.

6.2 Role of the actin cytoskeleton in the presynaptic release:

Our results indicated that HIC-1 is required for maintaining the presynaptic actin cytoskeleton and Wnt release, these data prompted us to ask whether there was any correlation between a normal actin cytoskeleton and Wnt release. Our experiments indicate that disrupting the actin cytoskeleton allows for increased Wnt secretion from the cholinergic motor neurons. How the actin cytoskeleton is involved in Wnt release is an important question that would require further experimentation.

The actin cytoskeleton is involved in a myriad of processes at the nerve terminals ranging from neurogenesis, axon branching, cellular trafficking and signaling, synaptic vesicles release and synaptogenesis among others (Morales et al., 2000;

Zhang and Benson, 2002) and reviewed in (Cingolani and Goda, 2008)). Interestingly, conflicting reports can be found on the role of local F-actin with respect to neurotransmitter release function. An earlier report claims that depolymerization of F-actin blocks neurotransmitter release (Bernstein and Bamburg, 1989), while more recent studies suggest an increase in neurotransmitter release upon actin depolymerization (Morales et al., 2000) or impaired recycling of synaptic vesicles after acute actin perturbations (Shupliakov et al., 2002). These findings warrant more studies to pinpoint the role of the actin cytoskeleton on neurotransmitter release.

Apart from affecting neurotransmitter release, the actin cytoskeleton has been shown to indirectly activate the Wnt/β-catenin signaling in mesenchymal cells (Galli et al., 2012). However, this work does not indicate a role for the actin cytoskeleton in the secretion of Wnt.

For a very long time, Wnts were considered to be just developmental molecules regulating embryonic development and early patterning of the embryo (reviewed in (Cadigan and Nusse, 1997)). Recent studies highlight more diverse functions of the Wnt signaling in the development and function of synapses and more specifically in maintaining acetylcholine receptor levels at the synapse ((Babu et al., 2011b; Barik et al., 2014b; Henriquez et al., 2008a; Jensen et al., 2012c; Kamimura et al., 2013; Klassen and Shen, 2007b; Messeant et al., 2017; Pandey et al., 2017) and reviewed in (Henriquez and Salinas, 2012; Jensen et al., 2012a; Koles and Budnik, 2012a, c)).

Despite the knowledge we have so far for the role of Wnts in the normal functioning of NMJs, there is no clear experimental evidence on how Wnts are

secreted from the Wnt-producing neurons. Kole and Budnik have described the cellular machinery used in the release of Wnts from the *Drosophila* larval NMJs. They propose that Wnt/Wg is encapsulated in exosomes in conjunction with Wntless/Evi (MIG-14 in *C.elegans*), then Wnt/Wg containing exosomes are sorted into multivesicular bodies at the presynaptic termini, these multivesicular bodies are then fused to the presynaptic membrane at a site near the active zone; the Periactive zone. They then release their exosomal content into the synaptic cleft at this site (Koles and Budnik, 2012a). Interestingly, the Periactive zone is also enriched with F-actin (Dunaevsky and Connor, 2000), this could, in turn, correspond to the site of Wnt vesicle release allowing for F-actin cytoskeleton to play a major role in Wnt release. Further experimentation using approaches that will allow one to image minute details across the pre-synaptic termini could help with further understanding the role of F-actin in Wnt release.

We have demonstrated through BiFC and genetic experiments, that HIC-1 is directly interacting with the actin-binding protein, Neurabin, which is reported to be localized at the periactive zone of the synapse (Sieburth et al., 2005b). Based on previous reports and our findings we are proposing that HIC-1 could be present at the periactive region of cholinergic neurons where it is regulates local F-actin dynamics which in turn allows for normal secretion of Wnt vesicles (illustrated in **Figure 6.1**). In-depth knowledge of the functioning of the actin cytoskeleton and its involvement in Wnt secretion warrants a lot more study.

6.3 The intracellular C-terminal region of HIC-1 acts as a claudin at the NMJ:

Out of 23 claudins in humans, 9 have been reported to have a conserved tyrosine residue at their C-terminus. It has been shown that modifications to this tyrosine

residue (phosphorylation) can alter the affinity of claudin-1 and claudin-2 towards the N-terminal PDZ domain of the ZO-1 protein (Nomme et al., 2015). We found the presence of a tyrosine residue in HIC-1 at the conserved C-terminus site similar to what is seen in other claudins in that region and that could be a putative PDZ binding motif for HIC-1. Furthermore, claudins interact with cytoplasmic scaffolding proteins particularly ZO-1,2,3 which indirectly connect claudins to the actin cytoskeleton and thereby stabilize tight junction assembly and their barrier functions (Umeda et al., 2006). A deletion construct of HIC-1 which removed the putative PDZ binding motif (last 4 amino acids at C-terminus including the tyrosine residue) failed to rescue the aldicarb defects of HIC-1 and was not able to bind to the PDZ domain of the actin-binding protein, Neurabin. Together these data indicate that HIC-1 could be behaving in a manner similar to other bonafide claudins intracellularly, using its C-terminal PDZ binding motif.

Claudins are known to make homo or heterophilic interactions via their two highly conserved extracellular loops which we found in HIC-1 to be poorly aligned with other claudins. This suggests that HIC-1 might not be functioning similarly to other claudins extracellularly. More studies are needed to understand how HIC-1 might be functioning extracellularly and whether it is involved in making cis or trans-interactions with other claudins, to other synaptic adhesion molecule or ligands present in the synaptic cleft. In summary, in this study, we have characterized the synaptic functions of a novel claudin-like molecule, HIC-1, in *C.elegans* and show that it is required for normal Wnt release in pre-synaptic motor neurons.

Areas of future investigation

1. We found that absence of HIC-1 leads to F-actin disruption and an enhanced Wnt release from the motor neurons in *C.elegans.* Removing actin pharmacologically also resulted in increased Wnt secretion. It would be interesting to see if the correlation between actin and Wnt secretion is indeed a conserved phenomenon across the species. Actin dynamics is regulated by Wnt signaling during axon remodeling (Stamatakou et al., 2015) and an actin regulator, Cortactin is regulated by Wnt signaling pathway which mediates synaptic plasticity across *Drosopholia* NMJs (Alicea et al., 2017). Although it has been established that actin cytoskeleton is regulated by Wnt pathway at the synapse but how actin cytoskeleton in turn regulates Wnt pathway is not very clear yet. Wnt proteins not only are required during early brain development, but they also play crucial roles in the mature brain (Inestrosa and Varela-Nallar, 2014; Oliva et al., 2013). Since we have seen the involvement of actin in maintaining a normal Wnt release in the adult *C.elegans,* One could perform cell culture experiments in the mouse or human neuronal culture. The outcome of this experiment should give insight whether actin cytoskeleton has a role in the secretion of Wnts in the mouse or human brain as well.

2. To further elucidate the correlation between Wnt and actin cytoskeleton in the neurons, one could go on to visualize these two entities under high magnification conditions. Transmission Electron microscopy (TEM) has revealed key structural features of the actin cytoskeleton (Svitkina, 2009), another such technique is stochastic optical reconstruction microscopy (STORM) which gives freedom to

visualize subcellular structures like actin at super-resolution limits (Stewart and Shen, 2015; Xu et al., 2013). The actin cytoskeleton makes a cage or ring-like structures at the neuronal terminals (Papandréou and Leterrier; Stewart and Shen, 2015). It is believed that in case of neuroendocrine cells, upon neuronal activity, these actin rings undergo structural changes, which leads to the release of secretory granules entrapped inside them (Malacombe et al., 2006). In the neuroendocrine cells, the release of secretory granules follows a path similar to neurotransmitter vesicles exocytosis to some extent. Here actin cytoskeleton plays a major role together with other proteins like RhoA, N-WASP, Arp3/3, and Cdc42 in maintaining reserved and a docked pool of these granules (Malacombe et al., 2006). Wnt secretion is increased during increased synaptic activity which leads to long-term potentiation in the hippocampal neurons (Chen et al., 2006). Our hypothesis is that Wnt vesicles might be trapped and stored in these cage-like structures of actin. During the neuronal activity, the actin dynamics could change in response to changes in the calcium transients in the cells, which in turn, could control the release of Wnts entrapped within them. In the neurons, similar to neurotransmitters release, the Wnt secretion could also be controlled, but unlike neurotransmitters, Wnt secretion would require actin dynamics machinery. To decipher whether Wnts are indeed sequestered inside the actin-like cage structures, one could look at these two structures under high magnification conditions.

3. Our studies on *hic-1* mutants have revealed secretion of Wnt ligands in an uncontrolled manner. To our knowledge, this is the first mutant in any system where increased Wnt secretion has been witnessed. We are interested in further elucidating what other molecules are deregulated during this scenario. To address

this, one could perform a genome-wide gene expression analysis in WT, *hic-1,* and *mig-14* mutants. This could further enrich our knowledge of the molecular details on Wnt secretion.

4. Our findings indicate that actin-binding protein, NAB-1 interacts directly to HIC-1 or in other words, NAB-1 acts as an adaptor to link HIC-1 with the actin cytoskeleton. It is still not clear whether NAB-1 alone is sufficient enough to link HIC-1 with actin cytoskeleton. There might be other protein(s) involved in this process. To evaluate what other molecules are required in this process, one could pull-down HIC-1::mCherry protein using mCherry antibodies from a translational fusion reporter line of *C.elegans* and then go for the mass-spectroscopy analysis. The outcome of this study should reveal the complete molecular machinery involved in linking HIC-1 with the actin cytoskeleton.

Appendix table 1: Collaborators and Contributions

Collaborators	Experiments performed	Displayed in section
Dr. Zhitao Hu and Dr. Lei Li, Queensland brain research Institute, Australia	Electrophysiology on *C.elegans* NMJs	Figure 3.21 and Figure 3.22
Diwakar Maraina, BS-MS student, IISER Mohali	Body bends and thrashing rates	Figure 3.23

Appendix table 2: Reagents used in the thesis

Lab	Reagent Strain/Plasmid	Citation
Josh Kaplan Lab	*nuIs32, nuIs152, nuIs376, nuIs159,nuIs299, nuIs283, nuIs169*	Babu et al.,2011, Sieburth et al.,2005, Hao et al.,2012
Andres Villu Maricq Lab	*akIs38*	Francis et al.,2005
Mei Zhen Lab	*hpIs66*	Hung et al.,2007
Derek Sieburth Lab	*vjIs30*	Staab et al.,2013
Mike Francis lab	*uIfs63*	Petrash et al.,2013

Bibliography

Abbas, L. (2003). Synapse formation: let's stick together. Curr Biol *13*, R25-27.
Abdelilah-Seyfried, S. (2010). Claudin-5a in developing zebrafish brain barriers: another brick in the wall. BioEssays *32*, 768-776.
Ackley, B.D., Harrington, R.J., Hudson, M.L., Williams, L., Kenyon, C.J., Chisholm, A.D., and Jin, Y. (2005). The two isoforms of the Caenorhabditis elegans leukocyte-common antigen related receptor tyrosine phosphatase PTP-3 function independently in axon guidance and synapse formation. The Journal of neuroscience : the official journal of the Society for Neuroscience *25*, 7517-7528.
Adenle, A.A., Johnsen, B., and Szewczyk, N.J. (2009). Review of the results from the International C. elegans first experiment (ICE-FIRST). Advances in space research : the official journal of the Committee on Space Research (COSPAR) *44*, 210-216.
Aktories, K., and Barbieri, J.T. (2005). Bacterial cytotoxins: targeting eukaryotic switches. Nature Reviews Microbiology *3*, 397.
Albelda, S.M. (1991). Endothelial and epithelial cell adhesion molecules. Am J Respir Cell Mol Biol *4*, 195-203.
Albuquerque, E.X., Pereira, E.F.R., Alkondon, M., and Rogers, S.W. (2009). Mammalian Nicotinic Acetylcholine Receptors: From Structure to Function. Physiological reviews *89*, 73-120.
Alfonso, A., Grundahl, K., Duerr, J.S., Han, H.-P., and Rand, J.B. (1993). The Caenorhabditis elegans unc-17 gene: a putative vesicular acetylcholine transporter. Science *261*, 617-619.
Alicea, D., Perez, M., Maldonado, C., Dominicci-Cotto, C., and Marie, B. (2017). Cortactin is a regulator of activity-dependent synaptic plasticity controlled by Wingless.
Alkondon, M., Pereira, E.F., and Albuquerque, E.X. (1998). α-Bungarotoxin-and methyllycaconitine-sensitive nicotinic receptors mediate fast synaptic transmission in interneurons of rat hippocampal slices. Brain research *810*, 257-263.
Alshbool, F.Z., and Mohan, S. (2014). Emerging Multifunctional Roles of Claudin Tight Junction Proteins in Bone. Endocrinology *155*, 2363-2376.
Anderson, J.L., Morran, L.T., and Phillips, P.C. (2010). Outcrossing and the Maintenance of Males within C. elegans Populations. Journal of Heredity *101*, S62-S74.
Asano, A., Asano, K., Sasaki, H., Furuse, M., and Tsukita, S. (2003a). Claudins in Caenorhabditis elegans. Current Biology *13*, 1042-1046.
Asano, A., Asano, K., Sasaki, H., Furuse, M., and Tsukita, S. (2003b). Claudins in Caenorhabditis elegans: their distribution and barrier function in the epithelium. Current Biology *13*, 1042-1046.
Babu, K., Hu, Z., Chien, S.-C., Garriga, G., and Kaplan, Joshua M. (2011a). The Immunoglobulin Super Family Protein RIG-3 Prevents Synaptic Potentiation and Regulates Wnt Signaling. Neuron *71*, 103-116.
Babu, K., Hu, Z., Chien, S.C., Garriga, G., and Kaplan, J.M. (2011b). The immunoglobulin super family protein RIG-3 prevents synaptic potentiation and regulates Wnt signaling. Neuron *71*, 103-116.
Barik, A., Zhang, B., Sohal, G.S., Xiong, W.-C., and Mei, L. (2014a). Crosstalk between Agrin and Wnt signaling pathways in development of vertebrate neuromuscular junction. Developmental Neurobiology *74*, 828-838.
Barik, A., Zhang, B., Sohal, G.S., Xiong, W.C., and Mei, L. (2014b). Crosstalk between Agrin and Wnt signaling pathways in development of vertebrate neuromuscular junction. Dev Neurobiol *74*, 828-838.

Benson, D.L., Schnapp, L.M., Shapiro, L., and Huntley, G.W. (2000). Making memories stick: cell-adhesion molecules in synaptic plasticity. Trends in Cell Biology *10*, 473-482.
Bernstein, B.W., and Bamburg, J.R. (1989). Cycling of actin assembly in synaptosomes and neurotransmitter release. Neuron *3*, 257-265.
Biederer, T., Sara, Y., Mozhayeva, M., Atasoy, D., Liu, X., Kavalali, E.T., and Sudhof, T.C. (2002). SynCAM, a synaptic adhesion molecule that drives synapse assembly. Science *297*, 1525-1531.
Brenner, S. (1974a). THE GENETICS OF CAENORHABDITIS ELEGANS. Genetics *77*, 71-94.
Brenner, S. (1974b). The genetics of Caenorhabditis elegans. Genetics *77*, 71-94.
Brumwell, C.L., Johnson, J.L., and Jacob, M.H. (2002). Extrasynaptic α7-nicotinic acetylcholine receptor expression in developing neurons is regulated by inputs, targets, and activity. Journal of Neuroscience *22*, 8101-8109.
Buckingham, S.D., and Sattelle, D.B. (2009). Fast, automated measurement of nematode swimming (thrashing) without morphometry. BMC Neuroscience *10*, 84.
Burkel, B.M., von Dassow, G., and Bement, W.M. (2007). Versatile fluorescent probes for actin filaments based on the actin-binding domain of utrophin. Cell Motil Cytoskeleton *64*, 822-832.
Burnett, P.E., Blackshaw, S., Lai, M.M., Qureshi, I.A., Burnett, A.F., Sabatini, D.M., and Snyder, S.H. (1998). Neurabin is a synaptic protein linking p70 S6 kinase and the neuronal cytoskeleton. Proceedings of the National Academy of Sciences of the United States of America *95*, 8351-8356.
Cadigan, K.M., and Nusse, R. (1997). Wnt signaling: a common theme in animal development. Genes Dev *11*, 3286-3305.
Cassada, R.C., and Russell, R.L. (1975). The dauerlarva, a post-embryonic developmental variant of the nematode Caenorhabditis elegans. Developmental biology *46*, 326-342.
Cattabeni, F. (2012). Neurabin: a key factor in the specific neuroprotection mediated by Adenosine. Purinergic Signalling *8*, 659-660.
Chalfie, M., Tu, Y., Euskirchen, G., Ward, W.W., and Prasher, D.C. (1994). Green fluorescent protein as a marker for gene expression. Science *263*, 802.
Chan, J.P., Staab, T.A., Wang, H., Mazzasette, C., Butte, Z., and Sieburth, D. (2013). Extrasynaptic Muscarinic Acetylcholine Receptors on Neuronal Cell Bodies Regulate Presynaptic Function in Caenorhabditis elegans. The Journal of Neuroscience *33*, 14146-14159.
Charles, P., Hernandez, M.P., Stankoff, B., Aigrot, M.S., Colin, C., Rougon, G., Zalc, B., and Lubetzki, C. (2000). Negative regulation of central nervous system myelination by polysialylated-neural cell adhesion molecule. Proceedings of the National Academy of Sciences *97*, 7585.
Cheerathodi, M., Avci, N.G., Guerrero, P.A., Tang, L.K., Popp, J., Morales, J.E., Chen, Z., Carnero, A., Lang, F.F., Ballif, B.A., *et al.* (2016). The Cytoskeletal Adapter Protein Spinophilin Regulates Invadopodia Dynamics and Tumor Cell Invasion in Glioblastoma. Molecular Cancer Research *14*, 1277-1287.
Chen, J., Park, C.S., and Tang, S.-J. (2006). Activity-dependent Synaptic Wnt Release Regulates Hippocampal Long Term Potentiation. Journal of Biological Chemistry *281*, 11910-11916.
Chen, Y., Liu, Y., Cottingham, C., McMahon, L., Jiao, K., Greengard, P., and Wang, Q. (2012). Neurabin Scaffolding of Adenosine Receptor and RGS4 Regulates Anti-Seizure Effect of Endogenous Adenosine. Journal of Neuroscience *32*, 2683-2695.
Chia, P.H., Li, P., and Shen, K. (2013). Cellular and molecular mechanisms underlying presynapse formation. The Journal of Cell Biology *203*, 11-22.

Chia, P.H., Patel, M.R., and Shen, K. (2012a). NAB-1 instructs synapse assembly by linking adhesion molecules and F-actin to active zone proteins. Nature Neuroscience *15*, 234-242.
Chia, P.H., Patel, M.R., and Shen, K. (2012b). NAB-1 instructs synapse assembly by linking adhesion molecules and F-actin to active zone proteins. Nat Neurosci *15*, 234-242.
Chien, S.C., Gurling, M., Kim, C., Craft, T., Forrester, W., and Garriga, G. (2015). Autonomous and nonautonomous regulation of Wnt-mediated neuronal polarity by the C. elegans Ror kinase CAM-1. Developmental biology *404*, 55-65.
Cingolani, L.A., and Goda, Y. (2008). Actin in action: the interplay between the actin cytoskeleton and synaptic efficacy. Nat Rev Neurosci *9*, 344-356.
Couchman, J.R. (2003). Syndecans: proteoglycan regulators of cell-surface microdomains? Nat Rev Mol Cell Biol *4*, 926-937.
Coue, M., Brenner, S.L., Spector, I., and Korn, E.D. (1987). Inhibition of actin polymerization by latrunculin A. FEBS Lett *213*, 316-318.
Cox, E.A. (2004). Sticky worms: adhesion complexes in C. elegans. Journal of Cell Science *117*, 1885-1897.
Cox, E.A., and Hardin, J. (2004). Sticky worms: adhesion complexes in C. elegans. J Cell Sci *117*, 1885-1897.
Cox, E.A., Tuskey, C., and Hardin, J. (2004). Cell adhesion receptors in C. elegans. J Cell Sci *117*, 1867-1870.
Culotti, J.G. (1994). Axon guidance mechanisms in Caenorhabditis elegans. Current Opinion in Genetics & Development *4*, 587-595.
Debell, J.T. (1965). A Long Look at Neuromuscular Junctions in Nematodes. The Quarterly Review of Biology *40*, 233-251.
Devaux, J., Fykkolodziej, B., and Gow, A. (2010). Claudin Proteins And Neuronal Function. Current topics in membranes *65*, 229-253.
Dickins, E.M., and Salinas, P.C. (2013). Wnts in action: from synapse formation to synaptic maintenance. Frontiers in Cellular Neuroscience *7*.
Dillon, C., and Goda, Y. (2005). THE ACTIN CYTOSKELETON: Integrating Form and Function at the Synapse. Annual Review of Neuroscience *28*, 25-55.
Dorsch, S., Klotz, K.N., Engelhardt, S., Lohse, M.J., and Bunemann, M. (2009). Analysis of receptor oligomerization by FRAP microscopy. Nature methods *6*, 225-230.
Dunaevsky, A., and Connor, E.A. (2000). F-actin is concentrated in nonrelease domains at frog neuromuscular junctions. The Journal of neuroscience : the official journal of the Society for Neuroscience *20*, 6007-6012.
Eisenmann, D.M., and Kim, S.K. (2000). Protruding vulva mutants identify novel loci and Wnt signaling factors that function during Caenorhabditis elegans vulva development. Genetics *156*, 1097-1116.
Ellis, H.M., and Horvitz, H.R. (1986). Genetic control of programmed cell death in the nematode C. elegans. Cell *44*, 817-829.
Fares, H., and Greenwald, I. (2001). Genetic analysis of endocytosis in Caenorhabditis elegans: coelomocyte uptake defective mutants. Genetics *159*, 133-145.
Fire, A., Xu, S., Montgomery, M.K., Kostas, S.A., Driver, S.E., and Mello, C.C. (1998). Potent and specific genetic interference by double-stranded RNA in Caenorhabditis elegans. Nature *391*, 806.

Firestein, B.L., and Rongo, C. (2001). DLG-1 is a MAGUK similar to SAP97 and is required for adherens junction formation. Molecular Biology of the Cell *12*, 3465-3475.
Fitzgerald, K., Harrington, A., and Leder, P. (2000). Ras pathway signals are required for notch-mediated oncogenesis. Oncogene *19*, 4191.
Fradkin, L.G. (2005). Wnt Signaling in Neural Circuit Development. Journal of Neuroscience *25*, 10376-10378.
Francis, M.M., Evans, S.P., Jensen, M., Madsen, D.M., Mancuso, J., Norman, K.R., and Maricq, A.V. (2005a). The Ror Receptor Tyrosine Kinase CAM-1 Is Required for ACR-16-Mediated Synaptic Transmission at the C. elegans Neuromuscular Junction. Neuron *46*, 581-594.
Francis, M.M., Evans, S.P., Jensen, M., Madsen, D.M., Mancuso, J., Norman, K.R., and Maricq, A.V. (2005b). The Ror receptor tyrosine kinase CAM-1 is required for ACR-16-mediated synaptic transmission at the C. elegans neuromuscular junction. Neuron *46*, 581-594.
Frøkjær-Jensen, C., Davis, M.W., Hopkins, C.E., Newman, B.J., Thummel, J.M., Olesen, S.-P., Grunnet, M., and Jorgensen, E.M. (2008). Single-copy insertion of transgenes in Caenorhabditis elegans. Nature genetics *40*, 1375.
Frotscher, M., Studer, D., Graber, W., Chai, X., Nestel, S., and Zhao, S. (2014). Fine structure of synapses on dendritic spines. Frontiers in Neuroanatomy *8*, 94.
Galli, C., Piemontese, M., Lumetti, S., Ravanetti, F., Macaluso, G.M., and Passeri, G. (2012). Actin cytoskeleton controls activation of Wnt/beta-catenin signaling in mesenchymal cells on implant surfaces with different topographies. Acta Biomater *8*, 2963-2968.
Gill, M.S., Olsen, A., Sampayo, J.N., and Lithgow, G.J. (2003). An automated high-throughput assay for survival of the nematode Caenorhabditis elegans. Free Radical Biology and Medicine *35*, 558-565.
Goncalves, A., Ambrosio, A.F., and Fernandes, R. (2013). Regulation of claudins in blood-tissue barriers under physiological and pathological states. Tissue Barriers *1*, e24782.
Gong, J., Yuan, Y., Ward, A., Kang, L., Zhang, B., Wu, Z., Peng, J., Feng, Z., Liu, J., and Xu, X.Z. (2016). The C. elegans Taste Receptor Homolog LITE-1 Is a Photoreceptor. Cell *167*, 1252-1263 e1210.
Gotti, C., and Clementi, F. (2004). Neuronal nicotinic receptors: from structure to pathology. Progress in neurobiology *74*, 363-396.
Gregorieff, A., and Clevers, H. (2005). Wnt signaling in the intestinal epithelium: from endoderm to cancer. Genes & development *19*, 877-890.
Gunzel, D., and Yu, A.S. (2013). Claudins and the modulation of tight junction permeability. Physiol Rev *93*, 525-569.
Hallam, S., Singer, E., Waring, D., and Jin, Y. (2000). The C. elegans NeuroD homolog cnd-1 functions in multiple aspects of motor neuron fate specification. Development *127*, 4239-4252.
Hao, Y., Hu, Z., Sieburth, D., and Kaplan, J.M. (2012). RIC-7 promotes neuropeptide secretion. PLoS genetics *8*, e1002464.
Hawkins, N.C., Ellis, G.C., Bowerman, B., and Garriga, G. (2005). MOM-5 frizzled regulates the distribution of DSH-2 to control C. elegans asymmetric neuroblast divisions. Developmental biology *284*, 246-259.
Henriquez, J.P., and Salinas, P.C. (2012). Dual roles for Wnt signalling during the formation of the vertebrate neuromuscular junction. Acta Physiol (Oxf) *204*, 128-136.

Henriquez, J.P., Webb, A., Bence, M., Bildsoe, H., Sahores, M., Hughes, S.M., and Salinas, P.C. (2008a). Wnt signaling promotes AChR aggregation at the neuromuscular synapse in collaboration with agrin. Proceedings of the National Academy of Sciences of the United States of America *105*, 18812-18817.

Henriquez, J.P., Webb, A., Bence, M., Bildsoe, H., Sahores, M., Hughes, S.M., and Salinas, P.C. (2008b). Wnt signaling promotes AChR aggregation at the neuromuscular synapse in collaboration with agrin. Proceedings of the National Academy of Sciences *105*, 18812-18817.

Hilliard, M.A., and Bargmann, C.I. (2006). Wnt signals and frizzled activity orient anterior-posterior axon outgrowth in C. elegans. Developmental Cell *10*, 379-390.

Hillier, L.W., Coulson, A., Murray, J.I., Bao, Z., Sulston, J.E., and Waterston, R.H. (2005). Genomics in C. elegans: so many genes, such a little worm. Genome research *15*, 1651-1660.

Hogg, R., Raggenbass, M., and Bertrand, D. (2003). Nicotinic acetylcholine receptors: from structure to brain function. In Reviews of physiology, biochemistry and pharmacology (Springer), pp. 1-46.

Hsieh, Y.-W., Alqadah, A., and Chuang, C.-F. (2014). Asymmetric neural development in theCaenorhabditis elegansolfactory system. genesis *52*, 544-554.

Hu, Z., Hom, S., Kudze, T., Tong, X.J., Choi, S., Aramuni, G., Zhang, W., and Kaplan, J.M. (2012). Neurexin and Neuroligin Mediate Retrograde Synaptic Inhibition in C. elegans. Science *337*, 980-984.

Hu, Z., Tong, X.-J., and Kaplan, J.M. (2013). UNC-13L, UNC-13S, and Tomosyn form a protein code for fast and slow neurotransmitter release in Caenorhabditis elegans. eLife *2*, e00967.

Hung, W., Hwang, C., Po, M.D., and Zhen, M. (2007). Neuronal polarity is regulated by a direct interaction between a scaffolding protein, Neurabin, and a presynaptic SAD-1 kinase in Caenorhabditis elegans. Development *134*, 237-249.

Inestrosa, N.C., and Arenas, E. (2010). Emerging roles of Wnts in the adult nervous system. Nat Rev Neurosci *11*, 77-86.

Inestrosa, N.C., and Varela-Nallar, L. (2014). Wnt signaling in the nervous system and in Alzheimer's disease. Journal of Molecular Cell Biology *6*, 64-74.

Inestrosa, N.C., Varela-Nallar, L., Grabowski, C.P., and Colombres, M. (2007). Synaptotoxicity in Alzheimer's disease: the Wnt signaling pathway as a molecular target. IUBMB Life *59*, 316-321.

Jensen, A.A., Frølund, B., Liljefors, T., and Krogsgaard-Larsen, P. (2005). Neuronal nicotinic acetylcholine receptors: structural revelations, target identifications, and therapeutic inspirations. Journal of medicinal chemistry *48*, 4705-4745.

Jensen, M., Brockie, P.J., and Maricq, A.V. (2012a). Wnt signaling regulates experience-dependent synaptic plasticity in the adult nervous system. Cell Cycle *11*, 2585-2586.

Jensen, M., Hoerndli, Frédéric J., Brockie, Penelope J., Wang, R., Johnson, E., Maxfield, D., Francis, Michael M., Madsen, David M., and Maricq, Andres V. (2012b). Wnt Signaling Regulates Acetylcholine Receptor Translocation and Synaptic Plasticity in the Adult Nervous System. Cell *149*, 173-187.

Jensen, M., Hoerndli, F.J., Brockie, P.J., Wang, R., Johnson, E., Maxfield, D., Francis, M.M., Madsen, D.M., and Maricq, A.V. (2012c). Wnt signaling regulates acetylcholine receptor translocation and synaptic plasticity in the adult nervous system. Cell *149*, 173-187.

Jia, W., Lu, R., Martin, T.A., and Jiang, W.G. (2014). The role of claudin-5 in blood-brain barrier (BBB) and brain metastases (Review). Molecular Medicine Reports *9*, 779-785.

Jones, A.K., and Sattelle, D.B. (2004). Functional genomics of the nicotinic acetylcholine receptor gene family of the nematode,Caenorhabditis elegans. BioEssays *26*, 39-49.
Jorgensen, E.M., and Nonet, M.L. (1995). Neuromuscular junctions in the nematode C. elegans. Seminars in Developmental Biology *6*, 207-220.
Jospin, M., Qi, Y.B., Stawicki, T.M., Boulin, T., Schuske, K.R., Horvitz, H.R., Bessereau, J.-L., Jorgensen, E.M., and Jin, Y. (2009). A Neuronal Acetylcholine Receptor Regulates the Balance of Muscle Excitation and Inhibition in Caenorhabditis elegans. PLOS Biology *7*, e1000265.
Kamath, R.S., Fraser, A.G., Dong, Y., Poulin, G., Durbin, R., Gotta, M., Kanapin, A., Le Bot, N., Moreno, S., and Sohrmann, M. (2003). Systematic functional analysis of the Caenorhabditis elegans genome using RNAi. Nature *421*, 231.
Kamimura, K., Ueno, K., Nakagawa, J., Hamada, R., Saitoe, M., and Maeda, N. (2013). Perlecan regulates bidirectional Wnt signaling at the Drosophila neuromuscular junction. J Cell Biol *200*, 219-233.
Kerppola, T.K. (2013). Bimolecular Fluorescence Complementation (BiFC) Analysis of Protein Interactions in Live Cells. Cold Spring Harbor Protocols *2013*, pdb.prot076497.
Kim, S.S., Wang, H., Li, X.-Y., Chen, T., Mercaldo, V., Descalzi, G., Wu, L.-J., and Zhuo, M. (2011). Neurabin in the anterior cingulate cortex regulates anxiety-like behavior in adult mice. Molecular Brain *4*, 6.
Klassen, M.P., and Shen, K. (2007a). Wnt Signaling Positions Neuromuscular Connectivity by Inhibiting Synapse Formation in C. elegans. Cell *130*, 704-716.
Klassen, M.P., and Shen, K. (2007b). Wnt signaling positions neuromuscular connectivity by inhibiting synapse formation in C. elegans. Cell *130*, 704-716.
Kojima, T., Go, M., Takano, K., Kurose, M., Ohkuni, T., Koizumi, J., Kamekura, R., Ogasawara, N., Masaki, T., Fuchimoto, J.*, et al.* (2013). Regulation of tight junctions in upper airway epithelium. Biomed Res Int *2013*, 947072.
Koles, K., and Budnik, V. (2012a). Exosomes go with the Wnt. Cell Logist *2*, 169-173.
Koles, K., and Budnik, V. (2012b). Wnt Signaling in Neuromuscular Junction Development. Cold Spring Harbor Perspectives in Biology *4*, a008045-a008045.
Koles, K., and Budnik, V. (2012c). Wnt signaling in neuromuscular junction development. Cold Spring Harbor perspectives in biology *4*.
Kourtis, N., and Tavernarakis, N. (2008). Monitoring protein synthesis by fluorescence recovery after photobleaching (FRAP) _in vivo_.
Krause, G., Winkler, L., Mueller, S.L., Haseloff, R.F., Piontek, J., and Blasig, I.E. (2008a). Structure and function of claudins. Biochimica et Biophysica Acta (BBA) - Biomembranes *1778*, 631-645.
Krause, G., Winkler, L., Mueller, S.L., Haseloff, R.F., Piontek, J., and Blasig, I.E. (2008b). Structure and function of claudins. Biochim Biophys Acta *1778*, 631-645.
Lackner, M.R., Nurrish, S.J., and Kaplan, J.M. (1999). Facilitation of synaptic transmission by EGL-30 Gqα and EGL-8 PLCβ: DAG binding to UNC-13 is required to stimulate acetylcholine release. Neuron *24*, 335-346.
Lal-Nag, M., and Morin, P.J. (2009). The claudins. Genome Biol *10*, 235.
Langton, P.F., Kakugawa, S., and Vincent, J.-P. (2016). Making, Exporting, and Modulating Wnts. Trends in Cell Biology *26*, 756-765.

Legouis, R., Gansmuller, A., Sookhareea, S., Bosher, J.M., Baillie, D.L., and Labouesse, M. (2000). LET-413 is a basolateral protein required for the assembly of adherens junctions in Caenorhabditis elegans. Nature Cell Biology *2*, 415.
Liewald, J.F., Brauner, M., Stephens, G.J., Bouhours, M., Schultheis, C., Zhen, M., and Gottschalk, A. (2008). Optogenetic analysis of synaptic function. Nature Methods *5*, 895.
Lin, K., Dorman, J.B., Rodan, A., and Kenyon, C. (1997). daf-16: An HNF-3/forkhead family member that can function to double the life-span of Caenorhabditis elegans. Science *278*, 1319-1322.
Liu, D., and Thomas, J.H. (1994). Regulation of a periodic motor program in C. elegans. Journal of Neuroscience *14*, 1953-1962.
Liu, Q., Hollopeter, G., and Jorgensen, E.M. (2009). Graded synaptic transmission at the Caenorhabditis elegans neuromuscular junction. Proceedings of the National Academy of Sciences *106*, 10823-10828.
Livak, K.J., and Schmittgen, T.D. (2001). Analysis of Relative Gene Expression Data Using Real-Time Quantitative PCR and the 2−ΔΔCT Method. Methods *25*, 402-408.
Lukas, R.J., Changeux, J.-P., le Novère, N., Albuquerque, E.X., Balfour, D.J.K., Berg, D.K., Bertrand, D., Chiappinelli, V.A., Clarke, P.B.S., Collins, A.C.*, et al.* (1999). International Union of Pharmacology. XX. Current Status of the Nomenclature for Nicotinic Acetylcholine Receptors and Their Subunits. Pharmacological Reviews *51*, 397.
Mahoney, T.R., Liu, Q., Itoh, T., Luo, S., Hadwiger, G., Vincent, R., Wang, Z.-W., Fukuda, M., and Nonet, M.L. (2006a). Regulation of synaptic transmission by RAB-3 and RAB-27 in Caenorhabditis elegans. Molecular Biology of the Cell *17*, 2617-2625.
Mahoney, T.R., Luo, S., and Nonet, M.L. (2006b). Analysis of synaptic transmission in Caenorhabditis elegans using an aldicarb-sensitivity assay. Nature Protocols *1*, 1772-1777.
Malacombe, M., Bader, M.F., and Gasman, S. (2006). Exocytosis in neuroendocrine cells: new tasks for actin. Biochim Biophys Acta *1763*, 1175-1183.
Mariol, M.C., Walter, L., Bellemin, S., and Gieseler, K. (2013). A rapid protocol for integrating extrachromosomal arrays with high transmission rate into the C. elegans genome. J Vis Exp, e50773.
Martin, R.J., Robertson, A.P., Buxton, S.K., Beech, R.N., Charvet, C.L., and Neveu, C. (2012). Levamisole receptors: a second awakening. Trends in Parasitology *28*, 289-296.
McGehee, D.S., and Role, L.W. (1995). Physiological Diversity of Nicotinic Acetylcholine Receptors Expressed by Vertebrate Neurons. Annual Review of Physiology *57*, 521-546.
Mclntire, S.L., Jorgensen, E., and Horvitz, H.R. (1993). Genes required for GABA function in Caenorhabditis elegans. Nature *364*, 334.
Mello, C., and Fire, A. (1995). DNA transformation. Methods Cell Biol *48*, 451-482.
Messeant, J., Ezan, J., Delers, P., Glebov, K., Marchiol, C., Lager, F., Renault, G., Tissir, F., Montcouquiol, M., Sans, N.*, et al.* (2017). Wnt proteins contribute to neuromuscular junction formation through distinct signaling pathways. Development *144*, 1712-1724.
Miller, D.M., Stockdale, F.E., and Karn, J. (1986). Immunological identification of the genes encoding the four myosin heavy chain isoforms of Caenorhabditis elegans. Proceedings of the National Academy of Sciences *83*, 2305-2309.
Mishina, M., Takai, T., Imoto, K., Noda, M., Takahashi, T., Numa, S., Methfessel, C., and Sakmann, B. (1986). Molecular distinction between fetal and adult forms of muscle acetylcholine receptor. Nature *321*, 406.

Morales, M., Colicos, M.A., and Goda, Y. (2000). Actin-dependent regulation of neurotransmitter release at central synapses. Neuron *27*, 539-550.
Morgan, T.H. (1936). Further experiments on the formation of the antipolar lobe of Ilyanassa. Journal of Experimental Zoology *74*, 381-425.
Nakanishi, H., Obaishi, H., Satoh, A., Wada, M., Mandai, K., Satoh, K., Nishioka, H., Matsuura, Y., Mizoguchi, A., and Takai, Y. (1997a). Neurabin: a novel neural tissue-specific actin filament-binding protein involved in neurite formation. J Cell Biol *139*, 951-961.
Nakanishi, H., Obaishi, H., Satoh, A., Wada, M., Mandai, K., Satoh, K., Nishioka, H., Matsuura, Y., Mizoguchi, A., and Takai, Y. (1997b). Neurabin: A Novel Neural Tissue–specific Actin Filament–binding Protein Involved in Neurite Formation. The Journal of Cell Biology *139*, 951-961.
Niebur, E., and Erdös, P. (1991). Theory of the locomotion of nematodes: Dynamics of undulatory progression on a surface. Biophysical Journal *60*, 1132-1146.
Nomme, J., Antanasijevic, A., Caffrey, M., Van Itallie, C.M., Anderson, J.M., Fanning, A.S., and Lavie, A. (2015). Structural Basis of a Key Factor Regulating the Affinity between the Zonula Occludens First PDZ Domain and Claudins. J Biol Chem *290*, 16595-16606.
Nonet, M.L. (1999). Visualization of synaptic specializations in live C. elegans with synaptic vesicle protein-GFP fusions. Journal of neuroscience methods *89*, 33-40.
Nonet, M.L., Grundahl, K., Meyer, B.J., and Rand, J.B. (1993). Synaptic function is impaired but not eliminated in C. elegans mutants lacking synaptotagmin. Cell *73*, 1291-1305.
Nonet, M.L., Staunton, J.E., Kilgard, M.P., Fergestad, T., Hartwieg, E., Horvitz, H.R., Jorgensen, E.M., and Meyer, B.J. (1997). Caenorhabditis elegans rab-3 mutant synapses exhibit impaired function and are partially depleted of vesicles. Journal of Neuroscience *17*, 8061-8073.
Oliva, C.A., Vargas, J.Y., and Inestrosa, N.C. (2013). Wnts in adult brain: from synaptic plasticity to cognitive deficiencies. Frontiers in Cellular Neuroscience *7*, 224.
Oliver, C.J., Terry-Lorenzo, R.T., Elliott, E., Bloomer, W.A.C., Li, S., Brautigan, D.L., Colbran, R.J., and Shenolikar, S. (2002). Targeting Protein Phosphatase 1 (PP1) to the Actin Cytoskeleton: the Neurabin I/PP1 Complex Regulates Cell Morphology. Molecular and Cellular Biology *22*, 4690-4701.
Pan, C.L., Baum, P.D., Gu, M., Jorgensen, E.M., Clark, S.G., and Garriga, G. (2008). C. elegans AP-2 and retromer control Wnt signaling by regulating mig-14/Wntless. Developmental Cell *14*, 132-139.
Pan, C.L., Howell, J.E., Clark, S.G., Hilliard, M., Cordes, S., Bargmann, C.I., and Garriga, G. (2006). Multiple Wnts and frizzled receptors regulate anteriorly directed cell and growth cone migrations in Caenorhabditis elegans. Developmental Cell *10*, 367-377.
Pandey, P., Bhardwaj, A., and Babu, K. (2017). Regulation of WNT Signaling at the Neuromuscular Junction by the Immunoglobulin Superfamily Protein RIG-3 in Caenorhabditis elegans. Genetics *206*, 1521-1534.
Pandey, P., Bhardwaj, A., and Babu, K. (2017). The immunoglobulin super-family protein, RIG-3, regulates WNT signaling by interacting with the non-conventional Wnt Receptor, CAM-1 at the C. elegans Neuromuscular Junction. Under Revision.
Papandréou, M.-J., and Leterrier, C. The functional architecture of axonal actin. Molecular and Cellular Neuroscience.
Paul, D., Baena, V., Ge, S., Jiang, X., Jellison, E.R., Kiprono, T., Agalliu, D., and Pachter, J.S. (2016). Appearance of claudin-5+ leukocytes in the central nervous system during neuroinflammation: a novel role for endothelial-derived extracellular vesicles. Journal of Neuroinflammation *13*.

Petrash, H.A., Philbrook, A., Haburcak, M., Barbagallo, B., and Francis, M.M. (2013). ACR-12 ionotropic acetylcholine receptor complexes regulate inhibitory motor neuron activity in Caenorhabditis elegans. The Journal of neuroscience : the official journal of the Society for Neuroscience *33*, 5524-5532.
Philbrook, A., Barbagallo, B., and Francis, M.M. (2013). A tale of two receptors: Dual roles for ionotropic acetylcholine receptors in regulating motor neuron excitation and inhibition. Worm *2*, e25765.
Pollerberg, G.E., Thelen, K., Theiss, M.O., and Hochlehnert, B.C. (2013). The role of cell adhesion molecules for navigating axons: density matters. Mech Dev *130*, 359-372.
Raftery, M.A., Hunkapiller, M.W., Strader, C.D., and Hood, L.E. (1980). Acetylcholine receptor: complex of homologous subunits. Science *208*, 1454.
Reinhold, A.K., and Rittner, H.L. (2016). Barrier function in the peripheral and central nervous system—a review. Pflügers Archiv - European Journal of Physiology *469*, 123-134.
Reits, E.A., and Neefjes, J.J. (2001). From fixed to FRAP: measuring protein mobility and activity in living cells. Nat Cell Biol *3*, E145-147.
Richmond, J.E., and Jorgensen, E.M. (1999a). Nature Neuroscience *2*, 791-797.
Richmond, J.E., and Jorgensen, E.M. (1999b). One GABA and two acetylcholine receptors function at the C. elegans neuromuscular junction. Nat Neurosci *2*, 791-797.
Russell, J.S.a.D. (2001). Molecular Cloning: A Laboratory Manual.
Ryan, X.P., Alldritt, J., Svenningsson, P., Allen, P.B., Wu, G.-Y., Nairn, A.C., and Greengard, P. (2005). The Rho-Specific GEF Lfc Interacts with Neurabin and Spinophilin to Regulate Dendritic Spine Morphology. Neuron *47*, 85-100.
Saheki, Y., and Bargmann, C.I. (2009). Presynaptic CaV2 calcium channel traffic requires CALF-1 and the α 2 δ subunit UNC-36. Nature Neuroscience *12*, 1257.
Schoepfer, R., Conroy, W.G., Whiting, P., Gore, M., and Lindstrom, J. (1990). Brain?-bungarotoxin binding protein cDNAs and MAbs reveal subtypes of this branch of the ligand-gated ion channel gene superfamily. Neuron *5*, 35-48.
Schwarz, J., Lewandrowski, I., and Bringmann, H. (2011). Reduced activity of a sensory neuron during a sleep-like state in Caenorhabditis elegans. Current biology : CB *21*, R983-984.
Schwarz, J., Spies, J.P., and Bringmann, H. (2012). Reduced muscle contraction and a relaxed posture during sleep-like Lethargus. Worm *1*, 12-14.
Shah, K., and Rossie, S. (2017). Tale of the Good and the Bad Cdk5: Remodeling of the Actin Cytoskeleton in the Brain. Molecular Neurobiology.
Shen, K., and Bargmann, C.I. (2003). The immunoglobulin superfamily protein SYG-1 determines the location of specific synapses in C. elegans. Cell *112*, 619-630.
Shen, K., Fetter, R.D., and Bargmann, C.I. (2004). Synaptic specificity is generated by the synaptic guidepost protein SYG-2 and its receptor, SYG-1. Cell *116*, 869-881.
Shimohama, S., Greenwald, D., Shafron, D., Akaika, A., Maeda, T., Kaneko, S., Kimura, J., Simpkins, C., Day, A., and Meyer, E. (1998). Nicotinic α7 receptors protect against glutamate neurotoxicity and neuronal ischemic damage. Brain research *779*, 359-363.
Shupliakov, O., Bloom, O., Gustafsson, J.S., Kjaerulff, O., Low, P., Tomilin, N., Pieribone, V.A., Greengard, P., and Brodin, L. (2002). Impaired recycling of synaptic vesicles after acute perturbation

of the presynaptic actin cytoskeleton. Proceedings of the National Academy of Sciences of the United States of America *99*, 14476-14481.
Sieburth, D., Ch'ng, Q., Dybbs, M., Tavazoie, M., Kennedy, S., Wang, D., Dupuy, D., Rual, J.-F., Hill, D.E., Vidal, M.*, et al.* (2005a). Systematic analysis of genes required for synapse structure and function. Nature *436*, 510-517.
Sieburth, D., Ch'ng, Q., Dybbs, M., Tavazoie, M., Kennedy, S., Wang, D., Dupuy, D., Rual, J.F., Hill, D.E., Vidal, M.*, et al.* (2005b). Systematic analysis of genes required for synapse structure and function. Nature *436*, 510-517.
Sieburth, D., Madison, J.M., and Kaplan, J.M. (2006). PKC-1 regulates secretion of neuropeptides. Nature Neuroscience *10*, 49-57.
Sievers, F., Wilm, A., Dineen, D., Gibson, T.J., Karplus, K., Li, W., Lopez, R., McWilliam, H., Remmert, M., Soding, J.*, et al.* (2011). Fast, scalable generation of high-quality protein multiple sequence alignments using Clustal Omega. Mol Syst Biol *7*, 539.
Simske, J.S., Köppen, M., Sims, P., Hodgkin, J., Yonkof, A., and Hardin, J. (2003). The cell junction protein VAB-9 regulates adhesion and epidermal morphology in C. elegans. Nature Cell Biology *5*, 619.
Smith, C.J., O'Brien, T., Chatzigeorgiou, M., Spencer, W.C., Feingold-Link, E., Husson, S.J., Hori, S., Mitani, S., Gottschalk, A., and Schafer, W.R. (2013). Sensory neuron fates are distinguished by a transcriptional switch that regulates dendrite branch stabilization. Neuron *79*, 266-280.
Staab, T.A., Griffen, T.C., Corcoran, C., Evgrafov, O., Knowles, J.A., and Sieburth, D. (2013). The conserved SKN-1/Nrf2 stress response pathway regulates synaptic function in Caenorhabditis elegans. PLoS Genet *9*, e1003354.
Stamatakou, E., Hoyos-Flight, M., and Salinas, P.C. (2015). Wnt Signalling Promotes Actin Dynamics during Axon Remodelling through the Actin-Binding Protein Eps8. PLOS ONE *10*, e0134976.
Stewart, E., and Shen, K. (2015). STORMing towards a clear picture of the cytoskeleton in neurons. eLife *4*, e06235.
Stork, T., Engelen, D., Krudewig, A., Silies, M., Bainton, R.J., and Klämbt, C. (2008). Organization and Function of the Blood–Brain Barrier in Drosophila. The Journal of Neuroscience *28*, 587-597.
Svitkina, T. (2009). Imaging Cytoskeleton Components by Electron Microscopy. Methods in molecular biology (Clifton, NJ) *586*, 187-206.
Tabara, H., Grishok, A., and Mello, C.C. (1998). RNAi in C. elegans: Soaking in the Genome Sequence. Science *282*, 430-431.
Tabara, H., Sarkissian, M., Kelly, W.G., Fleenor, J., Grishok, A., Timmons, L., Fire, A., and Mello, C.C. (1999). The rde-1 gene, RNA interference, and transposon silencing in C. elegans. Cell *99*, 123-132.
Tallafuss, A., Constable, J.R., and Washbourne, P. (2010). Organization of central synapses by adhesion molecules. Eur J Neurosci *32*, 198-206.
Thapliyal, S., Vasudevan, A., Dong, Y., Bai, J., Koushika, S.P., and Babu, K. (2018). The C-terminal of CASY-1/Calsyntenin regulates GABAergic synaptic transmission at the Caenorhabditis elegans neuromuscular junction. PLOS Genetics *14*, e1007263.
Togashi, H., Sakisaka, T., and Takai, Y. (2009). Cell adhesion molecules in the central nervous system. Cell Adhesion & Migration *3*, 29-35.

Touroutine, D. (2009). Identification and regulation of a novel nicotinic receptor at the Caenorhabditis elegans NMJ (University of Illinois at Chicago).
Touroutine, D., Fox, R.M., Von Stetina, S.E., Burdina, A., Miller, D.M., and Richmond, J.E. (2005). acr-16 encodes an essential subunit of the levamisole-resistant nicotinic receptor at the Caenorhabditis elegans neuromuscular junction. Journal of Biological Chemistry *280*, 27013-27021.
Trent, C., Tsung, N., and Horvitz, H.R. (1983). Egg-laying defective mutants of the nematode Caenorhabditis elegans. Genetics *104*, 619-647.
Tsukita, S., and Furuse, M. (2000). The structure and function of claudins, cell adhesion molecules at tight junctions. Ann N Y Acad Sci *915*, 129-135.
Turksen, K. (2004). Barriers built on claudins. Journal of Cell Science *117*, 2435-2447.
Umeda, K., Ikenouchi, J., Katahira-Tayama, S., Furuse, K., Sasaki, H., Nakayama, M., Matsui, T., Tsukita, S., Furuse, M., and Tsukita, S. (2006). ZO-1 and ZO-2 independently determine where claudins are polymerized in tight-junction strand formation. Cell *126*, 741-754.
Valvezan, A., and Klein, P. (2012). GSK-3 and Wnt Signaling in Neurogenesis and Bipolar Disorder. Frontiers in Molecular Neuroscience *5*.
Van Itallie, C.M., and Anderson, J.M. (2006). CLAUDINS AND EPITHELIAL PARACELLULAR TRANSPORT. Annual Review of Physiology *68*, 403-429.
Van Itallie, C.M., Tietgens, A.J., Anderson, J.M., and Nusrat, A. (2017). Visualizing the dynamic coupling of claudin strands to the actin cytoskeleton through ZO-1. Molecular Biology of the Cell *28*, 524-534.
Vashlishan, A.B., Madison, J.M., Dybbs, M., Bai, J., Sieburth, D., Ch'ng, Q., Tavazoie, M., and Kaplan, J.M. (2008). An RNAi screen identifies genes that regulate GABA synapses. Neuron *58*, 346-361.
Walker, C.S., Brockie, P.J., Madsen, D.M., Francis, M.M., Zheng, Y., Koduri, S., Mellem, J.E., Strutz-Seebohm, N., and Maricq, A.V. (2006). Reconstitution of invertebrate glutamate receptor function depends on stargazin-like proteins. Proceedings of the National Academy of Sciences of the United States of America *103*, 10781-10786.
Wang, J., Ruan, N.-J., Qian, L., Lei, W.-l., Chen, F., and Luo, Z.-G. (2008a). Wnt/β-Catenin Signaling Suppresses Rapsyn Expression and Inhibits Acetylcholine Receptor Clustering at the Neuromuscular Junction. Journal of Biological Chemistry *283*, 21668-21675.
Wang, R., Walker, C.S., Brockie, P.J., Francis, M.M., Mellem, J.E., Madsen, D.M., and Maricq, A.V. (2008b). TARP Proteins Have Fundamental Roles in the Gating of Glutamate Receptors and the Tuning of Synaptic Function. Neuron *59*, 997-1008.
Wang, W., Xu, L., Liu, P., Jairam, K., Yin, Y., Chen, K., Sprengers, D., Peppelenbosch, M.P., Pan, Q., and Smits, R. (2016a). Blocking Wnt Secretion Reduces Growth of Hepatocellular Carcinoma Cell Lines Mostly Independent of beta-Catenin Signaling. Neoplasia *18*, 711-723.
Wang, Z., Li, B., Zhou, L., Yu, S., Su, Z., Song, J., Sun, Q., Sha, O., Wang, X., Jiang, W.*, et al.* (2016b). Prodigiosin inhibits Wnt/beta-catenin signaling and exerts anticancer activity in breast cancer cells. Proceedings of the National Academy of Sciences of the United States of America *113*, 13150-13155.
Witzemann, V., Barg, B., Nishikawa, Y., Sakmann, B., and Numa, S. (1987). Differential regulation of muscle acetylcholine receptor γ-and ϵ-subunit mRNAs. FEBS Letters *223*, 104-112.
Wu, H., Xiong, W.C., and Mei, L. (2010). To build a synapse: signaling pathways in neuromuscular junction assembly. Development *137*, 1017-1033.

Wu, Q., Li, Y., Tang, M., and Wang, D. (2012). in Nematode Caenorhabditis elegans.
Wu, V.M., Schulte, J., Hirschi, A., Tepass, U., and Beitel, G.J. (2004). Sinuous is a Drosophila claudin required for septate junction organization and epithelial tube size control. The Journal of Cell Biology *164*, 313-323.
Xu, K., Zhong, G., and Zhuang, X. (2013). Actin, spectrin and associated proteins form a periodic cytoskeletal structure in axons. Science (New York, NY) *339*, 10.1126/science.1232251.
Yamagata, M., Sanes, J.R., and Weiner, J.A. (2003a). Synaptic adhesion molecules. Current Opinion in Cell Biology *15*, 621-632.
Yamagata, M., Sanes, J.R., and Weiner, J.A. (2003b). Synaptic adhesion molecules. Curr Opin Cell Biol *15*, 621-632.
Yamagata, M., Weiner, J.A., and Sanes, J.R. (2002). Sidekicks: synaptic adhesion molecules that promote lamina-specific connectivity in the retina. Cell *110*, 649-660.
Yang, P.-T., Lorenowicz, M.J., Silhankova, M., Coudreuse, D.Y.M., Betist, M.C., and Korswagen, H.C. (2008). Wnt Signaling Requires Retromer-Dependent Recycling of MIG-14/Wntless in Wnt-Producing Cells. Developmental Cell *14*, 140-147.
Yang, Y., and Rosenberg, G.A. (2011). MMP-Mediated Disruption of Claudin-5 in the Blood–Brain Barrier of Rat Brain After Cerebral Ischemia. Methods in molecular biology (Clifton, NJ) *762*, 333-345.
Yeh, E., Kawano, T., Weimer, R.M., Bessereau, J.L., and Zhen, M. (2005). Identification of genes involved in synaptogenesis using a fluorescent active zone marker in Caenorhabditis elegans. The Journal of neuroscience : the official journal of the Society for Neuroscience *25*, 3833-3841.
Zhan, T., Rindtorff, N., and Boutros, M. (2017). Wnt signaling in cancer. Oncogene *36*, 1461-1473.
Zhang, J., Liss, M., Wolburg, H., Blasig, I.E., and Abdelilah-Seyfried, S. (2012). Involvement of claudins in zebrafish brain ventricle morphogenesis. Annals of the New York Academy of Sciences *1257*, 193-198.
Zhang, W., and Benson, D.L. (2002). Developmentally regulated changes in cellular compartmentation and synaptic distribution of actin in hippocampal neurons. J Neurosci Res *69*, 427-436.
Zhen, M., and Jin, Y. (1999). The liprin protein SYD-2 regulates the differentiation of presynaptic termini in C. elegans. Nature *401*, 371.
Zuo, J., Treadaway, J., Buckner, T.W., and Fritzsch, B. (1999). Visualization of α9 acetylcholine receptor expression in hair cells of transgenic mice containing a modified bacterial artificial chromosome. Proceedings of the National Academy of Sciences of the United States of America *96*, 14100-14105.
Zwaal, R.R., Broeks, A., van Meurs, J., Groenen, J., and Plasterk, R. (1993). Target-selected gene inactivation in Caenorhabditis elegans by using a frozen transposon insertion mutant bank. Proceedings of the National Academy of Sciences *90*, 7431-7435.